



HAL
open science

On statistical risk assessment for spatial processes

Manaf Ahmed

► **To cite this version:**

Manaf Ahmed. On statistical risk assessment for spatial processes. Statistics [math.ST]. Université de Lyon, 2017. English. NNT : 2017LYSE1098 . tel-01586218

HAL Id: tel-01586218

<https://theses.hal.science/tel-01586218>

Submitted on 12 Sep 2017

HAL is a multi-disciplinary open access archive for the deposit and dissemination of scientific research documents, whether they are published or not. The documents may come from teaching and research institutions in France or abroad, or from public or private research centers.

L'archive ouverte pluridisciplinaire **HAL**, est destinée au dépôt et à la diffusion de documents scientifiques de niveau recherche, publiés ou non, émanant des établissements d'enseignement et de recherche français ou étrangers, des laboratoires publics ou privés.



N° d'ordre NNT : 2017LYSE1098

THÈSE DE DOCTORAT DE L'UNIVERSITÉ DE LYON
opérée au sein de
l'Université Claude Bernard Lyon 1

École Doctorale 512
InfoMaths

Spécialité de doctorat : Mathématiques Appliquées/ Statistiques

Soutenue publiquement le 29/06/2017, par :
Manaf AHMED

**Sur l'évaluation statistique des risques pour les
processus spatiaux**
On statistical risk assessment for spatial processes

Devant le jury composé de :

Bacro Jean-Noël, Professeur, Université Montpellier
Brouste Alexandre, Professeur, Université du Maine

Rapporteur
Rapporteur

Bel Liliane, Professeur, AgroParisTech
Toulemonde Gwladys, Maître de conférences, Université Montpellier

Examinatrice
Examinatrice

Vial Céline, Maître de conférences, Université Claude Bernard Lyon 1 Directrice de thèse
Maume-Deschamps Véronique, Professeur, Université Claude Bernard Lyon 1 Co-Directrice de thèse
Ribereau Pierre, Maître de conférences, Université Claude Bernard Lyon 1 Co-Directeur de thèse

Résumé

La modélisation probabiliste des événements climatiques et environnementaux doit prendre en compte leur nature spatiale. Cette thèse porte sur l'étude de mesures de risque pour des processus spatiaux. Dans une première partie, nous introduisons des mesures de risque à même de prendre en compte la structure de dépendance des processus spatiaux sous-jacents pour traiter de données environnementales. Une deuxième partie est consacrée à l'estimation des paramètres de processus de type max-mélange.

La première partie de la thèse est dédiée aux mesures de risque. Nous étendons les travaux réalisés dans [44] d'une part à des processus gaussiens, d'autre part à d'autres processus max-stables et à des processus max-mélange, d'autres structures de dépendance sont ainsi considérées. Les mesures de risque considérées sont basées sur la moyenne $L(\mathcal{A}, \mathcal{D})$ de pertes ou de dommages \mathcal{D} sur une région d'intérêt \mathcal{A} . Nous considérons alors l'espérance et la variance de ces *dommages normalisés*. Dans un premier temps, nous nous intéressons aux propriétés axiomatiques des mesures de risque, à leur calcul et à leur comportement asymptotique (lorsque la taille de la région \mathcal{A} tend vers l'infini). Nous calculons les mesures de risque dans différents cas. Pour un processus gaussien, X , on considère la fonction d'excès : $\mathcal{D}_{X,u}^+ = (X - u)^+$ où u est un seuil fixé. Pour des processus max-stables et max-mélange X , on considère la fonction puissance : $\mathcal{D}_X^\nu = X^\nu$. Dans certains cas, des formules semi-explicites pour les mesures de risque correspondantes sont données. Une étude sur simulations permet de tester le comportement des mesures de risque par rapport aux nombreux paramètres en jeu et aux différentes formes de noyau de corrélation. Nous évaluons aussi la performance calculatoire des différentes méthodes proposées. Celle-ci est satisfaisante. Enfin, nous avons utilisé une étude précédente sur des données de pollution dans le Piémont italien, celle-ci peuvent être considérées comme gaussiennes. Nous étudions la mesure de risque associée au seuil légal de pollution donnée par la directive européenne 2008/50/EC.

Dans une deuxième partie, nous proposons une procédure d'estimation des paramètres

d'un processus max-mélange, alternative à la méthode d'estimation par maximum de vraisemblance composite. Cette méthode plus classique d'estimation par maximum de vraisemblance composite est surtout performante pour estimer les paramètres de la partie max-stable du mélange (et moins performante pour estimer les paramètres de la partie asymptotiquement indépendante). Nous proposons une méthode de moindres carrés basée sur le F-madogramme : minimisation de l'écart quadratique entre le F-madogramme théorique et le F-madogramme empirique. Cette méthode est évaluée par simulation et comparée à la méthode par maximum de vraisemblance composite. Les simulations indiquent que la méthode par moindres carrés du F-madogramme est plus performante pour estimer les paramètres de la partie asymptotiquement indépendante.

Mots clé : mesures de risque ; mesures de dépendance spatiale ; processus gaussiens ; processus max-stables ; processus max-mélange ; dépendance asymptotique ; indépendance asymptotique.

Abstract

When dealing with environmental or climatic changes, a natural spatial dependence aspect appears. This thesis is dedicated to the study of risk measures in this spatial context. In the first part (Chapters 3 and 4), we study risk measures, which include the natural spatial dependence structure in order to assess the risks due to extreme environmental events and in the last part (Chapter 5), we propose estimation procedures for underlying processes, such as isotropic and stationary max-mixture processes.

In the first part dedicated to risk measures, we extended the work in [44] in order to obtain spatial risk measures for various spatial processes and different dependence structures. We based these risk measures on the mean losses over a region \mathcal{A} of interest. Risk measures are then defined as the expectation $\mathbb{E}[L(\mathcal{A}, \mathcal{D})]$ and variance $\text{Var}(L(\mathcal{A}, \mathcal{D}))$ of the *normalized loss*. In the study of these measures, we focused on the axiomatic properties of asymptotic behavior (as the size of the region interest goes to infinity) and on computational aspects. We calculated two risk measures: risk measure for the gaussian process based on the damage function called *access damage* $\mathcal{D}_{X,u}^+$ and risk measure for extreme processes based on *the power damage* function \mathcal{D}_X^v . In simulation study and for each risk measure provided, we emphasized the theoretical results of asymptotic behavior by various parameters of a model and different Kernels for the correlation function. We also evaluated the performance of these risk measures. The results were encouraging. Finally, we implemented the risk measure corresponding to gaussian on the real data of pollution in Piemonte, Italy. We assessed the risks associated with this pollution when an excess of it was over the legal level determined by the European directive 2008/50/EC.

With respect to estimation, we proposed a semi-parametric estimation procedure in order to estimate the parameters of a max-mixture model and also of a max-stable model (inverse max-stable model) as an alternative to composite likelihood. A good estimation by the proposed estimator required the dependence measure to detect all dependence structures in the model, especially when dealing with the max-mixture

model. We overcame this challenge by using the *F-madogram*. The semi-parametric estimation was then based on a quasi least square method, by minimizing the square difference between the theoretical F-madogram and an empirical one. We evaluated the performance of this estimator through a simulation study. It was shown that on a mean, the estimation is performed well, although in some cases, it encountered some difficulties.

Keywords: Risk measures, spatial dependence measures, gaussian process, asymptotic dependence/independence, max-stable process, max-mixture process.

Acknowledgements

First of all, I would like to thank Prof. Véronique Maume-Deschamps, Asst. Prof. Céline Vial and Asst. Prof. Pierre Ribereau for being such great supervisors. Their unlimited support and remarkable knowledge guided me to the right direction during my research study. I extend my gratitude to all those who whole-heartedly supported me when writing this thesis; I am grateful to have known their experiences, gotten their encouragement and having the possibility to travel to several conferences. It is an honour for me to work with excellent professors.

Besides my advisors, my deep and sincere gratitude goes out to my thesis Committee - the referees Prof. Bacro Jean-Noël and Prof. Brouste Alexandre and the examiners Prof. Bell Liliane and Toulemonde Gwladys - not only for their time and extreme patience, but for their intellectual contributions and insightful comments.

My great thanks and gratitude goes to my great country Iraq represented by Higher Education and Scientific Research Ministry/ University of Mosul for their financial support during my study. I am grateful to every soldier and civilian who fought and sacrificed their lives for the freedom of the city of Mosul.

I owe my gratitude to the Laboratory of Research on Mathematics in Lyon, Institut Camille Jordan represented by its director Sylvie Benzoni-Gavage. They provided me with all the facilities that contributed to complete this study. Thanks to all the colleagues and staff in this institute.

A special thanks goes to my friend Khalil Said for his accompaniment and support in everything.

Last but not the least, I want to thank the most important persons in my life - my parents - you are truly great for being there for me in all my life -, my sisters, my brothers, my wife and my daughter Banan, thank you so much for being a part of my life.

Contents

1	Introduction	1
1.1	General introduction and motivation	1
1.2	Main definitions and tools used in this thesis	2
1.2.1	Spatial processes	3
1.2.2	Axioms for univariate risk measures	5
1.2.3	Spatial risk measures	7
1.3	Main realizations of the thesis	7
1.3.1	General properties of $\mathcal{R}_1(\mathcal{A}, \mathcal{D})$	8
1.3.2	Risk measures for Gaussian processes	8
1.3.3	Spatial risk measure for extreme processes	10
1.3.4	Estimation of the parameters of max-mixture processes.	11
1.4	Outline of the thesis	12
2	Spatial Risk measure	15
2.1	Introduction	15
2.2	General framework	15
2.2.1	Stochastic processes	15
2.2.2	Dependence measures	18
2.3	Extreme spatial processes	21
2.3.1	Max-stable model	22
2.3.2	Inverse Max-stable processes	28
2.3.3	Max-mixture model	29
2.4	Spatial risk measure	32
2.4.1	Normalized loss function	32
2.4.2	Spatial risk measure definition	33
2.5	Axiomatic properties of spatial risk measures	33
3	Calculating $\mathcal{R}(\mathcal{A}, \mathcal{D})$ on some spatial processes	37
3.1	Risk measure for spatial Gaussian process	37
3.1.1	Explicit forms of $\mathcal{R}(\mathcal{A}, \mathcal{D}_{X,u}^+)$	38

3.1.2	Behaviour of $\mathcal{R}_1(\lambda\mathcal{A}, \mathcal{D}_{X,u}^+)$ with respect to λ	43
3.2	Risk measures for max-mixture processes	44
3.2.1	General forms for $\mathcal{R}_1(\mathcal{A}, \mathcal{D}_X^\nu)$	44
3.2.2	Explicit form of $\mathcal{R}_1(\mathcal{A}, \mathcal{D}_X^\nu)$ for TEG max-stable process . . .	46
3.2.3	Behavior of $\mathcal{R}_1(\lambda\mathcal{A}, \mathcal{D}_X^\nu)$ with respect to λ for max-mixture processes.	48
4	Computational aspects of the risk measures	51
4.1	Computational aspects for Gaussian risk measure	51
4.1.1	Analysis of $\mathcal{G}(h, u)$ and $\mathcal{R}_1(\lambda\mathcal{A}, \mathcal{D}_{X,u}^+)$	51
4.1.2	Numerical computation	53
4.1.3	Piemonte case study	54
4.2	Computational aspects for extreme processes risk measure	57
4.2.1	Analysis of the covariance damage function $\mathcal{Q}(h, \nu)$	57
4.2.2	Numerical computation of $\mathcal{R}_1(\mathcal{A}, \mathcal{D}^\nu)$	60
4.2.3	Behavior of $\mathcal{R}_1(\lambda\mathcal{A}, \mathcal{D}^\nu)$	62
5	Estimation parameters of spatial max-mixture model	65
5.1	F -madogram for max-mixture spatial process	65
5.2	Model inference	70
5.2.1	Parametric Estimation using Composite Likelihood	70
5.2.2	Semi-parametric estimation using NLS of F-madogram	72
5.3	Simulation study	74
5.3.1	Analysis the behavior of $\nu^F(h)$	74
5.3.2	Comparison of the estimation performance of $\hat{\psi}_T$ and $\hat{\psi}_L$. . .	75
6	Conclusions	81
6.1	Conclusion Remarks	81
6.2	Future work	82
	Appendices	83
A		83
A.1	Moments of truncated bivariate Gaussian distribution	83
A.2	Proof Corollary 3.5	85
B	Semi-Parametric estimation using dependence measures	89
B.1	Estimation procedure	89
B.2	Evaluating the performance of the estimators	91
	Bibliography	93

Chapter 1

Introduction

This thesis is devoted to the definition and study of risk measures in a spatial context. We will focus on the axiomatic properties, the asymptotic behavior (as the size of the area of interest goes to infinity), and on the computation aspects of these risk measures. Our contribution follows and further develops the work by Erwan Koch [44]. We provide certain guidelines to compute the risk measures when the model is well specified for Gaussian processes, max-stable processes, and max-mixture processes. The last chapter is devoted to the parameter estimation for max-mixture processes.

This introductory chapter begins with some general statements on spatial modeling in environmental contexts. This is one of our motivations. Then, we recall some definitions and tools that will be useful and we present the main goals and realizations of the thesis.

1.1 General introduction and motivation

A heat wave is a prolonged period where maxima temperatures are unusually high with respect to the usual ones. Most of the times, these heat waves have a huge spatial component. For example, in 1936, an extremely severe heat wave hit North America. Many states recorded high temperatures during this canicule, and this stood until the canicule of 2012. In 2003, a major heat wave hit Europe (cf [20], [38]), specially France, resulting in over 70,000 deaths (around 15,000 only in France). In France, this climatic event was exceptional due to its intensity, since some cities registered eight consecutive days with temperatures greater than 40° , but it was also exceptional due to its spatial extent, covering almost all of the country. In probability, this means that the underlying spatial process has a strong spatial dependence, even

at a long distance.

On the other hand, a "classical" storm type in the south of France is a *cevenol* event. These storms are a particular kind of rainfall, usually hitting the *Cevennes* in France. They are characterized by extremely heavy and localized rainfalls that lead to severe floods. For example, in September 2002, the *Gard* department was hit by an exceptional storm. Some locations received more than 700 mm of rain in 24 hours. This event caused the death of 23 persons. Another example is that of the Draguignan sevely flooding on June 15th, 2010 (cf [56], [51]), leaving 27 dead and one billion euros worth of damages. Also, during December 1999, three storms hit Europe, causing insured losses above 10 billion Euros (see [69, 57, 30]). The storms may also have a huge spatial component; in other words, the underlying spatial process may have a strong spatial dependence even at a long distance.

In Norway, on January 1, 1992, a hurricane (high wind velocities) hit the western coast of Norway and cost around 20 million euros. More than 29,000 buildings were damaged; in some municipalities, 33% of the building stock was damaged.

In all these situations, one of the main characteristic of the event is its spatial dependence. The dependencies may be strong even for large distances as the heat waves or they may be strong at short distances and weak at larger distances, as the *cevenol* events. When trying to detect the dangerousness of a region using risk measures, the notion of spatial dependence must be taken into account. Many dependence structures may arise, for example, asymptotic dependence, asymptotic independence, or both [73].

The high economic impact of these environmental/climatic events motivated us to develop the theory of spatial risk measures [44]. The impact of the dependence structure will be one of our main concerns.

1.2 Main definitions and tools used in this thesis

We provide a general setting to define spatial risk measures. It should be applicable and relevant for various spatial processes and different dependence structures. It will also depend on damage functions over a region.

First, we quickly present the spatial processes considered in this work, as well as tools used to identify the spatial dependence structures. Then, we shall provide definitions of risk measures and present natural axioms about them. For completeness,

we recall the classical axioms for univariate risk measures.

1.2.1 Spatial processes

Throughout this thesis, the spatial process $X := \{X(s), s \in \mathbb{S}\}$, $\mathbb{S} \in \mathbb{R}^d$ is assumed to be strongly stationary and isotropic. This means that for any $k \in \mathbb{N}$, $(s_1, \dots, s_k) \in \mathbb{S}^k$ and h with $(s_1 + h, \dots, s_k + h) \in \mathbb{S}^k$, the random vector $(X_{s_1}, \dots, X_{s_k})$ has the same distribution as $(X_{s_1+h}, \dots, X_{s_k+h})$ (stationarity) and this common distribution depends only on $\|h\|$ (isotropy), where $\|\cdot\|$ denotes the euclidean norm in \mathbb{R}^d . For any set $\mathcal{A} \subset \mathcal{B}(\mathbb{R}^d)$, the volume of \mathcal{A} is denoted by $|\mathcal{A}|$, that is $|\mathcal{A}| = \lambda(\mathcal{A})$ with λ being the Lebesgue measure on \mathbb{R}^d .

Gaussian processes

The process $(X(s))_{s \in \mathbb{S}}$ is a Gaussian process if and only if, for any $d \in \mathbb{N}$, $(s_1, \dots, s_d) \in \mathbb{S}^d$, the random vector $(X(s_1), \dots, X(s_d))$ is a Gaussian vector. Of course, an isotropic stationary Gaussian process is determined by:

- $\mu = \mathbb{E}(X(s))$, $\sigma^2 = \text{Var}(X(s))$,
- the covariance structure: $\gamma(h) = \text{Cov}(X(s), X(s+h))$ or equivalently, the correlation function $\rho(h) = \text{Corr}(X(s), X(s+h))$.

φ denotes the density of a standard normal law, Φ its distribution function, and $\bar{\Phi} = 1 - \Phi$ its survival distribution function.

Max-stable processes

Gaussian processes are not well suited for many applications, e.g. rainfall and wind in some regions. Hence, we shall consider max-stable processes. Related definitions and a literature review are detailed in Chapter 2. If X is a simple max-stable process, it has unit Fréchet margins and its bivariate dependence structure is given by:

$$\mathbb{P}(X(s) \leq x) = e^{-\frac{1}{x}}, \quad \mathbb{P}(X(s) \leq x_1, X(t) \leq x_2) = \exp(-V_{s,t}(x_1, x_2)), \quad x > 0.$$

$V_{s,t}$ is called the exponent measure function. If the process is isotropic then $V_{s,t}(x_1, x_2)$ depends only on $h = \|t - s\|$ and is written as V_h .

Max-stable processes are *asymptotically dependent* in the sense that either $X(s)$ and $X(s+h)$ are independent or we have

$$\chi(h, u) = 2 - \frac{\log \mathbb{P}(F(X(s)) < u, F(X(t)) < u)}{\log \mathbb{P}(F(X(s)) < u)} > 0 \quad \forall h \in \mathbb{S}, u \in [0, 1],$$

such that, $\chi(h) = \lim_{u \rightarrow -1} \chi(h, u)$. χ is seen as a measure of asymptotic dependence of the process.

For completeness, let us mention two examples of max-stable processes.

Smith Model (Gaussian extreme value model)

$$V_h(x_1, x_2) = \frac{1}{x_1} \Phi \left(\frac{\tau(h)}{2} + \frac{1}{\tau(h)} \log \frac{x_2}{x_1} \right) + \frac{1}{x_2} \Phi \left(\frac{\tau(h)}{2} + \frac{1}{\tau(h)} \log \frac{x_1}{x_2} \right);$$

with $\tau(h) = \sqrt{h^T \Sigma^{-1} h}$.

Schlather Models (Extremal Gaussian Model)

$$V_h(x_1, x_2) = \frac{1}{2} \left(\frac{1}{x_1} + \frac{1}{x_2} \right) \left[1 + \sqrt{1 - 2(\rho(h) + 1) \frac{x_1 x_2}{(x_1 + x_2)^2}} \right].$$

Inverse max-stable processes

Let X' be a simple max-stable process as stated above, with exponent measure function V_h , consider

$$X(s) = g(X'(s)) = -\frac{1}{\log\{1 - e^{-1/X'(s)}\}} \quad s \in \mathbb{S}.$$

Then, X has unit Fréchet margin and bivariate survivor function

$$\mathbb{P}(X(s_1) > x_1, X(s+h) > x_2) = \exp(-V_h(g(x_1), g(x_2))).$$

Inverse max-stable processes have been defined in [47]. More details are given in Chapter 2.

Inverse max-stable processes are *asymptotically independent* in the sense that $\chi(h) = 0$ for any h . In order to measure the strength of asymptotic independence, the $\bar{\chi}$ measure is introduced.

$$\bar{\chi}(h, u) = \frac{2 \log \mathbb{P}(F(X(s)) > u)}{\log \mathbb{P}(F(X(s)) > u, F(Y(s+h)) > u)} - 1, \quad 0 \leq u \leq 1.$$

Such that, $\bar{\chi}(h) = \lim_{u \rightarrow 1} \bar{\chi}(h, u)$. We have $-1 \leq \bar{\chi}(h) \leq 1$ and the spatial process is asymptotically dependent if $\bar{\chi}(h) = 1$. Otherwise, it is asymptotically independent.

Max-mixture processes

Wadsworth and Tawn [73] proposed to mix max-stable and inverse max-stable processes. Let X be a simple max-stable process, with exponent measure function V_h^X . Let Y be an inverse max-stable process with and exponent measure function V_h^Y . Let $a \in [0, 1]$ and define

$$Z(s) = \max\{aX(s), (1-a)Y(s)\}, \quad s \in \mathbb{S}.$$

Z has unit Fréchet marginals. Its bivariate distribution function is given by

$$\mathbb{P}(Z(s) \leq z_1, Z(s+h) \leq z_2) = e^{-aV_h^X(z_1, z_2)} \left[e^{\frac{-(1-a)}{z_1}} + e^{\frac{-(1-a)}{z_2}} - 1 + e^{-V_h^Y(g_a(z_1), g_a(z_2))} \right],$$

where $g_a(z) = g\left(\frac{z}{1-a}\right)$.

For nontrivial max-mixture, i.e. $a \in]0, 1[$, we have $\chi(h) \neq 0$ and $\bar{\chi}(h) \neq 1$ for some values of h , which means that these processes are neither asymptotically dependent nor asymptotically independent (see Chapter 2 for the calculation of χ and $\bar{\chi}$ for max-mixture processes).

Throughout the thesis, max-stable and max-mixture processes will be referred to as *extreme processes*.

The F -madogram

We terminate this subsection on spatial processes with the definition of the F -madogram, which can be seen as another measure of dependence. We shall use it for the estimation of parameters of max-mixture processes. It has been introduced in [24] for processes for which the variogram is not defined (typically processes with Fréchet margin do not have an order 2 moment).

Definition 1.1. *Let X be a spatial process on \mathbb{S} with univariate margin F . The F -madogram of the process X is for all $(s, t) \in \mathbb{S}^2$*

$$\nu^F(s-t) = \frac{1}{2} \mathbb{E}|F(X(s)) - F(X(t))|.$$

If the process is asymptotically independent, then $\nu^F(h) = \frac{1}{6}$.

1.2.2 Axioms for univariate risk measures

Before introducing spatial risk measures, it seems useful to recall the widely used concepts on univariate risk measures.

Univariate risk measures

Consider a random variable X on Ω (it may be the wind speed, the temperature, a claim amount...). F_X is its distribution function.

A *risk measure* is a function of X , valued in \mathbb{R} , often denoted as ρ .

The choice of a risk measure depends on the purpose, it could be for examples:

- the expected value: $\mathbb{E}(X)$ which provides information of the mean behavior.
- the variance: $\text{Var} = \mathbb{E}((X - E(X))^2)$ which measures the average deviation of X with respect to its mean.
- Quantiles: let $\alpha \in]0, 1[$, the α -quantile is $q_\alpha = \inf\{t, F_X(t) \geq \alpha\}$, this is the value that X should not exceed with probability α .

Axioms for univariate risk measures

A risk measure ρ is:

- *invariant by translation* if for any $a \in \mathbb{R}$, $\rho(X + a) = \rho(X) + a$. It means that adding a constant risk increases the risk with that constant amount.
- *positive homogeneous* if for any $a > 0$, $\rho(aX) = a\rho(X)$. The measure is not affected by a change of unity.
- *sub-additive*, if for any random variables X and Y , $\rho(X + Y) \leq \rho(X) + \rho(Y)$. It consists of a diversification effect.
- *a.s. monotone*, if $X \leq Y$ a.s., then $\rho(X) \leq \rho(Y)$.

Following [6] a risk measure is *coherent* if it satisfies the four axioms stated above.

Remark 1. • $X \rightsquigarrow \mathbb{E}(X)$ and $X \rightsquigarrow \sqrt{\text{Var}(X)}$ are coherent.

- $X \rightsquigarrow q_\alpha(X)$ is not coherent (it is not sub-additive). Nevertheless, the quantile function is extensively used because it is imposed by regulatory rules in finance / insurance; also, it is related to the notion of return time in environment.
- $\alpha \rightsquigarrow q_\alpha(X)$ is increasing.

1.2.3 Spatial risk measures

Previous works ([42] or [44]) proposed to evaluate spatial risk through the expectation of an integrated loss function.

Consider a spatial process X and let \mathcal{D}_X be a positive function of X called a *damage function*, e.g., $\mathcal{D}_{X,u} = (X - u)^+$ or $\mathcal{D}_X^\nu = X^\nu$.

Definition 1.2 (Normalized loss function). *Let $\mathcal{A} \subset \mathbb{S}$,*

$$L(\mathcal{A}, \mathcal{D}_X) = \frac{1}{|\mathcal{A}|} \int_{\mathcal{A}} \mathcal{D}_X(s) \, ds.$$

We propose considering spatial risk measures composed of two components: the expectation and the variance of the normalized loss,

$$\begin{aligned} \mathcal{R}(\mathcal{A}, \mathcal{D}_X) &= \{\mathbb{E}[L(\mathcal{A}, \mathcal{D}_X)], \text{Var}(L(\mathcal{A}, \mathcal{D}_X))\}, \\ &=: \{\mathcal{R}_0(\mathcal{A}, \mathcal{D}_X), \mathcal{R}_1(\mathcal{A}, \mathcal{D}_X)\} \end{aligned}$$

For stationary processes, $\mathbb{E}[L(\mathcal{A}, \mathcal{D}_X)]$ provides information on the severity of the phenomenon.

$$\mathbb{E}[L(\mathcal{A}, \mathcal{D}_X)] = \frac{1}{|\mathcal{A}|} \int_{\mathcal{A}} \mathbb{E}(\mathcal{D}_X(s)) ds = \mathbb{E}(\mathcal{D}_X(s)) \text{ does not depend on } \mathcal{A}.$$

When $\text{Var}(L(\mathcal{A}, \mathcal{D}_X))$ is impacted by the dependence structure, we have

$$\text{Var}(L(\mathcal{A}, \mathcal{D}_X)) = \frac{1}{|\mathcal{A}|^2} \int_{\mathcal{A} \times \mathcal{A}} \text{Cov}(\mathcal{D}_X(s), \mathcal{D}_X(t)) ds dt.$$

Natural axioms for spatial risk measures are adaptations to the spatial context of coherence axioms by [6]. In this study, we have followed [44].

Consider $\mathcal{A}, \mathcal{A}_1, \mathcal{A}_2$ as subsets of \mathbb{S} . Consider \mathcal{R} both as a function of \mathcal{A} and of a damage function \mathcal{D} . We have considered the following axioms on \mathcal{R} .

1. *Invariance by translation.* For any $v \in \mathbb{S}$, $\mathcal{R}(\mathcal{A} + v, \mathcal{D}) = \mathcal{R}(\mathcal{A}, \mathcal{D})$.
2. *Anti-monotonicity* If $|\mathcal{A}_1| \leq |\mathcal{A}_2|$, then $\mathcal{R}(\mathcal{A}_2, \mathcal{D}) \leq \mathcal{R}(\mathcal{A}_1, \mathcal{D})$.
3. *Sub-additivity* If $\mathcal{A}_1 \cap \mathcal{A}_2 = \emptyset$, then $\mathcal{R}(\mathcal{A}_1 \cup \mathcal{A}_2, \mathcal{D}) \leq \mathcal{R}(\mathcal{A}_1, \mathcal{D}) + \mathcal{R}(\mathcal{A}_2, \mathcal{D})$.
4. *Super sub-additivity* If $\mathcal{A}_1 \cap \mathcal{A}_2 = \emptyset$, then $\mathcal{R}(\mathcal{A}_1 \cup \mathcal{A}_2, \mathcal{D}) \leq \min_{i=1,2} [\mathcal{R}(\mathcal{A}_i, \mathcal{D})]$.

1.3 Main realizations of the thesis

We are now in a position to state our main results.

1.3.1 General properties of $\mathcal{R}_1(\mathcal{A}, \mathcal{D})$

Let X be an isotropic spatial process. The risk measure $\mathcal{R}_1(\mathcal{A}, \mathcal{D})$ is invariant by translation and is sub-additive. The other axiomatic properties are more difficult to get. We first provide some general forms for $\mathcal{R}_1(\mathcal{A}, \mathcal{D})$ which will be useful to get axiomatic and asymptotic properties.

Let \mathcal{A} be either a disk or a square; $\mathcal{R}_1(\mathcal{A}, \mathcal{D}_X)$ may be rewritten (we proceed as in [44]).

When \mathcal{A} is a disk of radius R ,

$$\mathcal{R}_1(\mathcal{A}, \mathcal{D}_X) = \int_{h=0}^{2R} f_{disk}(h, R) \text{Cov}(\mathcal{D}_X(s), \mathcal{D}_X(s+h)) \, dh.$$

Where $f_{disk}(h, R)$ is the density of distance between two points uniformly drawn on a disk ([52]), that is

$$f_{disk}(h, R) = \frac{2h}{R^2} \left(\frac{2}{\pi} \arccos\left(\frac{h}{2R}\right) - \frac{h}{\pi R} \sqrt{1 - \frac{h^2}{4R^2}} \right).$$

When \mathcal{A} is a square with side R

$$\mathcal{R}_1(\mathcal{A}, \mathcal{D}_X) = \int_{h=0}^{\sqrt{2}R} f_{square}(h, R) \text{Cov}(\mathcal{D}_X(s), \mathcal{D}_X(s+h)) \, dh.$$

Where $f_{square}(h, R)$ is given by: for $h \in [0, R]$,

$f_{square}(h, R) = \frac{2\pi h}{R^2} - \frac{8h^2}{R^3} + \frac{2h^3}{R^4}$, and for $h \in [R, \sqrt{2}R]$, let $b = \frac{h^2}{R^2}$

$$f_{square}(h, R) = \frac{2h}{R^2} \left\{ -2 - b + 3\sqrt{b-1} + \frac{b+1}{\sqrt{b-1}} + 2\arcsin\left(\frac{2-b}{b}\right) - \frac{4}{b\sqrt{1 - \frac{(2-b)^2}{b^2}}} \right\},$$

These two formulas show that if you can compute $\text{Cov}(\mathcal{D}_X(s), \mathcal{D}_X(s+h))$, then the risk measure reduces to a one-dimensional integration.

1.3.2 Risk measures for Gaussian processes

In the case of Gaussian processes, explicit formulas for $\mathcal{R}_1(\mathcal{A}, \mathcal{D})$ may be obtained. Consider a fixed threshold u , $\mathcal{D}_{X,u} = (X - u)^+$. The choice of u will be according to

the purpose; it may, for example, be a regulatory threshold.

This means that $\mathcal{R}_1(\mathcal{A}, \mathcal{D}_{X,u}^+)$ is the variance of the mean of X over the threshold u on the area \mathcal{A} .

If we consider a standard Gaussian process (i.e. $\mu = 0$ and $\sigma = 1$) with a positive auto-correlation function ρ , a simple calculation provides the following result:

$$\mathcal{R}_0(\mathcal{A}, \mathcal{D}_{X,u}^+) = \mathbb{E}(L(\mathcal{A}, \mathcal{D}_{X,u}^+)) = \varphi(u) - u\bar{\Phi}(u).$$

The variance of $L(\mathcal{A}, \mathcal{D}_{X,u}^+)$ may be obtained by using the results [60] on moments of truncated bivariate normal distributions. If \mathcal{A} is a square,

$$\mathcal{R}_1(\mathcal{A}, \mathcal{D}_{X,u}^+) = \text{Var}(L(\mathcal{A}, \mathcal{D}_{X,u}^+)) = \int_{h=0}^{\sqrt{2}R} f_{\text{square}}(h, R) \mathcal{G}(h, u) dh.,$$

with

$$\begin{aligned} \mathcal{G}(h, u) = & \ell(u, u, \rho(h))(\rho(h) + u^2) - 2u\varphi(u)\bar{\Phi}\left(\frac{u(1 - \rho(h))}{(1 - \rho^2(h))^{1/2}}\right) \\ & + (1 - \rho^2(h))^{1/2} \varphi\left(\frac{u}{(1 + \rho(h))^{1/2}}\right)^2 - (\varphi(u) - u\bar{\Phi}(u))^2; \end{aligned}$$

and $\ell(u, v, \rho(h))$ is the total probability of a truncated bivariate standard normal distribution with correlation function ρ .

$$\ell(u, v, \rho(h)) = \frac{1}{2\pi(1 - \rho^2(h))^{1/2}} \int_u^\infty \int_v^\infty e^{\left\{\frac{-1}{2(1 - \rho(h))^2}[x^2 - 2\rho(h)xy + y^2]\right\}} dx dy.$$

As a corollary, we may express the risk measure for any Gaussian process. Let Y be an isotropic Gaussian process with mean μ and variance σ^2 . Let $X = \frac{Y - \mu}{\sigma}$; of course, X is a standard Gaussian process.

Corollary 1.1. *The spatial risk measure $\mathbb{R}(\mathcal{A}, \mathcal{D}_{Y,u}^+)$ satisfies the following*

$$\mathcal{R}(\mathcal{A}, \mathcal{D}_{Y,u}^+) = \left\{ \sigma \mathbb{E}[L(\mathcal{A}, \mathcal{D}_{X,u_0}^+)], \sigma^2 \text{Var}(L(\mathcal{A}, \mathcal{D}_{X,u_0}^+)) \right\},$$

with $u_0 = (u - \mu)/\sigma$.

Moreover, the previous formula provides the behavior of $\lambda \rightsquigarrow \mathcal{R}_1(\lambda\mathcal{A}, \mathcal{D}_{X,u}^+)$ and it implies anti-monotonicity for disk or square.

Corollary 1.2. *Let X be an isotropic Gaussian process with auto-correlation function ρ . Let $\mathcal{A} \subset \mathbb{S}$ be either a disk or a square.*

The mapping $\lambda \mapsto \mathcal{R}_1(\lambda\mathcal{A}, \mathcal{D}_{X,u}^+)$ is non-increasing if and only if $h \mapsto \rho(h)$, $h > 0$ is

non-increasing and non-negative.

If $h \mapsto \rho(h)$ decreases to 0 as h goes to infinity,

$$\lim_{\lambda \rightarrow \infty} \mathcal{R}_1(\lambda \mathcal{A}, \mathcal{D}_{X,u}^+) = 0.$$

Let \mathcal{A}_1 and \mathcal{A}_2 be either squares or disks with $|\mathcal{A}_1| \leq |\mathcal{A}_2|$; then,

$$\mathcal{R}_1(\mathcal{A}_2, \mathcal{D}_{X,u}^+) \leq \mathcal{R}_1(\mathcal{A}_1, \mathcal{D}_{X,u}^+).$$

The decreasing behaviors of $\mathcal{R}_1(\lambda \mathcal{A}, \mathcal{D}_{X,u}^+)$ means that there is a diversification effect as the size of the considered area increases. Moreover, if the process is independent at a large scale ($h \rightarrow \infty$) the risk measure goes to 0 as the size of the area goes to infinity.

Finally, a simulation study shows the different behaviors of $\mathcal{R}_1(\lambda \mathcal{A}, \mathcal{D}_{X,u}^+)$ with respect to the various parameters of the model and different Kernels for the correlation function. Also, we provide an application on real data that has been previously studied in [11]. It concerns data on pollution in Piemonte, measured by the concentration in PM_{10} . The observed values of PM_{10} are frequently larger than the legal level fixed by the European directive 2008/50/EC. It has been shown in [11] that the log of PM_{10} can be fitted on an isotropic Gaussian process and that our formulas apply.

1.3.3 Spatial risk measure for extreme processes

In the cases of extreme spatial processes (i.e. max-stable or max-mixture processes), the excess damage function considered before cannot be used; due to Fréchet margins, it has no moment of order 1. We shall consider the damage function

$$\mathcal{D}_X^\nu(s) = |X(s)|^\nu,$$

for $0 < \nu < \frac{1}{2}$ (so that the order two moment exists).

These kind of damage functions are used, for e.g., in analyzing the negative effects due to the wind speed (see [58] for more details). In [44], the risk measure associated to \mathcal{D}_X^ν is calculated for Smith processes. We propose a calculation for TEG max-stable processes as well as some computational tools for max-mixture processes.

The properties of moments of Fréchet distributions give that if X as a unit Fréchet marginal distributions,

$$\mathbb{E}(L(\mathcal{A}, \mathcal{D}_X^\nu)) = \Gamma(1 - \nu).$$

The variance is more difficult to compute in general. Nevertheless, if \mathcal{A} is a square of side R , we have:

$$\mathcal{R}_1(\mathcal{A}, \mathcal{D}_X^\nu) = \int_{h=0}^{\sqrt{2}R} \mathcal{Q}(h, \nu) f_{square}(h, R) dh,$$

with

$$\mathcal{Q}(h, \nu) = \nu^2 \int_0^\infty \int_0^\infty x_1^{\nu-1} x_2^{\nu-1} [G_h^X(x_1, x_2) - F(x_1)F(x_2)] dx_1 dx_2$$

and $G_h^X = \mathbb{P}(X(s) \leq x_1, X(s+h) \leq x_2)$. We have a similar result for disks. These formulas are useful to get the behavior of $\mathcal{R}_1(\mathcal{A}, \mathcal{D}_X^\nu)$.

Proposition 1.3. *Let Z be an isotropic and stationary max-mixture spatial process. Assume that the mappings $h \mapsto V_h^X(x_1, x_2)$ and $V_h^Y(x_1, x_2)$ are non-decreasing for any $(x_1, x_2) \in \mathbb{R}_+^2$. Moreover, we assume that*

$$V_h^X(x_1; x_2) \longrightarrow \frac{1}{x_1} + \frac{1}{x_2} \quad \text{and} \quad V_h^Y(x_1, x_2) \longrightarrow \frac{1}{x_1} + \frac{1}{x_2} \quad \text{as} \quad h \rightarrow \infty$$

$\forall x_1, x_2 \in \mathbb{R}_+$. Let $\mathcal{A} \subset \mathbb{S}$ be either a disk or a square,

$$\lim_{\lambda \rightarrow \infty} \mathcal{R}_1(\lambda \mathcal{A}, \mathcal{D}_Z^\nu) = 0.$$

If there exists V_0 (resp. V_1), an exponent measure function of a non-independent max-stable (resp. inverse max-stable) bivariate random vector, such that $V_h^X \longrightarrow V_0$ (resp. $V_h^Y \longrightarrow V_1$ as $h \rightarrow \infty$), then

$$\lim_{\lambda \rightarrow \infty} \mathcal{R}_1(\lambda \mathcal{A}, \mathcal{D}_Z^\nu) > 0.$$

This proposition shows that the risk measure contains some information on the dependence structure of the underlying process.

Finally, a simulation study shows the behavior of $\mathcal{R}_1(\mathcal{A}, \mathcal{D}_X^\nu)$ with respect to the various parameters of the model.

1.3.4 Estimation of the parameters of max-mixture processes.

We have provided some tools to compute the risk measure $\mathcal{R}_1(\mathcal{A}, \mathcal{D}_X^\nu)$ for max-mixture processes. The estimation of the parameters of these processes remains a difficulty. The usual way to estimate parameters in spatial contexts is to maximize the composite likelihood.

For example, in [55], [26] and many others, the composite likelihood maximization is used to estimate the parameters of max-stable processes. In [9] and [73], it is used to estimate the parameters of max-mixture processes. Nevertheless, the estimation does not perform well in some cases; moreover, it seems to have difficulties estimating the inverted max-stable part.

In section 5.2.2, we propose a semi-parametric estimation procedure as an alternative to composite likelihood maximization for max-mixture and also for max-stable (resp.

inverse max-stable) processes. Our procedure is a least square method on the F -madogram; that is, we minimize the difference between the theoretical F -madogram and the empirical one. Some of literature deals with semi-parametric estimation in modeling spatial extremes. For example, [54] and [2] provided semi-parametric estimators of extremal indexes. In [16], another semi-parametric procedure to estimate model parameters is introduced. It is based on fitting the theoretical extremogram with the empirical one by non-linear least square for the isotropic space-time Brown-Resnick max-stable process. The semi-parametric procedure proposed in this thesis is based on this article.

The performance of this estimator is evaluated by a simulation study in Section 5.3.2. It shows, in general, that the estimation performs well, although it encounters some difficulties, which are discussed. Let us mention that we have also tried to estimate the parameters by using least squares on empirical tail dependence measures $\chi(h, u)$ and $\bar{\chi}(h, u)$. This procedure shows similar performance (it can be seen in Appendix B).

1.4 Outline of the thesis

Chapter 2 is devoted to spatial risk measures. It is divided as follows. Section 2.2 is dedicated to the general framework; it contains definitions, notations, examples and properties of the mathematical objects that we have used throughout this thesis. In Section 2.3, we present three different extreme spatial processes with different dependence structures (asymptotic dependence/independence and a mixture of them). Definition of spatial risk measures and the axiomatic properties are introduced in Section 2.4. The expressions and theoretical behaviors of the spatial risk measures for each spatial process considered in this thesis is provided in Chapter 3. The computational aspects related to risk measures will be presented in Chapter 4. In this chapter, the behavior of these risk measures is numerically analyzed by a simulation study. In this simulation study, for each risk measure contains two parts. The first one concerns the behavior of the covariance damage functions and variance of normalized losses. In the second part, numerical computations of the risk measures are presented. The estimation procedure is introduced in Chapter 5. In Section 5.1, we calculate an expression for the F -madogram of max-mixture models. Section 5.2 is devoted to the least square F -madogram estimation of the parameters of max-mixture processes. A simulation study is conducted, which allows us to evaluate the performance of the estimation procedure (Section 5.3). Finally, concluding remarks are discussed in Chapter 6 and some auxiliary results and simulations are provided in the Appendix.

The results of Chapters 2, 3 and 4 are contained in two different submitted articles:

M. Ahmed, V. Maume-Deschamps, P. Ribereau, C. Vial, *Spatial risk measures for Gaussian processes*, [3].

M. Ahmed, V. Maume-Deschamps, P. Ribereau, C. Vial, *Risk measures for max-stable and max-mixture spatial processes*, [4].

The results of Chapter 5 will be presented in a submitted article within few months.

Chapter 2

Spatial Risk measure

2.1 Introduction

In this chapter, we state our general framework: we recall definitions on gaussian processes, max-stable processes, inverse max-stable processes and max-mixtures. We also present the notions of asymptotic dependence and asymptotic independence. Finally, we consider quite general spatial risk measures and develop the axiomatic setting of [43].

2.2 General framework

In this section we provide the fundamental definitions, notations, examples and properties of mathematical objects that we are using throughout this thesis.

2.2.1 Stochastic processes

Definition 2.1. (*Stochastic process*) *Let us consider a probability space $(\Omega, \mathcal{F}, \mathbb{P})$ and a set $\mathbb{S} \subset \mathbb{R}^d$. A stochastic process X is a collection $(X(s), s \in \mathbb{S})$, such that $\forall s \in \mathbb{S}; X(s)$ is a random variable.*

In particular, we will speak in spatial processes when $\mathbb{S} \in \mathbb{R}^2$. Typically, observations of precipitations at certain station may be considered as realizations of a spatial process.

Definition 2.2. (Second-order processes) *The process X on \mathbb{S} is second order, if for any $s \in \mathbb{S}$, $\mathbb{E}[X(s)^2] < \infty$. In this case, the covariance function exists and is a positive semi-definite function, say $c : \mathbb{S} \times \mathbb{S} \rightarrow \mathbb{R}$, such that for each $(s, t) \in \mathbb{S}^2$*

$$c(s, t) = \mathbb{E}[X(s)X(t)] - \mathbb{E}[X(s)]\mathbb{E}[X(t)].$$

Under the second-order assumption, the *variance function* of the process X exists and is denoted by

$$\sigma^2(s) = c(s, s), \quad \text{for any } s \in \mathbb{S}.$$

We may also define the *auto-correlation function*, denoted by

$$\rho(s, t) = \frac{c(s, t)}{\sigma(s)\sigma(t)}, \quad \text{for any } (s, t) \in \mathbb{S}^2.$$

In the spatial context, the auto-correlation function is usually assumed to be non-negative, that is, for all $(s, t) \in \mathbb{S}^2$, $\rho(s, t) \geq 0$. Nevertheless, negative dependency rarely occurs in practice; see [35] for more discussion on this topic.

In what follows, we shall consider non-negative correlation functions. The most classical isotropic auto-correlation functions are the following (see [1]), for all $\tau > 0$

1. Spherical auto-correlation function:

$$\rho_{\theta}^{sph}(\tau) = \left[1 - 1.5\left(\frac{\tau}{\theta}\right) + 0.5\left(\frac{\tau}{\theta}\right)^3 \right] \mathbb{1}_{\{\tau < \theta\}};$$

2. Cubic auto-correlation function:

$$\rho_{\theta}^{cub}(\tau) = \left[1 - 7\left(\frac{\tau}{\theta}\right) + \frac{35}{2}\left(\frac{\tau}{\theta}\right)^2 - \frac{7}{2}\left(\frac{\tau}{\theta}\right)^5 + \frac{3}{5}\left(\frac{\tau}{\theta}\right)^7 \right] \mathbb{1}_{\{\tau < \theta\}};$$

3. Exponential auto-correlation function:

$$\rho_{\theta}^{exp}(\tau) = \exp \left[-\frac{\tau}{\theta} \right];$$

4. Gaussian auto-correlation function:

$$\rho_{\theta}^{gau}(\tau) = \exp \left[-\left(\frac{\tau}{\theta}\right)^2 \right];$$

5. Matérn auto-correlation function:

$$\rho_{mat}(\tau) = \frac{1}{\Gamma(\varphi)2^{\varphi-1}}(\theta\tau)^{\varphi}K_{\varphi}(\theta\tau);$$

where $\theta \in \mathbb{R}$ is a truncation parameter, $\Gamma(\cdot)$ is the gamma function, $K_\varphi(\cdot)$ is the modified Bessel function of second kind, and φ is a non-negative parameter. The parameter θ is a scaling parameter, also called the correlation length or the range parameter.

We represent below several graphs of the correlation functions for the different models and for various parameters.

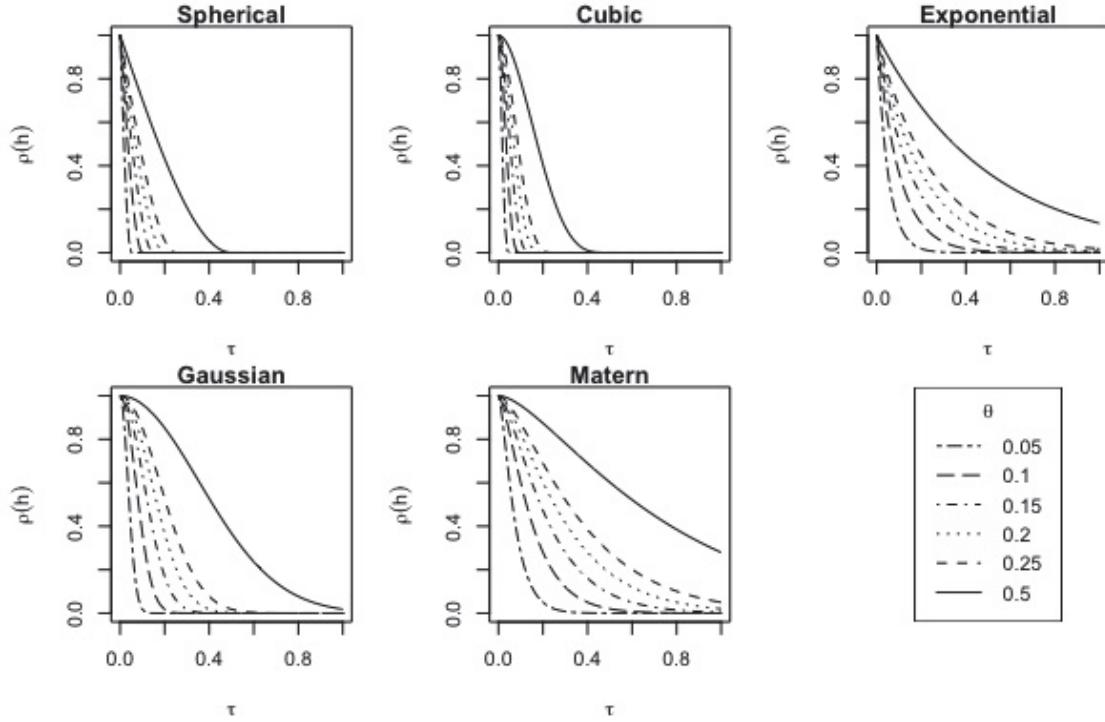


Figure 2.1: Dependence structure for different isotropic and non-negative spatial correlation functions, respectively spherical, cubic, exponential, gaussian, and matern with different scaling parameter $\theta := \{0.05, 0.1, 0.15, 0.20, 0.25, 0.5\}$ and distance $\tau \in [0, 1]$.

Definition 2.3. (Weakly stationary process) A second-order process X is weakly stationary if $\forall s \in \mathbb{S}$, $m(s) := \mathbb{E}[X(s)] = m$ and $c(s, t) = c(s + v, t + v) \quad \forall s, t \in \mathbb{S}$, with $s + v, t + v \in \mathbb{S}$.

Definition 2.4. (Strongly stationary processes) A process X on \mathbb{S} is strongly stationary if $\forall k \in \mathbb{N}^+$, $\forall (s_1, \dots, s_k) \in \mathbb{S}^k$, $\forall v \in \mathbb{S}$, such that $(s_1 + v, \dots, s_k + v) \in \mathbb{S}^k$

$$(X(s_1), \dots, X(s_k)) \stackrel{\mathcal{L}}{=} (X(s_1 + v), \dots, X(s_k + v))$$

An immediate consequence is that a second-order process which is strongly stationary is also weakly stationary but not vice versa. This property is much more restrictive than the weakly stationarity. For simplicity, in what follows, we shall say *stationary* for strongly stationary. Weakly stationary or *second-order stationary* will be used indifferently.

Definition 2.5. (Isotropic process) *A weakly stationary process X on \mathbb{S} is isotropic, if for each $(s, t) \in \mathbb{S}^2$, the covariance value $c(s, t)$ depends only on the distance $\|s - t\|$; that is, for each $(s, t) \in \mathbb{S}^2$*

$$c(s, t) = c_0(\|s - t\|)$$

An important class of processes is the one of Gaussian processes defined as follows.

Definition 2.6. (Gaussian process) *X is a Gaussian process if for any $k \in \mathbb{N}^+$ and any $(s_1, \dots, s_k) \in \mathbb{S}^k$, $(X_{s_1}, \dots, X_{s_k})$ is a k -dimensional Gaussian vector.*

Let us notice that a second-order stationary Gaussian process is stationary. Furthermore, if X is an isotropic standard Gaussian process, then we can get an explicit form for the bivariate cumulative distribution function between $X(s)$ and $X(t)$, for all $(s, t) \in \mathbb{S}^2$, that is, for all $(u, v) \in \mathbb{R}^2$

$$\begin{aligned} F_{s,t}(u, v) &:= \mathbb{P}(X(s) \leq u, X(t) \leq v), \\ &= \int_{-\infty}^u \int_{-\infty}^v \left((2\pi) \sqrt{1 - \rho^2(\tau_{s,t})} \right)^{-1} \exp \left\{ -\frac{x^2 - 2\rho(\tau_{s,t})xy + y^2}{2(1 - \rho(\tau_{s,t}))^2} \right\} dx dy, \end{aligned} \quad (2.2.1)$$

where $\tau_{s,t} = \|s - t\|$.

2.2.2 Dependence measures

Important properties of a process are described by its dependence structure and lots of measures are defined in the literature to better understand the dependence in real spatial data. In what follows, we will introduce some of them in the context of a spatial process.

First of all, let us introduce the notion of negative or positive association of two locations of a process when dealing with their extremal behaviour. The following definition extend the notion of Positive Quadrant Dependence introduced by [48] for a pair of random variables. This concept explains how the two variables behave together when they are simultaneously small (or large).

Definition 2.7. (Positive Quadrant Dependence) *The process X on \mathbb{S} is positively quadrant-dependent (or positively associated) if the following inequality is fulfilled for all $(s, t) \in \mathbb{S}^2$ and $(u, v) \in \mathbb{R}^2$*

$$\mathbb{P}(X(s) \leq u, X(t) \leq v) \geq \mathbb{P}(X(s) \leq u)\mathbb{P}(X(t) \leq v) \quad (2.2.2)$$

or equivalently

$$\mathbb{P}(X(s) > u, X(t) > v) > \mathbb{P}(X(s) > u)\mathbb{P}(X(t) > v) \quad (2.2.3)$$

For example, a Gaussian process X is positively-quadrant dependent if $0 \leq \rho(s, t) < 1$ for all $(s, t) \in \mathbb{S}^2$ and negatively-quadrant dependent if $-1 < \rho(s, t) \leq 0$ for all $(s, t) \in \mathbb{S}^2$; see the details in Example 9 of [46] and other examples therein.

Now, we will focus on different quantitative measures introduced in the literature to better understand the strength of dependence in the extremes. At first, we consider the **upper tail dependence coefficient** introduced by [65]. Dealing with a pair of variables, this coefficient allows to distinguish between two different forms of extremal dependence: asymptotic dependence and independence. In a spatial context, this tool measures the association degree between the processes at two locations and becomes a function depending on the distance between the two sites; see[10]

Definition 2.8. *Let X be a stationary spatial process on \mathbb{S} with univariate margin cumulative distribution function F . The **upper tail dependence function** χ is defined for all $s \in \mathbb{S}$ and $h \in \mathbb{S}$ such that $s + h \in \mathbb{S}$,*

$$\chi(h) = \lim_{u \rightarrow 1^-} \mathbb{P}(F(X(s+h)) > u | F(X(s)) > u). \quad (2.2.4)$$

If $\chi(h) = 0$, the pair $(X(s+h), X(s))$ is said to be asymptotically independent (AI). If $\chi(h) \neq 0$, the pair $(X(s+h), X(s))$ is said to be asymptotically dependent (AD). The process is said AI (resp. AD) if for all $h \in \mathbb{S}$ $\chi(h) = 0$ (resp. $\chi(h) \neq 0$).

Under the assumptions of the theorem 2.1 below, for any h the coefficient $\chi(h)$ can alternatively be expressed; see [22], as the limit when $u \rightarrow 1^-$ of the function defined on $\mathbb{S} \times [0, 1]$ into $[0, 1]$, by

$$\chi(h, u) = 2 - \frac{\log \mathbb{P}(F(X(s)) < u, F(X(t)) < u)}{\log \mathbb{P}(F(X(s)) < u)}, \text{ for } h \in \mathbb{S}, u \in [0, 1[. \quad (2.2.5)$$

Such that, $\chi(h) = \lim_{u \rightarrow -1} \chi(h, u)$. More details and comments on the coefficient χ can be found in [10].

These notions are spatial versions of the dependence measures usually defined in multivariate contexts; see [23]. It is well known that a Gaussian pair with correlation $\rho \in (0, 1)$ is asymptotically independent. But the behaviour of the conditional probability with respect to u suggests that the asymptotic independence could not be detected as it appears for u very near to 1. Thus, it suggests that the function χ is more useful to study asymptotic dependence than asymptotic independence. This is why, in [22], the authors introduced an alternative dependence coefficient called **lower tail dependence coefficient** $\bar{\chi}$. This quantity measures the strength of asymptotic independence of a process.

Definition 2.9. For a stationary spatial process X on $\mathbb{S} \subset \mathbb{R}^2$ with margin F , the function $\bar{\chi}$ defined from \mathbb{S} into $] - 1, 1[$ and for any $(s, s + h) \in \mathbb{S}^2$

$$\bar{\chi}(h, u) = \frac{2 \log \mathbb{P}(F(X(s)) > u)}{\log \mathbb{P}(F(X(s)) > u, F(X(s+h)) > u)} - 1, \quad 0 \leq u \leq 1 \quad (2.2.6)$$

is the lower tail dependence coefficient, such that, $\bar{\chi}(h) = \lim_{u \rightarrow 1} \bar{\chi}(h, u)$.

If $\bar{\chi}(h) = 1$ for all h , the spatial process is asymptotically dependent. Otherwise, the process is said to be asymptotically independent. Furthermore, if $\bar{\chi} \in]0, 1[$ (resp. $] - 1, 0[$) the two locations s and $s + h$ (for any s) are asymptotically positively associated (resp. asymptotically negatively associated).

Coming back to the Gaussian example, for a Gaussian process, the function $\bar{\chi}$ equals the correlation function ρ ; then, it gives a quantitative measure of the strength of dependence even in the asymptotically independent case.

Another important measure of dependence was introduced by [18] in the case of bivariate random variable and extended by [63] to the spatial case in the following way.

Definition 2.10. Let X be a stationary spatial process on $\mathbb{S} \in \mathbb{R}^2$ with marginal distribution function F . We define the extremal coefficient between two locations s and $s + h$ for any $s \in \mathbb{S}$ and $s + h \in \mathbb{S}$, and for any $x \in \mathbb{R}$ by

$$\theta_F(h, x) = \frac{\log(P(X(s) < x, X(s+h) < x))}{\log(P(X(s) < x))}.$$

This parameter is related to the upper tail dependence parameter; indeed if $\lim_{x \rightarrow x_F} \theta_F(h, x) = \theta_F(h)$ exists, we have the following relation [10].

$$\chi(h) = 2 - \theta_F(h),$$

where $x_F = \sup\{x | F(x) < 1\}$. Then, $P(X(s) < x, X(s+h) < x)$ may be approximated by $F(x)^{\theta_F(h)}$ for x large.

This coefficient is of particular interest in the context of extremal distribution and spatial processes as we will see in the following section. It is also particularly useful when dealing with asymptotic dependence, but useless in case of asymptotic independence.

To overcome this problem, [47] proposed a model allowing to gather all the different cases of dependence depending on the value of a parameter in another words, smoothly linking asymptotic dependence and independence.

Let X be a stationary process with unit Fréchet margin; then, for all $(s, s + h) \in \mathbb{S}^2$

$$\mathbb{P}(X(s) > x, X(s + h) > x) = \mathcal{L}_h(x)x^{-1/\eta(h)}, \quad \text{as } x \rightarrow \infty \quad (2.2.7)$$

and

$$\mathbb{P}(X(s) > x | X(s + h) > x) = \mathcal{L}_h(x)x^{1-1/\eta(h)}, \quad \text{as } x \rightarrow \infty \quad (2.2.8)$$

where \mathcal{L}_h is a slowly varying function and $\eta(h) \in (0, 1]$ is the **tail dependence coefficient**. This coefficient determines the decay rate of the bivariate tail probability for large x . The interest of this simple modelisation, which appears to be quite general, is that the coefficient $\eta(h)$ provides a measure of the extremal dependence of $X(s)$ and $X(s + h)$. In fact, we can describe four dependence classes for X , satisfying the model above; see [10, 47] for more details:

- $\eta(h) = 1$ and $\mathcal{L}(x) \not\rightarrow 0$, corresponds to asymptotic dependence;
- $0 < \eta(h) < 1/2$ and $\mathcal{L}(x) \not\rightarrow 0$, corresponds to asymptotic negative association;
- $1/2 < \eta(h) < 1$ and $\mathcal{L}(x) \not\rightarrow 0$, corresponds to asymptotic positive association;
- $\eta(h) = 1/2$ and $\mathcal{L}(x) \geq 1$ (resp. $\mathcal{L}(x) \equiv 1$), corresponds to near independence case (resp. exact independence).

It is also important to notice that the last three cases correspond to asymptotic independence and the coefficient $\eta(h)$ measures the dependence in the asymptotic independence case.

Finally, it is important to see the relations between η and $\bar{\chi}$. If equation (2.2.7) is satisfied, then $\bar{\chi}(h) \rightarrow 2\eta(h) - 1$, (see proof of proposition 2.3 and [22]).

2.3 Extreme spatial processes

In this section, we present three different extreme spatial processes with different dependence structures. The first one (max-stable process) is either asymptotically

dependent or independent. The second one (inverse max-stable process) is asymptotically independent. The third one is a max-mixture process between the two above.

2.3.1 Max-stable model

First definitions

Max-stable processes are the extension of the multivariate extreme value theory to the infinite dimensional setting [16].

Definition 2.11. (*max-stable process*) A process X is **max-stable** if for all $n \in \mathbb{N}$ and X_1, \dots, X_n i.i.d. copies of X , there exist two continuous functions $(a_n(\cdot) > 0, n \in \mathbb{N})$ and $(b_n(\cdot) \in \mathbb{R}, n \in \mathbb{N})$ such that

$$\max_{i=1, \dots, n} \frac{X_i - b_n}{a_n} \stackrel{d}{=} X.$$

When for all $n \in \mathbb{N}$, $a_n = 1$ and $b_n = 0$, the margin distribution of the process X is unit Fréchet, that is for any $s \in \mathbb{S}$ and $x > 0$,

$$F(x) := P(X(s) \leq x) = \exp[-1/x].$$

In that case, the process is called a **simple max-stable process**.

The following result explains the importance of max-stable processes in the spatial extreme domain.

Theorem 2.1 ([29]). (*max-stable process*) Let $T := (T(s), s \in \mathbb{S})$ be a stochastic process. If there exist two sequences of continuous functions $(a_n(\cdot) > 0, n \in \mathbb{N})$ and $(b_n(\cdot) \in \mathbb{R}, n \in \mathbb{N})$ such that for all $n \in \mathbb{N}$ and n i.i.d. X_1, \dots, X_n and X a process, such that

$$\max_{i=1, \dots, n} \frac{X_i - b_n}{a_n} \xrightarrow{d} X, \quad n \rightarrow \infty, \quad (2.3.1)$$

then $X := \{X(s), s \in \mathbb{S}\}$ is a max-stable process.

[28] proved that a max-stable process X can be constructed by using a random process and a Poisson process. This representation is named the **spectral representation**. More precisely we have the following results

Theorem 2.2 ([28]). *spectral representation* Let X be a max-stable process on \mathbb{S} . Then there exists $\{\xi_i, i \geq 1\}$ i.i.d Poisson point process on $(0, \infty)$, with intensity $d\xi/\xi^2$ and a sequence $\{W_i, i \geq 1\}$ of i.i.d. copies of a positive process $W = (W(s), s \in \mathbb{S})$, such that $\mathbb{E}[W(s)] = 1$ for all $s \in \mathbb{S}$ such that

$$X \stackrel{d}{=} \max_{i \geq 1} \xi_i W_i. \quad (2.3.2)$$

This representation is in particular useful for the simulation of a max-stable process and provides examples of such processes by choosing special sequences $\{\xi_i, i \geq 1\}$ and $\{W_i, i \geq 1\}$. We may also deduce from its proof an explicit form for the k -dimensional multivariate distribution, which is

$$\mathbb{P}(X(s_1) \leq x_1, \dots, X(s_k) \leq x_k) = \exp \left\{ -\mathbb{E} \left[\max_{\ell=1, \dots, k} \left(\frac{W(s_\ell)}{x_\ell} \right) \right] \right\}. \quad (2.3.3)$$

Furthermore, using the result (2.3.1) and the multivariate extreme value theory, we already know that for all $k \in \mathbb{N}$ and $(x_1, \dots, x_k) \in \mathbb{R}^k$

$$\mathbb{P}(X(s_1) \leq x_1, \dots, X(s_k) \leq x_k) = \exp\{-V(x_1, \dots, x_k)\}, \quad (2.3.4)$$

where the function V is homogenous of order -1 and is named *the exponent measure*. Then, in the case of max-stable processes from (2.3.3) and (2.3.4), we have

$$V(x_1, \dots, x_k) = \mathbb{E} \left[\max_{\ell=1, \dots, k} \left(\frac{W(s_\ell)}{x_\ell} \right) \right]. \quad (2.3.5)$$

One of the interests of the exponent measure is its interpretation in terms of dependence. In fact, the homogeneity of the exponent measure V implies

$$\max\{1/x_1, \dots, 1/x_k\} \leq V(x_1, \dots, x_k) \leq \{1/x_1 + \dots + 1/x_k\}. \quad (2.3.6)$$

See [12], section 8.2.2. In the inequalities (2.3.6), the lower (resp. upper) bound corresponds to complete dependence (resp. independence). The relation (2.3.6) may also be used to obtain inequalities for the cumulative distribution function of the k -dimensional random vector $(X(s_1), \dots, X(s_k))$, say $G_d(x_1, \dots, x_d)$, that is

$$F(x_1) \dots F(x_k) \leq G_k(x_1, \dots, x_k) \leq \min\{F(x_1), \dots, F(x_k)\}, \quad \forall (x_1, \dots, x_k) \in \mathbb{R}^k, \quad (2.3.7)$$

where F is the unit Fréchet margin distribution function. Consequently, X satisfies the positively quadrant dependence (PQD); see [48].

Dependence structure

In this subsection, we present various relationships between the different dependence coefficients introduced above and max-stable processes. A convenient measure of dependence for max-stable processes is the **d-dimensional extremal coefficient function** Θ_d , [22, 63] which is completely characterized through the exponent measure V .

Definition 2.12. Let X be a simple max-stable process on \mathbb{S} . The d -dimensional extremal coefficient function is defined for all $(s_1, \dots, s_d) \in \mathbb{S}^d$, by

$$\Theta_d(s_1, \dots, s_d) = -x \log (\mathbb{P}(X(s_1) \leq x, \dots, X(s_d) \leq x)), x \in \mathbb{R}^+. \quad (2.3.8)$$

Rk. For simple max stable processes, the coefficients Θ and θ_F coincide. Equation (2.3.5) implies that Θ_d is well defined and does not depend on x :

$$\Theta_d(s_1, \dots, s_d) = \mathbb{E}[\max\{W(s_1), \dots, W(s_d)\}] = V(1_1, \dots, 1_d) \in [1, d]. \quad (2.3.9)$$

If $\Theta_d(s_1, \dots, s_d) = 1$, for any $(s_1, \dots, s_d) \in \mathbb{S}^d$, the process is completely dependent (its marginals are comonotonic). If $\Theta_d(s_1, \dots, s_d) = d$, for any $(s_1, \dots, s_d) \in \mathbb{S}^d$, the process is independent.

We are particularly interested in the spatial case, i.e. $d = 2$, the extremal coefficient function defined and studied in [62, 63].

Definition 2.13. Let X be a simple max-stable process on \mathbb{S} . The extremal coefficient function for any pairs of sites $(s, s+h) \in \mathbb{S}^2$ is the function Θ defined on \mathbb{S} (or in \mathbb{R}^+ in isotropic case) with values in $[1, 2]$ by

$$\mathbb{P}(X(s) \leq x, X(s+h) \leq x) = \exp\{-\Theta(h)/x\}, x > 0 \quad (2.3.10)$$

where,

$$\Theta(h) = \mathbb{E}[\max\{W(s), W(s+h)\}] = V(1, 1) \in [1, 2]. \quad (2.3.11)$$

If for any $h \in \mathbb{S}$, $\Theta(h) = 1$ (resp. $\Theta(h) = 2$), then we have complete dependence (resp. complete independence). The case $1 < \Theta(h) < 2$, for all $h \in \mathbb{S}$ corresponds to asymptotic dependence.

Furthermore, it is easy to see the relationship between Θ and χ ; see [73] for any $h \in \mathbb{S}$

$$\Theta(h) = 2 - \chi(h). \quad (2.3.12)$$

Another classical tool often used in geostatistics is the variogram. But for max-stable processes, the quantity of dependence strength will not exist in variogram, because the marginal laws are Fréchet, and thus, have no order 2 moments. We shall use the **F-madogram** introduced in [24].

Definition 2.14. Let X be a spatial process on \mathbb{S} with univariate margin F . The F -madogram of the process X is for all $(s, t) \in \mathbb{S}^2$

$$\nu^F(s-t) = \frac{1}{2} \mathbb{E}|F(X(s)) - F(X(t))|. \quad (2.3.13)$$

In the max-stable case, [24] gives the relation for all $h \in \mathbb{S}$,

$$\Theta(h) = \frac{1 + 2\nu^F(h)}{1 - 2\nu^F(h)}, \quad (2.3.14)$$

which appears to be helpful to estimate the extremal coefficient Θ .

Examples of some max-stable models

In this section, we provide some examples of well-known max-stable models. We will use the spectral representation (see Theorem 2.2) with different sequences (ξ_i) and (W_i) .

1. Smith Model (Gaussian extreme value model)

[66] introduced the so-called *Gaussian extreme value* model. It is defined in $\mathbb{S} = \mathbb{R}^d$. Its dependence structure is contained in a covariance matrix Σ . Let $\{(\xi_i, s_i)\}$ be a Poisson point process on $(0, \infty) \times \mathbb{R}^d$ with intensity $\xi^{-2}d\xi ds$ and consider the d -dimensional Gaussian probability density function $\varphi_d(\cdot; \Sigma)$ with mean 0 and covariance matrix Σ . For all $s \in \mathbb{R}^d$, define $W_i(s) = \varphi_d(s - s_i; \Sigma)$ and

$$X(s) = \max_{i \geq 1} \{\xi_i \varphi_d(s - s_i; \Sigma)\}. \quad (2.3.15)$$

Then, X is a max-stable process on $\mathbb{S} = \mathbb{R}^d$ with unit Fréchet margin. The pairwise distribution function is given by the following equation, for all $(s, s+h) \in \mathbb{S}^2$,

$$\mathbb{P}(X(s) \leq x_1, X(s+h) \leq x_2) = \exp\{-V_h(x_1, x_2)\}, \quad (2.3.16)$$

where

$$V_h(x_1, x_2) = \frac{1}{x_1} \Phi\left(\frac{\tau(h)}{2} + \frac{1}{\tau(h)} \log \frac{x_2}{x_1}\right) + \frac{1}{x_2} \Phi\left(\frac{\tau(h)}{2} + \frac{1}{\tau(h)} \log \frac{x_1}{x_2}\right); \quad (2.3.17)$$

$\tau(h) = \sqrt{h^T \Sigma^{-1} h}$ and $\Phi(\cdot)$ the standard normal cumulative distribution function.

The pairwise extremal coefficient equals

$$\Theta(h) = 2\Phi\left(\frac{\tau(h)}{2}\right). \quad (2.3.18)$$

Equation (2.3.12) gives

- for $h = 0$, we have $\chi(0) = 1$, which corresponds to complete dependence;
- for $h > 0$, $\chi(h) \in (0, 1)$, which corresponds to asymptotic dependence.
- $\lim_{h \rightarrow \infty} \chi(h) = 0$, which means that the asymptotic dependence vanishes at infinite distances.

Note that if the covariance matrix is diagonal $\Sigma = \sigma \mathbf{I}_d$, the process X is isotropic, as its bivariate distribution depends only on h through the function $\tau(h) = \sqrt{\frac{1}{\sigma} \|h\|^2}$.

2. Schlather Models (Extremal Gaussian Model)

This model introduced by [61] provides a class based on stationary random field with finite expectation. Let $W := \{W(s), s \in \mathbb{S}\}$ be a stationary random field, with $\mathbb{E}[W^+(s)] = \mu \in (0, \infty)$, where $W^+(s) = \max\{0, W(s)\}$. Let $\{\xi_i, i \geq 1\}$ be a Poisson point process on $(0, \infty)$, with intensity $d\xi/\xi^2$ and $\{W_i, i \geq 1\}$ as iid copies of $W(s)$. Consider

$$X(s) = \mu^{-1} \max_{i \geq 1} \xi_i W_i^+(s), \quad s \in \mathbb{S}; \quad (2.3.19)$$

it defines a stationary max-stable process. Schlather proposed such a model with a stationary Gaussian process $W(s)$ with correlation function $\rho(\cdot)$ and $\mu^{-1} = \sqrt{2\pi}$. In this case, the resulting max-stable process X is called *Extremal Gaussian process (EG)*. The pairwise distribution function is

$$\mathbb{P}(X(s) \leq x_1, X(t) \leq x_2) = \exp\{-V_h(x_1, x_2)\} \quad (2.3.20)$$

where

$$V_h(x_1, x_2) = \frac{1}{2} \left(\frac{1}{x_1} + \frac{1}{x_2} \right) \left[1 + \sqrt{1 - 2(\rho(h) + 1) \frac{x_1 x_2}{(x_1 + x_2)^2}} \right]. \quad (2.3.21)$$

The extremal coefficient is given by

$$\Theta(h) = 1 + \left(\frac{1 - \rho(h)}{2} \right)^{1/2}. \quad (2.3.22)$$

We have $\Theta(h)$ is in the interval $[1, 1.838]$ with boundary values corresponding to $\rho(h) = 1$ and $\rho(h) = 0$ respectively. Thus, $\lim_{h \rightarrow \infty} \chi(h) \neq 0$. In other words, the asymptotic dependence persists even at infinite distances. This might be unrealistic in applications. To overcome this problem a truncated version of $W(s)$ can be used. Let $\{r_i\}$ be a homogenous Poisson point process of unit

rate on \mathbb{S} and $\mu^{-1} = \sqrt{2\pi}(\mathbb{E}[|\mathcal{B}|])^{-1}$. Then, for a stationary Gaussian process $W_i(s)$, define

$$X(s) = \max_{i \geq 1} \xi_i W_i(s) \mathbf{1}_{\mathcal{B}_i}(s - r_i), \quad s \in \mathbb{S} \quad (2.3.23)$$

with $\mathcal{B} \subset \mathbb{S}$ a compact random set and \mathcal{B}_i i.i.d. copies of \mathcal{B} . The process X is a *truncated extremal Gaussian process (TEG)*. The pairwise distribution functions are given by

$$\mathbb{P}(X(s) \leq x_1, X(t) \leq x_2) = \exp\{-V_h(x_1, x_2)\} \quad (2.3.24)$$

where

$$V_h(x_1, x_2) = \left(\frac{1}{x_1} + \frac{1}{x_2} \right) \left[1 - \frac{\alpha(h)}{2} \left(1 - \sqrt{1 - 2(\rho(h) + 1) \frac{x_1 x_2}{(x_1 + x_2)^2}} \right) \right]. \quad (2.3.25)$$

The extremal coefficient is given by

$$\Theta(h) = 2 - \alpha(h) \left\{ 1 - \left(\frac{1 - \rho(h)}{2} \right)^{1/2} \right\} \quad (2.3.26)$$

where $\alpha(h) = \mathbb{E}\{|\mathcal{B} \cap (h + \mathcal{B})|\} / \mathbb{E}[|\mathcal{B}|]$,

where \mathcal{B} is a random set. When modeling a spatial phenomena, the choice of the set \mathcal{B} is to be delicate. For the sake of simplicity, we may consider \mathcal{B} as a simple form, for example, a disk with fixed radius r . Such that, the area of the intersection of \mathcal{B} and $h + \mathcal{B}$ is

$$|\mathcal{B} \cap (h + \mathcal{B})| = \left[2r^2 (\cos^{-1}(\|h\|/2r) - (\|h\|/2r) \sqrt{1 - \|h\|^2/2r^2}) \right] \mathbf{1}_{[0, 2r]}(\|h\|) \quad (2.3.27)$$

and we can approximate it by $\pi r^2 [1 - \|h\|/2r]_+$. This choice leads to $\alpha(h) = \{1 - h/2r\}_+$. In such a case, $\chi(h) = 0, \forall h \geq 2r$. In other words, the process X is independent for all $h \geq 2r$. For more details, see section 2(e) in [26].

3. Brown-Resnik Model

[41] introduced a generalization of the Brown-Resnik model, which was proposed by [15]. Let $W_i(s) = \exp\{e_i(s) - \gamma(s)\}$, where $e_i(s)$ is a stationary Gaussian process, with mean zero and variogram $\gamma(s)$, and let $\{\xi_i, i \geq 1\}$ be a Poisson point process on $(0, \infty)$; then,

$$X(s) = \max_{i \geq 1} \xi_i (e_i(s) - \gamma(s)), \quad s \in \mathbb{S} \quad (2.3.28)$$

is a max-stable process called *Brown-Rensik model*, which is sometimes called the Geometric Gaussian model. The pairwise distribution function is then

$$\mathbb{P}(X(s) \leq x_1, X(t) \leq x_2) = \exp\{-V(x_1, x_2; h)\}, \quad (2.3.29)$$

where

$$V(x_1, x_2; h) = \frac{1}{x_1} \Phi\left(\frac{\sqrt{2\gamma(h)}}{2} + \frac{1}{\sqrt{2\gamma(h)}} \log \frac{x_2}{x_1}\right) + \frac{1}{x_2} \Phi\left(\frac{\sqrt{2\gamma(h)}}{2} + \frac{1}{\sqrt{2\gamma(h)}} \log \frac{x_1}{x_2}\right). \quad (2.3.30)$$

The pairwise extremal coefficient given by

$$\Theta(h) = 2\Phi\left(\frac{\sqrt{2\gamma(h)}}{2}\right). \quad (2.3.31)$$

2.3.2 Inverse Max-stable processes

If we choose a threshold too low, we may miss the dependence structure. In other words, in theoretical study, the limiting distribution of extremes tends to be independent but in practice, this limit could never be achieved (see [27, 67]). [73] proposed a class of asymptotically independent processes obtained by inverting max-stable processes. These processes are called **inverse max-stable processes**; they satisfy the survivor function (2.2.7).

Definition 2.15. Let $X' := \{X'(s), s \in \mathbb{S}\}$ be a max-stable process with unit Fréchet margin, such that for all $s \in \mathbb{S} \subset \mathbb{R}^2$

$$X'(s) = \mu^{-1} \max_{i \geq 1} W_i^+(s) / \xi_i, \quad s \in \mathbb{S} \quad (2.3.32)$$

where ξ_i is a Poisson point process on $(0, \infty)$ with intensity $d\xi$ and $W_i(s)$ are i.i.d. copies of a continuous process W independent of $\{\xi_i\}$. Let $g : (0, \infty) \mapsto (0, \infty)$ be defined by $g(x) = -1/\log\{1 - e^{-1/x}\}$. Set $X(s) = g(X'(s))$,

Then, $X := \{X(s), s \in \mathbb{S}\}$ is an asymptotic independent spatial process with unit Fréchet margin. The d -dimensional joint survivor function is

$$\mathbb{P}(X(s_1) > x_1, \dots, X(s_d) > x_d) = \exp\{-V(g(x_1), \dots, g(x_d))\} \quad (2.3.33)$$

where V is the exponent measure of the process X' defined in equation (2.3.5). Moreover, X satisfies the positive quadrant dependence property. The tail dependent coefficient is given by $\eta(h) = 1/\Theta(h)$, where $\Theta(h)$ is the extremal coefficient of the max-stable process X' . Moreover, we have $\tilde{\chi}(h) = 2/\Theta(h) - 1$.

Another class of asymptotically independent processes may be constructed from a Gaussian process (see [47]). Let $X' := \{X'(s), s \in \mathbb{S}\}$ be a stationary and standard Gaussian process with correlation function ρ . Let $X = -1/\log(\Phi(X'))$; it defines an asymptotically independent spatial process with unit Fréchet margin and satisfies the equation (2.2.7). Its survivor function satisfies

$$\mathbb{P}(Y(s_1) > z, Y(s_2) > z) \sim \mathcal{C}_h z^{-2/(1+\rho(h))} (\log z)^{-\rho(h)/(1+\rho(h))} \quad (2.3.34)$$

with

$$\mathcal{C}_h = (1 + \rho(h))^{3/2} (1 - \rho(h))^{-1/2} (4\pi)^{-\rho(h)/(1+\rho(h))} \quad (2.3.35)$$

The tail dependence coefficient is given by $\eta(h) = (1 + \rho(h))/2$. Moreover, we have $\tilde{\chi}(h) = \rho(h)$.

2.3.3 Max-mixture model

In spatial contexts, specifically in an environmental domain, many scenarios of dependence could arise and AD and AI might cohabite. The work by [73] provides a flexible model called max-mixture.

Definition 2.16. (*Max-Mixture model*) Let $X := \{X(s), s \in \mathbb{S}\}$ be a max-stable process with extremal coefficient $\Theta(h)$ and bivariate distribution function F_X , and let $Y := \{Y(s), s \in \mathbb{S}\}$ be an asymptotically independent spatial process whose coefficient tail dependence $\eta(h)$ is well defined, has the bivariate distribution function F_Y and satisfies the asymptotic relation (2.2.7). Assume that X and Y are independent, and that each of them has Fréchet margin. Let $a \in [0, 1]$ and

$$Z(s) = \max\{aX(s), (1-a)Y(s)\}, \quad s \in \mathbb{S}, \quad (2.3.36)$$

then Z is a max-mixture process has unit Fréchet marginals and bivariate distribution function

$$F_Z(z_1, z_2) = e^{-aV_X(z_1, z_2)} F_Y\left(\frac{z_1}{1-a}, \frac{z_2}{1-a}\right). \quad (2.3.37)$$

Proposition 2.3 ([9, 73]). Let Z be a max-mixture process. Through the definition 2.16, the pairwise survivor function of Z satisfies

$$\mathbb{P}(Z(s) > z, Z(t) > z) \sim \frac{a\{2 - \Theta(h)\}}{z} + \frac{(1-a)^{1/\eta(h)}}{z^{1/\eta(h)}} + O(z^{-2}), \quad z \rightarrow \infty. \quad (2.3.38)$$

Assume there exists finite $h^* = \inf\{h : \Theta(h) \neq 0\}$; then,

$$\chi(h) = a(2 - \Theta(h)) \quad (2.3.39)$$

and

$$\bar{\chi}(h) = \mathbb{1}_{[h^* < h]}(h) + (2\eta(h) - 1)\mathbb{1}_{[h^* \geq h]}. \quad (2.3.40)$$

Rk. If there exists finite $h^* = \inf\{h : \Theta(h) \neq 0\}$, then Z is asymptotically dependent up to distance h^* and asymptotically independent for larger distances. Only asymptotic dependence or asymptotical independence in Z is achieved by the bounds $a = 0$ and $a = 1$, respectively.

Proof. From definition 2.16, we have

$$\begin{aligned} \mathbb{P}(Z(s) > z, Z(t) > z) = \\ 1 - 2e^{-\frac{1}{z}} + e^{-\frac{a\Theta(h)}{z}} \left[2e^{-\frac{(1-a)}{z}} - 1 + \mathcal{L}_h\left(\frac{z}{1-a}\right) \left(\frac{z}{1-a}\right)^{-1/\eta(h)} \right]. \end{aligned}$$

By the Taylor series and limiting behavior

$$\begin{aligned} \mathbb{P}(Z(s) > z, Z(t) > z) \sim \\ \frac{a\{2 - \Theta(h)\}}{z} + O(z^{-2}) + \left(1 - \frac{a\Theta(h)}{z} + O(z^{-2})\right) \mathcal{L}_h\left(\frac{z}{1-a}\right) \left(\frac{z}{1-a}\right)^{-1/\eta(h)}, \text{ as } z \rightarrow \infty \\ \sim \frac{a\{2 - \Theta(h)\}}{z} + O(z^{-2}) + \mathcal{L}_h\left(\frac{z}{1-a}\right) \left(\frac{z}{1-a}\right)^{-1/\eta(h)} - \frac{a\Theta(h)}{z} \mathcal{L}_h\left(\frac{z}{1-a}\right) \left(\frac{z}{1-a}\right)^{-1/\eta(h)} \\ + \mathcal{L}_h\left(\frac{z}{1-a}\right) O(z^{-2-\frac{1}{\eta(h)}}). \end{aligned}$$

In PQD property, we have $1/2 \leq \eta \leq 1$, then $O(z^{-2}) > O(z^{-2-\frac{1}{\eta(h)}})$, and therefore

$$\mathbb{P}(Z(s) > z, Z(t) > z) \sim \frac{a\{2 - \Theta(h)\}}{z} + \mathcal{L}_h\left(\frac{z}{1-a}\right) \frac{(1-a)^{1/\eta(h)}}{z^{1/\eta(h)}} + O(z^{-2}) \text{ as } z \rightarrow \infty.$$

From assuming the asymptotically independence of z , we have $\mathcal{L}_h\left(\frac{z}{1-a}\right) \rightarrow 1$ as $z \rightarrow \infty$. Then, 2.3.38 is satisfied.

From the definition of upper tail dependence coefficient in 2.2.5, we have

$$\begin{aligned} \chi(h, z) = 2 - a\Theta(h) + z \log \left[2e^{-\frac{(1-a)}{z}} - 1 + \mathcal{L}_h\left(\frac{z}{1-a}\right) \left(\frac{z}{1-a}\right)^{-1/\eta(h)} \right] \\ \sim 2 - a\Theta(h) + z \log \left[1 - \frac{2(1-a)}{z} + \mathcal{L}_h\left(\frac{z}{1-a}\right) \left(\frac{z}{1-a}\right)^{-1/\eta(h)} + O(z^{-2}) \right] \end{aligned}$$

Let $V = \frac{2(1-a)}{z} - \mathcal{L}_h\left(\frac{z}{1-a}\right) \left(\frac{z}{1-a}\right)^{-1/\eta(h)} - O(z^{-2})$. Then,

$$\begin{aligned} \chi(h, z) \sim 2 - a\Theta(h) + z \log(1 - V) \\ \sim a\{2 - \Theta(h)\} + \mathcal{L}_h\left(\frac{z}{1-a}\right) (1-a)^{-1/\eta(h)} z^{1-1/\eta(h)} + O(z^{-1}) + zO(V^2). \end{aligned}$$

We have $O(z^{-1}) = O(V^2)$ forming the limits of η . Then,

$$\chi(h) = \lim_{z \rightarrow \infty} \chi(h, z) = a(2 - \theta(h)), \quad \forall h \neq 0$$

which satisfies 2.3.12 for asymptotic dependence case ($a = 1$).

From the definition 2.9 of the lower tail dependence coefficient, we have

$$\begin{aligned} \bar{\chi}(h, z) &= \frac{2 \log \mathbb{P}(Z(s) > z)}{\log \mathbb{P}(X(s) > \frac{z}{a}, X(t) > \frac{z}{a}) + \log \mathbb{P}(Y(s) > \frac{z}{1-a}, Y(t) > \frac{z}{1-a})} - 1 \\ &= \frac{2 \log(1 - \exp(\frac{-1}{z}))}{\log(1 - 2 \exp(\frac{-a}{z}) + \exp(\frac{-a\Theta(h)}{z})) + \log(\mathcal{L}_h(\frac{z}{1-a})(\frac{z}{1-a})^{-1/\eta(h)})} - 1 \\ &\sim \frac{2 \log(\frac{1}{z} + O(z^{-2}))}{\log(\frac{a(2-\Theta(h))}{z} + O(z^{-2})) + \log(\mathcal{L}_h(\frac{z}{1-a})(\frac{z}{1-a})^{-1/\eta(h)})} - 1. \end{aligned}$$

If $(2 - \Theta(h)) \neq 0$, then

$$\begin{aligned} \bar{\chi}(h, z) &\sim \frac{-2 \log(z) + O(\log(z))}{\log(a(2 - \Theta(h))) - \log(z) + \log(\mathcal{L}_h(\frac{z}{1-a})) - \frac{1}{\eta(h)}(\log(z) - \log(1-a)) + O(\log(z))} - 1 \\ &\sim \frac{-2 + o(1)}{\frac{\log(a(2-\Theta(h)))}{\log(z)} + \frac{\log(\mathcal{L}_h(\frac{z}{1-a}))}{\log(z)} - \frac{1}{\eta(h)}(1 - \frac{\log(1-a)}{\log(z)}) - 1 + o(1)} - 1. \end{aligned}$$

Therefore,

$$\bar{\chi}(h) = \lim_{z \rightarrow \infty} \bar{\chi}(h, z) = \frac{-2}{-\frac{1}{\eta(h)} - 1} - 1 = 1. \quad (2.3.41)$$

If $(2 - \Theta(h)) = 0$, then

$$\begin{aligned} \bar{\chi}(h, z) &\sim \frac{-2 \log(z) + O(\log(z))}{\log(\mathcal{L}_h(\frac{z}{1-a})) - \frac{1}{\eta(h)}(\log(z) - \log(1-a)) + O(\log(z))} - 1 \\ &\sim \frac{-2 + o(1)}{\frac{\log(\mathcal{L}_h(\frac{z}{1-a}))}{\log(z)} - \frac{1}{\eta(h)}(1 - \frac{\log(1-a)}{\log(z)}) + o(1)} - 1. \end{aligned}$$

Therefore,

$$\bar{\chi}(h) = \lim_{z \rightarrow \infty} \bar{\chi}(h, z) = \frac{-2}{-\frac{1}{\eta(h)}} - 1 = 2\eta(h) - 1. \quad (2.3.42)$$

leads to satisfy the lower tail coefficient in 2.3.40 and satisfies 2.3.42 when $a = 0$. \square

[9] used this kind of models to allow asymptotical dependence and independence to be present at a short and intermediate distance respectively; furthermore, the process is independent at a long distance. This structure has been made by combining the truncated Gaussian extremal max-stable process with an asymptotically independent process. The estimation of the model parameters has been done by using maximum composite likelihood and using CLIC (composite likelihood information criterion) to select the model.

2.4 Spatial risk measure

Considering a process X , we will define a risk measure associated to X on a region $\mathcal{A} \subset \mathbb{R}^2$ of the space. It will be a non-negative quantity, which represents an average damage or cost due to X on \mathcal{A} . We follow the ideas developed in [44] or [43].

2.4.1 Normalized loss function

A damage function \mathcal{D} represents the relationship between the aggregate losses (e.g economic, health) and the environmental (climate) indicator (e.g air pollution, temperature levels), some economic interpretations may be found in [14].

Definition 2.17. (Normalized loss function) Consider a damage function $\mathcal{D} : \mathbb{R}^d \rightarrow \mathbb{R}^+$. For any set $\mathcal{A} \in \mathcal{B}(\mathbb{R}^d)$, the normalized aggregate loss function on \mathcal{A} is

$$L(\mathcal{A}, \mathcal{D}) = \frac{1}{|\mathcal{A}|} \int_{\mathcal{A}} \mathcal{D}(s) \, ds, \quad (2.4.1)$$

where $|\mathcal{A}|$ stands for the volume (or the Lebesgue measure) of \mathcal{A} .

The quantity $\int_{\mathcal{A}} \mathcal{D}(s) ds$ represents the aggregated loss over the region \mathcal{A} . Therefore, the function $L(\mathcal{A}, \mathcal{D})$ is the proportion of loss on \mathcal{A} . In our context, \mathcal{D} will be a function of the process X , denoted \mathcal{D}_X .

We will focus on two damage functions. The first one is the excess damage function: let $u > 0$ be the fixed threshold for $s \in \mathbb{S}$,

$$\mathcal{D}_{X,u}^+(s) = (X(s) - u)^+. \quad (2.4.2)$$

For example, when considering air pollutants (like in [11]), u is a regulatory level which is determined by experts. This damage function will be used on Gaussian processes.

The second damage function corresponds to a power of the spatial process X . For a fixed power coefficient $0 < \nu < 1/2$ and for any $s \in \mathbb{S}$, we define a damage function

$$\mathcal{D}_X^\nu(s) = |X(s)|^\nu. \quad (2.4.3)$$

This damage function will be used on processes with Fréchet marginals; this is why we have to take $0 < \nu < 1/2$ which guarantes that $L(\mathcal{A}, \mathcal{D}_X^\nu)$ has an order 2 moment. It has an economic interpretation when X is the wind speed: damages due to the wind are generally proportional to some power of the wind speed (see [58]).

2.4.2 Spatial risk measure definition

As already mentioned, in spatial contexts, spatial dependency is an important characteristic. Considering the risk measure as the expectation of a normalized loss will not take into account the spatial dependency; however, it is useful to quantify the magnitude of risk. We shall consider the spatial risk measure composed from two components: expectation and variance of the normalized loss,

$$\begin{aligned} \mathcal{R}(\mathcal{A}, \mathcal{D}_X) &= \{\mathbb{E}[L(\mathcal{A}, \mathcal{D}_X)], \text{Var}(L(\mathcal{A}, \mathcal{D}_X))\}, \\ &=: \{\mathcal{R}_0(\mathcal{A}, \mathcal{D}_X), \mathcal{R}_1(\mathcal{A}, \mathcal{D}_X)\} \end{aligned} \quad (2.4.4)$$

For stationary processes, the expectation component provide information on the severity of the phenomenon, while the variance component is impacted by the dependence structure.

Let us remark that

$$\mathcal{R}_1(\mathcal{A}, \mathcal{D}_X) = \frac{1}{|\mathcal{A}|^2} \int_{\mathcal{A} \times \mathcal{A}} \text{Cov}(\mathcal{D}_X(s), \mathcal{D}_X(t)) ds dt. \quad (2.4.5)$$

We shall focus on the properties of $\mathcal{R}_1(\mathcal{A}, \mathcal{D}_X)$.

2.5 Axiomatic properties of spatial risk measures

In [6],[45],[68] and others, axioms and the behavior of univariate risk measures are presented, while [44] provides an axiomatic setting of risk measures in a spatial context.

In this section, we will present a set of spatial axiomatic properties describing the behavior of a real valued spatial risk measure $\mathcal{R}^*(\mathcal{A}, \mathcal{D})$. Axioms 1 and 4 below have been introduced in [44] and studied for some max-stable processes.

Definition 2.18. *Let $\mathcal{A} \subset \mathbb{R}^2$ be a region of the space.*

1. **Spatial invariance under translation**

Let $\mathcal{A} + v \subset \mathbb{R}^2$ be the region \mathcal{A} translated by a vector $v \in \mathbb{R}^2$. Then for $v \in \mathbb{R}^2$, $\mathcal{R}^*(\mathcal{A} + v, \mathcal{D}) = \mathcal{R}^*(\mathcal{A}, \mathcal{D})$.

2. **Spatial anti-monotonicity**

Let \mathcal{A}_1 and $\mathcal{A}_2 \subset \mathbb{R}^2$ be two regions such that $|\mathcal{A}_1| \leq |\mathcal{A}_2|$; then $\mathcal{R}^*(\mathcal{A}_2, \mathcal{D}) \leq \mathcal{R}^*(\mathcal{A}_1, \mathcal{D})$.

3. **Spatial sub-additivity**

Let \mathcal{A}_1 and $\mathcal{A}_2 \subset \mathbb{R}^2$ be two disjointed regions, then $\mathcal{R}^*(\mathcal{A}_1 \cup \mathcal{A}_2, \mathcal{D}) \leq \mathcal{R}^*(\mathcal{A}_1, \mathcal{D}) + \mathcal{R}^*(\mathcal{A}_2, \mathcal{D})$.

4. **Spatial super sub-additivity**

Let \mathcal{A}_1 and $\mathcal{A}_2 \subset \mathbb{R}^2$ be two disjointed regions, then $\mathcal{R}^*(\mathcal{A}_1 \cup \mathcal{A}_2, \mathcal{D}) \leq \min_{i=1,2} [\mathcal{R}^*(\mathcal{A}_i, \mathcal{D})]$.

5. **Spatial homogeneity**

Let $\lambda > 0$ and $\mathcal{A} \subset \mathbb{R}^2$ then, $\mathcal{R}^*(\lambda\mathcal{A}, \mathcal{D}) = \lambda^k \mathcal{R}^*(\mathcal{A}, \mathcal{D})$, that is \mathcal{R}^* is homogeneous of order k , where $\lambda\mathcal{A}$ is the set $\{\lambda x, x \in \mathcal{A}\}$.

In [44], the following damage functions are considered for some max-stable processes: $\mathcal{D}_X(s) = \mathbf{1}_{\{X(s) > u\}}$, $\mathcal{D}_X(s) = X(s)^\beta$. The author proves the invariance by translation; in this context, he also proves the monotonicity and super sub-additivity in the case where $\mathcal{A}_1, \mathcal{A}_2$ are either disks or squares.

Theorem 2.4. *Let X be a stationary process and \mathcal{D}_X be a positive damage function of X . The risk measure $\mathcal{R}_1(\cdot, \mathcal{D}_X)$ is invariant by translation and sub-additive.*

Proof. The invariance by translation follows directly from the stationarity. On one other hand, consider \mathcal{A}_1 and $\mathcal{A}_2 \subset \mathbb{R}^2$ as two disjointed regions.

$$\begin{aligned}
\mathcal{R}_1(\mathcal{A}_1 \cup \mathcal{A}_2, \mathcal{D}_X) &= \text{Var}(L(\mathcal{A}_1 \cup \mathcal{A}_2, \mathcal{D}_X)) \\
&= \frac{1}{(|\mathcal{A}_1| + |\mathcal{A}_2|)^2} \left[|\mathcal{A}_1|^2 \mathcal{R}_1(\mathcal{A}_1, \mathcal{D}_X) + |\mathcal{A}_2|^2 \mathcal{R}_1(\mathcal{A}_2, \mathcal{D}_X) \right. \\
&\quad \left. + 2\text{Cov} \left(\int_{\mathcal{A}_1} \mathcal{D}_X(s) ds, \int_{\mathcal{A}_2} \mathcal{D}_X(s) ds \right) \right] \\
&\leq \frac{1}{(|\mathcal{A}_1| + |\mathcal{A}_2|)^2} \left[|\mathcal{A}_1|^2 \mathcal{R}_1(\mathcal{A}_1, \mathcal{D}_X) + |\mathcal{A}_2|^2 \mathcal{R}_1(\mathcal{A}_2, \mathcal{D}_X) \right. \\
&\quad \left. + 2|\mathcal{A}_1||\mathcal{A}_2| \sqrt{\mathcal{R}_1(\mathcal{A}_1, \mathcal{D}_X)} \sqrt{\mathcal{R}_1(\mathcal{A}_2, \mathcal{D}_X)} \right] \\
&\quad \text{by using the Cauchy-Schwarz inequality,} \\
&\leq \mathcal{R}_1(\mathcal{A}_1, \mathcal{D}_X) + \mathcal{R}_1(\mathcal{A}_2, \mathcal{D}_X).
\end{aligned}$$

Thus, we have proved sub-additivity. □

The calculations of the next chapter will lead to prove the anti-monotonicity for squares or disks of $\mathcal{R}_1(\mathcal{A}, \mathcal{D}_{X,u}^+)$ for isotropic Gaussian processes. The same result will be given for $\mathcal{R}_1(\mathcal{A}, \mathcal{D}_X^u)$ with X as a max-stable or a max-mixture process, which develops the results in [44].

Chapter 3

Calculating $\mathcal{R}(\mathcal{A}, \mathcal{D})$ on some spatial processes

In this chapter, we aim at providing simple expressions for $\mathcal{R}(\mathcal{A}, \mathcal{D}_{X,u}^+)$, where X is a Gaussian process and $\mathcal{R}(\mathcal{A}, \mathcal{D}_X^\nu)$, for some max-stable or max-mixture processes X . We consider a max-stable case that has not been treated in [44]. We shall see that $\mathcal{R}_1(\mathcal{A}, \mathcal{D}_{X,u}^+)$ and $\mathcal{R}_1(\mathcal{A}, \mathcal{D}_X^\nu)$ may reduce to a one-dimensional integration and can thus be efficiently computed. We shall also study anti-monotonicity and (asymptotic) homogeneity properties.

3.1 Risk measure for spatial Gaussian process

In this section, we consider $X := \{X(s), s \in \mathbb{S}\}$ as a stationary Gaussian process with auto-correlation function ρ and for a fixed threshold $u > 0$, the risk measure $\mathcal{R}(\mathcal{A}, \mathcal{D}_{X,u}^+)$ associated to the damage function $\mathcal{D}_{X,u}^+ = (X - u)^+$.

In what follows, φ is the density of the univariate standard Gaussian distribution, $\bar{\Phi}$ is the survival function of the standard Gaussian distribution, and $\ell(u, v, w)$ is the total probability of a truncated bivariate standard Gaussian distribution with correlation w , that is

$$\ell(u, v, w) = \frac{1}{2\pi(1-w^2)^{1/2}} \int_u^\infty \int_v^\infty e^{\left\{\frac{-1}{2(1-w^2)}[x^2 - 2wxy + y^2]\right\}} dx dy. \quad (3.1.1)$$

In this section, we first provide explicit forms for the risk measure; following this, we will study the behavior of $\mathcal{R}_1(\lambda\mathcal{A}, \mathcal{D}_{X,u}^+)$ with respect to λ .

3.1.1 Explicit forms of $\mathcal{R}(\mathcal{A}, \mathcal{D}_{X,u}^+)$

We are interested in the explicit calculation of the expectation and variance of $L(\mathcal{A}, \mathcal{D}_{X,u}^+)$ with

$$L(\mathcal{A}, \mathcal{D}_{X,u}^+) = \frac{1}{|\mathcal{A}|} \int_{\mathcal{A}} (X(s) - u)^+ ds.$$

Proposition 3.1. *Consider $X := \{X(s), s \in \mathbb{S}\}$ as an isotropic standard Gaussian process with auto-correlation function ρ . Let $u \in \mathbb{R}_+$ be a fixed threshold. We will then have the following:*

$$\mathcal{R}_0(\mathcal{A}, \mathcal{D}_{X,u}^+) = \varphi(u) - u\bar{\Phi}(u), \quad (3.1.2)$$

and

$$\mathcal{R}_1(\mathcal{A}, \mathcal{D}_{X,u}^+) = \frac{1}{|\mathcal{A}|^2} \int_{\mathcal{A} \times \mathcal{A}} \mathcal{G}(\tau_{s,t}, u) \, ds dt, \quad (3.1.3)$$

with $\tau_{s,t} = \|s - t\|$ and for any $h, s \in \mathbb{S}$

$$\begin{aligned} \mathcal{G}(h, u) &:= \text{Cov}(\mathcal{D}_{X,u}^+(s), \mathcal{D}_{X,u}^+(s+h)); \\ \mathcal{G}(h, u) &= (\rho(h) + u^2)\ell(u, u, \rho(h)) - 2u\varphi(u)\bar{\Phi}\left(\frac{u(1-\rho(h))}{(1-\rho^2(h))^{1/2}}\right) \\ &\quad + (1-\rho^2(h))^{1/2}\varphi\left(\frac{u}{(1+\rho(h))^{1/2}}\right)^2 - (\varphi(u) - u\bar{\Phi}(u))^2. \end{aligned} \quad (3.1.4)$$

Proof. Let X be an isotropic standard Gaussian process and $u \in \mathbb{R}_+$,

$$\begin{aligned} \mathbb{E}[L(\mathcal{A}, \mathcal{D}_{X,u}^+)] &= \frac{1}{|\mathcal{A}|} \int_{\mathcal{A}} \mathbb{E}[(X(s) - u)^+] ds \\ &= \frac{1}{|\mathcal{A}|} \int_{\mathcal{A}} \left[\int_u^\infty x\varphi(x) dx - u \int_u^\infty \varphi(x) dx \right] ds \\ &= \frac{1}{|\mathcal{A}|} \int_{\mathcal{A}} (\varphi(u) - u\bar{\Phi}(u)) ds \\ &= \varphi(u) - u\bar{\Phi}(u). \end{aligned} \quad (3.1.5)$$

On the other hand,

$$\text{Var}(L(\mathcal{A}, \mathcal{D}_{X,u}^+)) = \frac{1}{|\mathcal{A}|^2} \int_{\mathcal{A} \times \mathcal{A}} \text{Cov}(\mathcal{D}_{X,u}^+(s), \mathcal{D}_{X,u}^+(t)) ds dt.$$

We calculate $\text{Cov}(\mathcal{D}_{X,u}^+(s), \mathcal{D}_{X,u}^+(t))$ by using the results from [60] on moments m_{10}, m_{11} of truncated bivariate Gaussian distributions. See Appendix A.1. Let f_{X_1, X_2} be the

density function of the random vector (X_1, X_2) .

$$\begin{aligned}\mathbb{E}[\mathcal{D}_{X,u}^+(s)\mathcal{D}_{X,u}^+(t)] &= \int_u^\infty \int_u^\infty (xy - 2ux + u^2)f_{X(s),X(t)}(x,y) dx dy \\ &= \ell(u, u, \rho(\tau_{s,t}))m_{11} - 2u\ell(u, u, \rho(\tau_{s,t}))m_{10} + u^2\ell(u, u, \rho(\tau_{s,t})),\end{aligned}\tag{3.1.6}$$

with

$$\begin{aligned}\ell(u, v, \rho)m_{10} &= \frac{1}{2\pi(1-\rho^2)^{1/2}} \int_u^\infty \int_v^\infty x \exp\left\{-\frac{1}{2(1-\rho^2)}[x^2 + 2\rho xy + y^2]\right\} dx dy, \\ &= \varphi(u)\bar{\Phi}\left(\frac{v-\rho u}{(1-\rho^2)^{1/2}}\right) + \rho\varphi(v)\bar{\Phi}\left(\frac{u-\rho v}{(1-\rho^2)^{1/2}}\right);\end{aligned}$$

and

$$\begin{aligned}\ell(u, v, \rho)m_{11} &= \frac{1}{2\pi(1-\rho^2)^{1/2}} \int_u^\infty \int_v^\infty xy \exp\left\{-\frac{1}{2(1-\rho^2)}[x^2 + 2\rho xy + y^2]\right\} dx dy, \\ &= \rho\ell(u, v, \rho) + \rho u\varphi(u)\bar{\Phi}\left(\frac{v-\rho u}{(1-\rho^2)^{1/2}}\right) + \rho v\varphi(v)\bar{\Phi}\left(\frac{u-\rho v}{(1-\rho^2)^{1/2}}\right) \\ &\quad + \frac{(1-\rho^2)^{1/2}}{\sqrt{2\pi}}\varphi\left(\frac{(u^2 - 2\rho uv + v^2)^{1/2}}{(1-\rho^2)^{1/2}}\right).\end{aligned}$$

For $v = u$, we have,

$$\ell(u, u, \rho)m_{10} = (1 + \rho)\varphi(u)\bar{\Phi}\left(\frac{u(1-\rho)}{(1-\rho^2)^{1/2}}\right)$$

and

$$\ell(u, u, \rho)m_{11} = \rho\ell(u, u, \rho) + 2\rho u\varphi(u)\bar{\Phi}\left(\frac{u(1-\rho)}{(1-\rho^2)^{1/2}}\right) + \frac{(1-\rho^2)^{1/2}}{\sqrt{2\pi}}\varphi\left(\frac{(2u^2(1-\rho))^{1/2}}{(1-\rho^2)^{1/2}}\right).$$

Finally, we get

$$\begin{aligned}
\mathbb{E}[\mathcal{D}_{X,u}^+(s)\mathcal{D}_{X,u}^+(t)] &= \frac{(1 - \rho^2(\tau_{s,t}))^{1/2}}{\sqrt{2\pi}} \varphi\left(\frac{(2u^2(1 - \rho(\tau_{s,t})))^{1/2}}{(1 - \rho^2(\tau_{s,t}))^{1/2}}\right) \\
&\quad + 2u\rho(\tau_{s,t})\varphi(u)\bar{\Phi}\left(\frac{u(1 - \rho(\tau_{s,t}))}{(1 - \rho^2(\tau_{s,t}))^{1/2}}\right) \\
&\quad + \rho(\tau_{s,t})\ell(u, u, \rho(\tau_{s,t})) - 2u(1 + \rho(\tau_{s,t}))\varphi(u)\bar{\Phi}\left(\frac{u(1 - \rho(\tau_{s,t}))}{(1 - \rho^2(\tau_{s,t}))^{1/2}}\right) \\
&\quad + u^2\ell(u, u, \rho(\tau_{s,t})) \\
&= \ell(u, u, \rho(\tau_{s,t}))(\rho(\tau_{s,t}) + u^2) - 2u\varphi(u)\bar{\Phi}\left(\frac{u(1 - \rho(\tau_{s,t}))}{(1 - \rho^2(\tau_{s,t}))^{1/2}}\right) \\
&\quad + (1 - \rho^2(\tau_{s,t}))^{1/2} \varphi\left(\frac{u}{(1 + \rho(\tau_{s,t}))^{1/2}}\right)^2.
\end{aligned}$$

The result follows. \square

Corollary 3.2. *Let $Y := \{Y(s), s \in \mathbb{S}\}$ be an isotropic Gaussian process with mean μ and variance σ^2 . Let $X = \frac{Y - \mu}{\sigma}$ be an isotropic and standard Gaussian process. The spatial risk measure $\mathcal{R}(\mathcal{A}, \mathcal{D}_{Y,u}^+)$ satisfies*

$$\mathcal{R}(\mathcal{A}, \mathcal{D}_{Y,u}^+) = \left\{ \sigma \mathbb{E}[L(\mathcal{A}, \mathcal{D}_{X,u_0}^+)], \sigma^2 \text{Var}(L(\mathcal{A}, \mathcal{D}_{X,u_0}^+)) \right\}, \quad (3.1.7)$$

with $u_0 = (u - \mu)/\sigma$.

Proof. From the definition of $\mathcal{D}_{Y,u}^+$, we have:

$$\begin{aligned}
\mathbb{E}[L(\mathcal{A}, \mathcal{D}_{Y,u}^+)] &= \frac{1}{|\mathcal{A}|} \int_{\mathcal{A}} \mathbb{E}(Y(s) - u)^+ ds \\
&= \frac{1}{|\mathcal{A}|} \int_{\mathcal{A}} \mathbb{E}(\mu + \sigma X(s) - u)^+ ds \\
&= \frac{\sigma}{|\mathcal{A}|} \int_{\mathcal{A}} \mathbb{E}(X(s) - (\frac{u - \mu}{\sigma}))^+ ds \\
&= \sigma \mathbb{E}[L(\mathcal{A}, \mathcal{D}_{X,u_0}^+)].
\end{aligned} \quad (3.1.8)$$

On the other hand,

$$\begin{aligned}
\text{Var}(L(\mathcal{A}, \mathcal{D}_{Y,u}^+)) &= \frac{1}{|\mathcal{A}|^2} \int_{\mathcal{A} \times \mathcal{A}} \mathbb{E}[\mathcal{D}_{Y,u}^+(s)\mathcal{D}_{Y,u}^+(t)] - \mathbb{E}[\mathcal{D}_{Y,u}^+(s)]\mathbb{E}[\mathcal{D}_{Y,u}^+(t)] \, dsdt \\
&= \frac{1}{|\mathcal{A}|^2} \int_{\mathcal{A} \times \mathcal{A}} \mathbb{E}[(Y(s) - u)^+(Y(t) - u)^+] - \mathbb{E}[(Y(s) - u)^+]\mathbb{E}[(Y(t) - u)^+] \, dsdt \\
&= \frac{1}{|\mathcal{A}|^2} \int_{\mathcal{A} \times \mathcal{A}} \sigma^2 \mathbb{E}[(X(s) - u_0)^+(X(t) - u_0)^+] - \sigma^2 \mathbb{E}[(X(s) - u_0)^+]\mathbb{E}[(X(t) - u_0)^+] \, dsdt \\
&= \frac{\sigma^2}{|\mathcal{A}|^2} \int_{\mathcal{A} \times \mathcal{A}} \mathbb{E}[\mathcal{D}_{X_s, u_0}^+(s)\mathcal{D}_{X_t, u_0}^+(s)] - \mathbb{E}[\mathcal{D}_{X_s, u_0}^+(s)]\mathbb{E}[\mathcal{D}_{X_t, u_0}^+(s)] \, ds \, dt
\end{aligned}$$

Therefore,

$$\text{Var}(L(\mathcal{A}, \mathcal{D}_{Y,u}^+)) = \sigma^2 \text{Var}(L(\mathcal{A}, \mathcal{D}_{X, u_0}^+)). \quad (3.1.9)$$

□

Corollary 3.2 implies that without loss generality, we may calculate the risk measure for an isotropic standard Gaussian process; expressions for an isotropic non-standard Gaussian process will follow. Furthermore, from these results, we can see that $\mathcal{R}_0(\mathcal{A}, \mathcal{D}_{Y,u}^+)$ does not depend on the region \mathcal{A} but only on the characteristics of the underlying Gaussian process. Then, in the following study of the risk measure, we will focus on the component $\mathcal{R}_1(\mathcal{A}, \mathcal{D}_{Y,u}^+)$.

The following theorem is useful to compute the risk measure because it reduces to a one-dimension integration.

Theorem 3.3. *Let $X := \{X(s), s \in \mathbb{S}\}$ be an isotropic standard Gaussian process. If the region \mathcal{A} is either a disk or a square, the expression $\text{Var}(L(\mathcal{A}, \mathcal{D}_{X,u}^+))$ reduces to a one dimensional integration.*

When \mathcal{A} is a disk of radius R ,

$$\text{Var}(L(\mathcal{A}, \mathcal{D}_{X,u}^+)) = \int_{h=0}^{2R} \mathcal{G}(h, u) f_{disk}(h, R) dh, \quad (3.1.10)$$

where

$$f_{disk}(h, R) = \frac{2h}{R^2} \left(\frac{2}{\pi} \arccos\left(\frac{h}{2R}\right) - \frac{h}{\pi R} \sqrt{1 - \frac{h^2}{4R^2}} \right), \quad (3.1.11)$$

and \mathcal{G} is defined in equation (3.1.4).

When \mathcal{A} is a square of side R

$$\text{Var}(L(\mathcal{A}, \mathcal{D}_{X,u}^+)) = \int_{h=0}^{\sqrt{2}R} \mathcal{G}(h, u) f_{\text{square}}(h, R) dh, \quad (3.1.12)$$

where, for $h \in [0, R]$

$$f_{\text{square}}(h, R) = \frac{2\pi h}{R^2} - \frac{8h^2}{R^3} + \frac{2h^3}{R^4}$$

and for $h \in [R, \sqrt{2}R]$,

$$f_{\text{square}}(h, R) = \frac{2h}{R^2} \left[-2 - b + 3\sqrt{b-1} + \frac{b+1}{\sqrt{b-1}} + 2\arcsin\left(\frac{2-b}{b}\right) - \frac{4}{b\sqrt{1 - \frac{(2-b)^2}{b^2}}} \right], \quad (3.1.13)$$

where $b = \frac{h^2}{R^2}$.

Proof. The strategy of proof is the one adopted in [44] for some max-stable processes. Let S and T be two independent random variables uniformly distributed on \mathcal{A} . For any function γ defined on \mathbb{R}^+ , we have

$$\mathbb{E}[\gamma(\|S - T\|)] = \frac{1}{|\mathcal{A}|^2} \int_{\mathcal{A} \times \mathcal{A}} \gamma(\|s - t\|) ds dt.$$

Using [52], if \mathcal{A} is a square of side R ,

$$\mathbb{E}[\gamma(\|S - T\|)] = \int_{h=0}^{\sqrt{2}R} \gamma(h) f_{\text{square}}(h, R) dh, \quad (3.1.14)$$

with f_{square} given by equation (3.1.13). If \mathcal{A} is a disk of radius R then,

$$\mathbb{E}[\gamma(\|S - T\|)] = \int_{h=0}^{2R} \gamma(h) f_{\text{disk}}(h, R) dh. \quad (3.1.15)$$

Moreover, by (3.1.3)

$$\text{Var}(L(\mathcal{A}, \mathcal{D}_{X,u}^+)) = \mathbb{E}[\mathcal{G}(\|S - T\|, u)].$$

Using (3.1.14) and (3.1.15) with the function $\gamma(h) = \mathcal{G}(h, u)$; we obtain the expressions (3.2.1) and (3.2.2). \square

In what follows, we write our results for square regions \mathcal{A} , but the results hold for disks as well.

3.1.2 Behaviour of $\mathcal{R}_1(\lambda\mathcal{A}, \mathcal{D}_{X,u}^+)$ with respect to λ

The following expression of $\mathcal{R}_1(\lambda\mathcal{A}, \mathcal{D}_{X,u}^+)$ is a keystone to understand its behavior.

Lemma 3.4. *Let $\lambda \geq 0$ and \mathcal{A} be a square of side R ; then,*

$$\mathcal{R}_1(\lambda\mathcal{A}, \mathcal{D}_{X,u}^+) = \int_{h=0}^{\sqrt{2}R} f_{\text{square}}(h, R) \mathcal{G}(\lambda h, u) dh. \quad (3.1.16)$$

Proof. Theorem 3.3 gives:

$$\begin{aligned} \mathcal{R}_1(\lambda\mathcal{A}, \mathcal{D}_{X,u}^+) = \text{Var}(L(\lambda\mathcal{A}, \mathcal{D}_{X,u}^+)) &= \int_{h=0}^{\sqrt{2}\lambda R} f_{\text{square}}(h, \lambda R) \mathcal{G}(h, u) dh. \\ &= \int_{h=0}^{\sqrt{2}R} f_{\text{square}}(\lambda h, \lambda R) \mathcal{G}(\lambda h, u) \lambda dh. \end{aligned}$$

Remark that $f_{\text{square}}(\lambda h, \lambda R) = \lambda^{-1} f_{\text{square}}(h, R)$. Thus,

$$\mathcal{R}_1(\lambda\mathcal{A}, \mathcal{D}_{X,u}^+) = \int_{h=0}^{\sqrt{2}R} f_{\text{square}}(h, R) \mathcal{G}(\lambda h, u) dh.$$

The same calculations would give the same result if \mathcal{A} is a disk of radius R (by replacing f_{square} by f_{disk}). \square

Lemma 3.4 provides the following two results on the behavior of the mapping $\lambda \mapsto \mathcal{R}_1(\lambda\mathcal{A}, \mathcal{D}_{X,u}^+)$.

Corollary 3.5. *Let X be an isotropic standard Gaussian process on $\mathbb{S} \subset \mathbb{R}^2$ with the auto-correlation function ρ . Let $\mathcal{A} \subset \mathbb{S}$ be either a disk or a square. The mapping $\lambda \mapsto \mathcal{R}_1(\lambda\mathcal{A}, \mathcal{D}_{X,u}^+)$ is non-increasing if and only if $h \mapsto \rho(h)$, $h > 0$ is non-increasing and non-negative.*

Proof. It suffices to remark that by its definition, for any $h > 0$, the function $\lambda \mapsto \mathcal{G}(\lambda h, u)$ is non-increasing, provided the auto-correlation function is non-negative and non-increasing. For compactness, see Appendix A.2. \square

Corollary 3.6. *Let $X := \{X(s), s \in \mathbb{S}\}$ be an isotropic standard Gaussian process with auto-correlation function satisfying the following criterion: decreases to 0 as h goes to infinity. Then, for \mathcal{A} , either a disk or a square, we have*

$$\lim_{\lambda \rightarrow \infty} \mathcal{R}_1(\lambda\mathcal{A}, \mathcal{D}_{X,u}^+) = 0. \quad (3.1.17)$$

Proof. Let \mathcal{A} be a square of side R ,

$$\mathcal{R}_1(\lambda\mathcal{A}, \mathcal{D}_{X,u}^+) = \int_{h=0}^{\sqrt{2}R} f_{\text{square}}(h, R) \mathcal{G}(\lambda h, u) dh, \quad (3.1.18)$$

Then, the monotonic convergence theorem gives:

$$\lim_{\lambda \rightarrow \infty} \mathcal{R}_1(\lambda\mathcal{A}, \mathcal{D}_{X,u}^+) = \int_{h=0}^{\sqrt{2}R} f_{\text{square}}(h, R) \lim_{\lambda \rightarrow \infty} \mathcal{G}(\lambda h, u) dh. \quad (3.1.19)$$

Since $\rho(h)$ goes to 0 as h goes to infinity,

$$\lim_{\lambda \rightarrow \infty} \mathcal{G}(\lambda h, u) = u^2 \ell(u, u, 0) - u^2 \bar{\Phi}^2(u).$$

The result follows. \square

Thus, Lemma 3.4 proves the anti-monotonicity for regions $\mathcal{A}_1, \mathcal{A}_2$ which are either disks or squares.

Property 3.7. *Let $X := \{X(s), s \in \mathbb{S}\}$ be an isotropic standard Gaussian process with non-negative and non-increasing auto-correlation function; let $\mathcal{A}_1, \mathcal{A}_2$ be either squares or disks, such that $|\mathcal{A}_1| \leq |\mathcal{A}_2|$, then*

$$\mathcal{R}_1(\lambda\mathcal{A}_2, \mathcal{D}_{X,u}^+) \leq \mathcal{R}_1(\lambda\mathcal{A}_1, \mathcal{D}_{X,u}^+).$$

Proof. Let us do the proof in the square case. By invariance by translation, we may assume $\mathcal{A}_1 = \lambda\mathcal{A}_2$ for some $\lambda \leq 1$. Equation (3.1.16) gives the result. \square

A simulation study and a real data case will be provided in Chapter 4 for $\mathcal{R}(\lambda\mathcal{A}_2, \mathcal{D}_{X,u}^+)$.

3.2 Risk measures for max-mixture processes

Let X be an isotropic and stationary process, with unit Fréchet margin and let the power coefficient $0 < \nu < 1/2$ be a fixed. For a given damage function \mathcal{D}_X^ν , the interest risk measure in this section is $\mathcal{R}(\mathcal{A}, \mathcal{D}_X^\nu)$

3.2.1 General forms for $\mathcal{R}_1(\mathcal{A}, \mathcal{D}_X^\nu)$

By theorem 3.3, we may reduce $\mathcal{R}_1(\mathcal{A}, \mathcal{D}_X^\nu)$ to smaller dimension integral.

Lemma 3.8. *Let $X := \{X(s), s \in \mathbb{S}\}$ be an isotropic and stationary spatial process. Let $\mathcal{Q}(h) = \text{Cov}(\mathcal{D}_X^\nu(s), \mathcal{D}_X^\nu(s+h))$.*

Consider $\mathcal{A} \subset \mathbb{R}^2$ to be a disk of radius R , for a fixed $0 < \nu < 1/2$, we have:

$$\mathcal{R}_1(\mathcal{A}, \mathcal{D}_X^\nu) = \text{Var}(L(\mathcal{A}, \mathcal{D}_X^\nu)) = \int_{h=0}^{2R} \mathcal{Q}(h) f_{\text{disk}}(h, R) dh, \quad (3.2.1)$$

Consider $\mathcal{A} \subset \mathbb{R}^2$ to be a square of side R , we have:

$$\mathcal{R}_1(\mathcal{A}, \mathcal{D}_X^\nu) = \text{Var}(L(\mathcal{A}, \mathcal{D}_X^\nu)) = \int_{h=0}^{\sqrt{2}R} \mathcal{Q}(h) f_{\text{square}}(h, R) dh, \quad (3.2.2)$$

In what follows, results are written for square regions \mathcal{A} , but the results hold for disks as well.

Remark 2. *Properties of moments of Fréchet distributions give that if X as unit Fréchet marginal distributions,*

$$\mathbb{E}(L(\mathcal{A}, \mathcal{D}_X^\nu)) = \Gamma(1 - \nu).$$

Proposition 3.9. *Consider $X := \{X(s), s \in \mathbb{S}\}$ as an isotropic and stationary spatial process with unit Fréchet margin F and pairwise distribution function $G_h^X = \mathbb{P}(X(s) \leq x_1, X(s+h) \leq x_2)$. Let \mathcal{A} be a square of side R . We have*

$$\mathcal{R}_1(\mathcal{A}, \mathcal{D}_X^\nu) = \int_{h=0}^{\sqrt{2}R} \mathcal{Q}(h, \nu) f_{\text{square}}(h, R) dh, \quad (3.2.3)$$

with

$$\begin{aligned} \mathcal{Q}(h, \nu) &= \text{Cov}(\mathcal{D}_X^\nu(s), \mathcal{D}_X^\nu(s+h)); \\ \mathcal{Q}(h, \nu) &= \int_0^\infty \int_0^\infty [G_h^X(x_1^{1/\nu}, x_2^{1/\nu}) - F(x_1^{1/\nu})F(x_2^{1/\nu})] dx_1 dx_2 \end{aligned} \quad (3.2.4)$$

or equivalently

$$\mathcal{Q}(h, \nu) = \nu^2 \int_0^\infty \int_0^\infty x_1^{\nu-1} x_2^{\nu-1} [G_h^X(x_1, x_2) - F(x_1)F(x_2)] dx_1 dx_2. \quad (3.2.5)$$

Proof. Since X is a non-negative process, Hoeffding's identity ([39] and [64]) gives:

$$\begin{aligned}
& \text{Cov}(\mathcal{D}_X^\nu(s), \mathcal{D}_X^\nu(s+h)) \\
&= \iint_{\mathbb{R}_+^2} [\mathbb{P}(X(s)^\nu \leq x_1, X(s+h)^\nu \leq x_2) \\
&\quad - \mathbb{P}(X(s)^\nu \leq x_1)\mathbb{P}(X(s+h)^\nu \leq x_2)] dx_1 dx_2 \\
&= \nu^2 \iint_{\mathbb{R}_+^2} x_1^{\nu-1} x_2^{\nu-1} [\mathbb{P}(X(s) \leq x_1, X(s+h) \leq x_2) \\
&\quad - \mathbb{P}(X(s) \leq x_1)\mathbb{P}(X(s+h) \leq x_2)] dx_1 dx_2.
\end{aligned} \tag{3.2.6}$$

□

3.2.2 Explicit form of $\mathcal{R}_1(\mathcal{A}, \mathcal{D}_X^\nu)$ for TEG max-stable process

Equation (3.2.3) shows that the computation of $\mathcal{R}_1(\mathcal{A}, \mathcal{D}_X^\nu)$ reduces to the integration of $\mathcal{Q}(h, \nu)f_{square}$ (resp. $\mathcal{Q}(h, \nu)f_{disk}$). In [43], the computation of $\mathcal{Q}(h, \nu)f_{square}$ for the Smith model has been done. In that case, the computation of $\mathcal{R}_1(\mathcal{A}, \mathcal{D}_X^\nu)$ is thus reduced to a one-dimensional integration. In this section, we do the computation for a TEG model.

Corollary 3.10. *Let $X := \{X(s), s \in \mathbb{S}\}$ be a truncated extremal Gaussian TEG max-stable process with unit Fréchet margin, correlation function ρ and truncated parameter r . For $0 < \nu < 1/2$, we have*

$$\begin{aligned}
& \mathcal{Q}(h, \nu) = \\
& \int_0^{+\infty} w^\nu \left[\Gamma(2(1-\nu))\mathcal{T}_2(w, h)\mathcal{T}_1(w, h)^{2(\nu-1)} + \Gamma(1-2\nu)\mathcal{T}_3(w, h)\mathcal{T}_1(w, h)^{2\nu-1} \right] dw \\
& \quad - [\Gamma(1-\nu)]^2
\end{aligned} \tag{3.2.7}$$

where,

$$\mathcal{T}_1(w, h) = \frac{w+1}{w} \left[1 - \frac{\alpha(h)}{2} (1 - \mathcal{K}(w, h)) \right]; \tag{3.2.8}$$

$$\begin{aligned}
\mathcal{T}_2(w, h) &= \left[1 - \frac{\alpha(h)}{2} (1 - \mathcal{K}(w, h)) - \frac{\alpha(h)(\rho(h)+1)(1-w)}{2\mathcal{K}(w, h)(w+1)^2} \right] \\
&\quad \times \left[\frac{1}{w^2} - \frac{\alpha(h)}{2w^2} (1 - \mathcal{K}(w, h)) - \frac{\alpha(h)(\rho(h)+1)(w-1)}{2w\mathcal{K}(w, h)(w+1)^2} \right];
\end{aligned} \tag{3.2.9}$$

$$\mathcal{T}_3(w, h) = \alpha(h) \left[\frac{(\rho(h) + 1)}{\mathcal{K}(w, h)(w + 1)^3} - \frac{(\rho(h) + 1)^2(w - 1)^2}{2\mathcal{K}(w, h)^3(w + 1)^5} \right]; \quad (3.2.10)$$

$$\mathcal{K}(w, h) = \left[1 - \frac{2w(\rho(h) + 1)}{(w + 1)^2} \right]^{1/2} \quad (3.2.11)$$

and $\alpha(h)$ defined in (2.3.27).

Proof. We have,

$$\text{Cov}(\mathcal{D}_X^\nu(s), \mathcal{D}_X^\nu(s + h)) = \mathbb{E}[\mathcal{D}_X^\nu(s)\mathcal{D}_X^\nu(s + h)] - [\mathbb{E}[\mathcal{D}_X^\nu(s)]]^2.$$

From remark 2. we have $\mathbb{E}[\mathcal{D}_X^\nu(s)] = \Gamma(1 - \nu)$, and we also have

$$\mathbb{E}[\mathcal{D}_X^\nu(s)\mathcal{D}_X^\nu(s + h)] = \int_0^\infty \int_0^\infty x_1^\nu x_2^\nu f_{(X(s), X(s+h))}(x_1, x_2) dx_1 dx_2,$$

where $f_{(X(s), X(s+h))}(x_1, x_2)$ is the bivariate density function of the TEG model.

It rewrites:

$$\mathbb{E}[\mathcal{D}^\nu(s)\mathcal{D}^\nu(s + h)] = \int_0^{+\infty} \int_0^{+\infty} u^{2\nu+1} w^\nu f(u, uw) du dw.$$

The bivariate density function of a TEG model satisfies

$$f_{(X(s), X(s+h))}(u, uw) = \left[\frac{1}{u^4} \mathcal{T}_2(w, h) + \frac{1}{u^3} \mathcal{T}_3(w, h) \right] e^{-\frac{1}{u} \mathcal{T}_1(w, h)}$$

where $\mathcal{T}_1(w, h)$, $\mathcal{T}_2(w, h)$ and $\mathcal{T}_3(w, h)$ are introduced in (3.2.8), (3.2.9), and (3.2.10). Therefore,

$$\begin{aligned} \mathbb{E}[\mathcal{D}^\nu(s)\mathcal{D}^\nu(s + h)] = \\ \int_0^{+\infty} w^\nu \left[\mathcal{T}_2(w, h) \int_0^{+\infty} u^{2\nu-3} e^{-\frac{1}{u} \mathcal{T}_1(w, h)} du + \mathcal{T}_3(w, h) \int_0^{+\infty} u^{2\nu-2} e^{-\frac{1}{u} \mathcal{T}_1(w, h)} du \right] dw. \end{aligned}$$

Moment Properties of Fréchet distributions give

$$\int_0^{+\infty} u^{2\nu-3} e^{-\frac{1}{u} \mathcal{T}_1(w, h)} du = \frac{1}{\mathcal{T}_1(w, h)} \cdot \mu_{(2\nu-1)},$$

with $\mu_{(2\nu-1)}$, the moment of order $k = (2\nu - 1)$. That is,

$$\mu_{(2\nu-1)} = \mathcal{T}_1(w, h)^{(2\nu-1)} \Gamma[2(\nu - 1)].$$

In the same way, we get

$$\int_0^{+\infty} u^{2\nu-2} e^{\frac{-1}{u}} \mathcal{T}_1(w, h) du = \mathcal{T}_1(w, h)^{(2\nu-1)} \Gamma(1-2\nu).$$

Then,

$$\mathbb{E}[\mathcal{D}_X^\nu(s) \mathcal{D}_X^\nu(s+h)] = \int_0^{+\infty} w^\nu \left[\mathcal{T}_2(w, h) \mathcal{T}_1(w, h)^{2(\nu-1)} \Gamma(2\nu-1) + \mathcal{T}_3(w, h) \mathcal{T}_1(w, h)^{(2\nu-1)} \Gamma(1-2\nu) \right] dw,$$

and the result follows. \square

3.2.3 Behavior of $\mathcal{R}_1(\lambda\mathcal{A}, \mathcal{D}_Z^\nu)$ with respect to λ for max-mixture processes.

In what follows, we consider an isotropic and stationary max-mixture spatial process with unit Fréchet margin F . We denote X and V_h^X the process and the exponent measure function corresponding to the max-stable part and Y and V_h^Y the process and the exponent measure function corresponding to the inverse max-stable process Y . Let $a \in [0, 1]$, $Z = \max(aX, (1-a)Y)$. We shall study the behavior of $\mathcal{R}_1(\lambda\mathcal{A}, \mathcal{D}_Z^\nu)$ with respect to λ . Of course, the case $a = 1$ gives results for max-stable processes and $a = 0$ gives results for inverse max-stable processes. Recall that the bivariate distribution function is given by

$$G_h^Z(x_1, x_2) = e^{-aV_h^X(x_1, x_2)} \left[e^{\frac{-(1-a)}{x_1}} + e^{\frac{-(1-a)}{x_2}} - 1 + e^{-V_h^Y(g_a(x_1), g_a(x_2))} \right],$$

where $g(z) = -\frac{1}{\log(1-e^{-\frac{1}{z}})}$ and $g_a(z) = g(\frac{z}{1-a})$.

Lemma 3.8 and Proposition 3.9 are a keystone to describe the behaviour of $\mathcal{R}_1(\lambda\mathcal{A}, \mathcal{D}_Z^\nu)$. As in Lemma 3.4, we get for any $\lambda > 0$:

$$\mathcal{R}_1(\lambda\mathcal{A}, \mathcal{D}_Z^\nu) = \int_{h=0}^{\sqrt{2}R} f_{square}(h, R) \mathcal{Q}(\lambda h, \nu) dh. \quad (3.2.12)$$

Corollary 3.11. *Let Z be an isotropic and stationary max-mixture spatial process as above. Assume that the mappings $h \mapsto V_h^X(x_1, x_2)$ and $V_h^Y(x_1, x_2)$ are non-decreasing for any $(x_1, x_2) \in \mathbb{R}_+^2$. Let $\mathcal{A} \subset \mathbb{S}$ be either a disk or a square; then, the mapping $\lambda \mapsto \mathcal{R}_1(\lambda\mathcal{A}, \mathcal{D}_Z^\nu)$ is non-increasing.*

Proof. We use (3.2.12) and from Proposition 3.9,

$$\mathcal{Q}(\lambda h, \nu) = \nu^2 \int_0^\infty \int_0^\infty x_1^{\nu-1} x_2^{\nu-1} [G_h^Z(x_1, x_2) - F(x_1)F(x_2)] dx_1 dx_2.$$

Since $h \mapsto V_h^X(x_1, x_2)$ and $V_h^Y(x_1, x_2)$ are non-decreasing, $h \mapsto G_h^Z(x_1, x_2)$ is non-increasing and the result follows. \square

Remark 3. For a spatial max-stable or inverse max-stable process X , the fact that $h \mapsto V_h^X(x_1, x_2)$ is non-decreasing implies that the dependence between $X(t)$ and $X(t+h)$ decreases as h increases, which seems reasonable in applications. On the other hand, if, $V_h^X(x_1, x_2)$ goes to $\frac{1}{x_1} + \frac{1}{x_2}$ as h goes to infinity, $X(t)$, $X(t+h)$ tend to behave independently as h goes to infinity.

Corollary 3.12. Let Z be an isotropic and stationary max-mixture spatial process as above. Assume that the mappings $h \mapsto V_h^X(x_1, x_2)$ and $V_h^Y(x_1, x_2)$ are non-decreasing for any $(x_1, x_2) \in \mathbb{R}_+^2$. Moreover, we assume that

$$V_h^X(x_1; x_2) \longrightarrow \frac{1}{x_1} + \frac{1}{x_2} \quad \text{as } h \rightarrow \infty$$

and

$$V_{hh}^Y(x_1, x_2) \longrightarrow \frac{1}{x_1} + \frac{1}{x_2} \quad \text{as } h \rightarrow \infty$$

$\forall x_1, x_2 \in \mathbb{R}_+$. Let $\mathcal{A} \subset \mathbb{S}$ be either a disk or a square ,

$$\lim_{\lambda \rightarrow \infty} \mathcal{R}_1(\lambda \mathcal{A}, \mathcal{D}_Z^\nu) = 0.$$

If there exists V_0 (resp. V_1), an exponent measure function of a non independent max-stable (resp. inverse max-stable) bivariate random vector, such that $V_h^X \longrightarrow V_0$ and $V_h^Y \longrightarrow V_1$ as $h \rightarrow \infty$, then

$$\lim_{\lambda \rightarrow \infty} \mathcal{R}_1(\lambda \mathcal{A}, \mathcal{D}_Z^\nu) > 0.$$

Proof. In the case of A a square of side R , we use

$$\mathcal{Q}(\lambda h, \nu) = \nu^2 \int_0^\infty \int_0^\infty x_1^{\nu-1} x_2^{\nu-1} [G_h^Z(x_1, x_2) - F(x_1)F(x_2)] dx_1 dx_2.$$

If $V_h^W(x_1; x_2)$ is non-decreasing to $\frac{1}{x_1} + \frac{1}{x_2}$ as $h \rightarrow \infty$ for $W = X$ and $W = Y$, then $G_h^Z(x_1, x_2)$ is non-increasing to $F(x_1)F(x_2)$ and we derive a conclusion by using the monotone convergence theorem. \square

Corollary 3.13. *Let Z be isotropic and stationary max-mixture as above. Assume that $h \mapsto V_h^W(x_1, x_2)$ is non-increasing, with $W = X$ and $W = Y$. Let \mathcal{A}_1 and \mathcal{A}_2 be either disks or squares, such that $|\mathcal{A}_1| \leq |\mathcal{A}_2|$; then,*

$$\mathcal{R}_1(\lambda\mathcal{A}_2, \mathcal{D}_Z^\nu) \leq \mathcal{R}_1(\lambda\mathcal{A}_1, \mathcal{D}_Z^\nu).$$

Proof. Since the risk measure $\mathcal{R}_1(\mathcal{A}, \mathcal{D}_Z^\nu)$ is invariant by translation, we may assume that $\mathcal{A}_1 = \lambda\mathcal{A}_2$ for some $\lambda \geq 1$. Then, equation (3.2.12) gives the result. \square

Chapter 4

Computational aspects of the risk measures

In this Chapter, we study the behavior of the proposed spatial risk measures $\mathcal{R}(\mathcal{A}, \mathcal{D}_X)$, through some simulations.

4.1 Computational aspects for Gaussian risk measure

4.1.1 Analysis of $\mathcal{G}(h, u)$ and $\mathcal{R}_1(\lambda\mathcal{A}, \mathcal{D}_{X,u}^+)$

We begin this simulation section with the study of the covariance damage function \mathcal{G} which plays a central role in the behavior of $\mathcal{R}(\mathcal{A}, \mathcal{D}_{X,u}^+)$. We consider five Gaussian models depending on the choice of the correlation structure introduced in Section 2.2.1.

In order to emphasize the dependence of the damage covariance function \mathcal{G} to the correlation parameter, we will denote it by $\mathcal{G}_\theta(h, u)$ for any triplet (h, u, θ) .

Figure 4.1.(a) shows the behavior of the spatial covariance between two damage functions $\mathcal{D}_{X,u}^+(\cdot)$ and $\mathcal{D}_{X,u}^+(\cdot+h)$ with respect to the distance h , when the correlation range is set to $\theta = 0.50$ and the threshold to $u = \Phi^{-1}(0.75)$, where Φ^{-1} is the quantile function of the standard normal distribution. It shows that $\mathcal{G}_\theta(h, u)$ tends to 0 as h tends to infinity with different decreasing speed. This is obviously the expected behavior, because the process $(\mathcal{D}_{X,u}^+(s), s \in \mathbb{S})$ is (spatially) asymptotically independent. Whereas, for spherical and cubic correlation functions, $\mathcal{G}_\theta(h, u) = 0$ as soon as $h > \theta$, which means that the process $(\mathcal{D}_{X,u}^+(s), s \in \mathbb{S})$ is θ -independent (independent at a distance larger than θ).

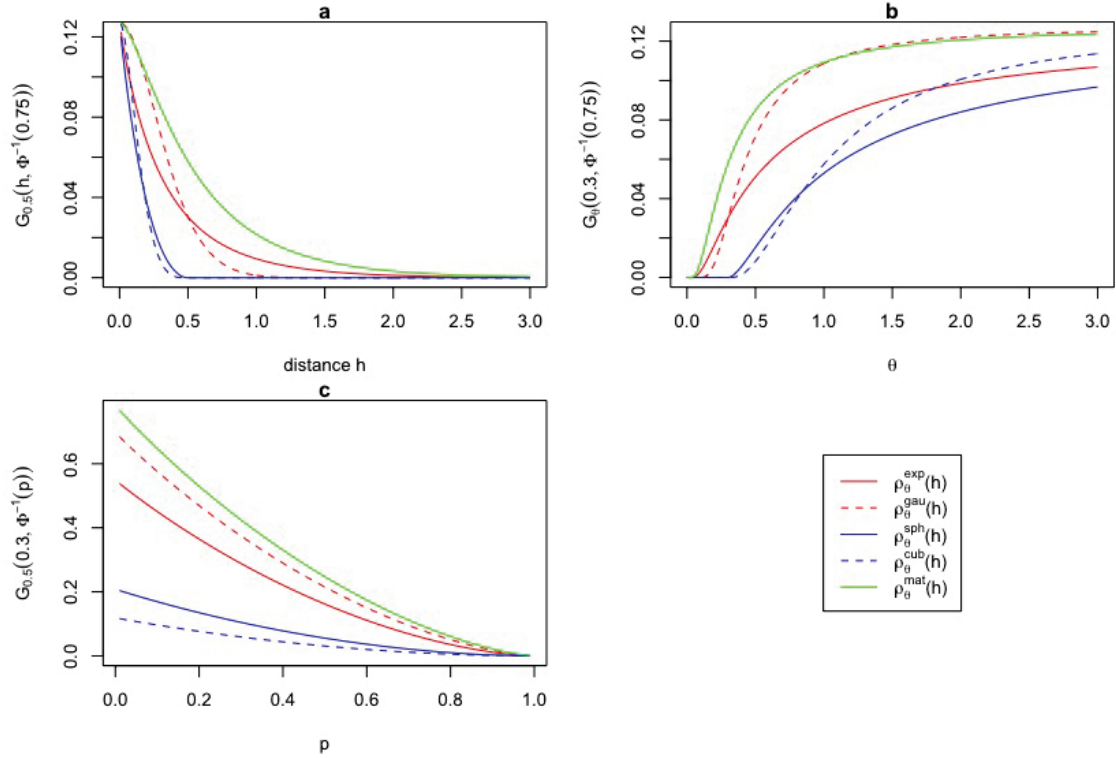


Figure 4.1: Behavior of $\mathcal{G}_{\theta}(h, u)$ with respect to the threshold u , the correlation length θ and the distance h . Five non-negative correlation functions (exponential, Gaussian, spherical, cubic and Matérn with $\kappa = 1$) have been examined. The graphs (a), (b) and (c) show the behavior of $\mathcal{G}(\cdot, \cdot)$ with respect to the following: (a) the distance h , when $u = \Phi^{-1}(0.75)$ and $\theta = 0.50$; (b) the correlation length θ , when $u = \Phi^{-1}(0.75)$ and $h = 0.30$; (c) the threshold $u = \Phi^{-1}(p)$, $p \in [0, 1]$, when $\theta = 0.50$ and $h = 0.30$.

In order to study the behavior of the damage covariance function with respect to θ , we set the threshold $u = \Phi^{-1}(0.75)$ and the distance $h = 0.30$. In Figure 4.1.(b) we remark that $\mathcal{G}_{\theta}(h, u)$ is increasing with θ .

Finally, we study the behavior of the damage covariance function with respect to the threshold $u = \Phi^{-1}(p)$, $p \in [0, 1]$. We set $\theta = 0.50$ and $h = 0.30$. Remark (see Figure 4.1.(c)) that even if h is small, $\mathcal{G}_{\theta}(h, \Phi^{-1}(p))$ goes to zero as p goes to 1, so that it will be difficult to approximate correctly the covariance damage function when u is large.

Figure 4.2. focusses on the behavior of $\mathcal{R}_1(\lambda \mathcal{A}, \mathcal{D}_{X,u}^+)$ with respect to (λ, u, θ) , when \mathcal{A} is a square of side $R = 1$. In order to see the influence of the homothety rate λ , we set $u = \Phi^{-1}(0.75)$ and $\theta = 0.50$.

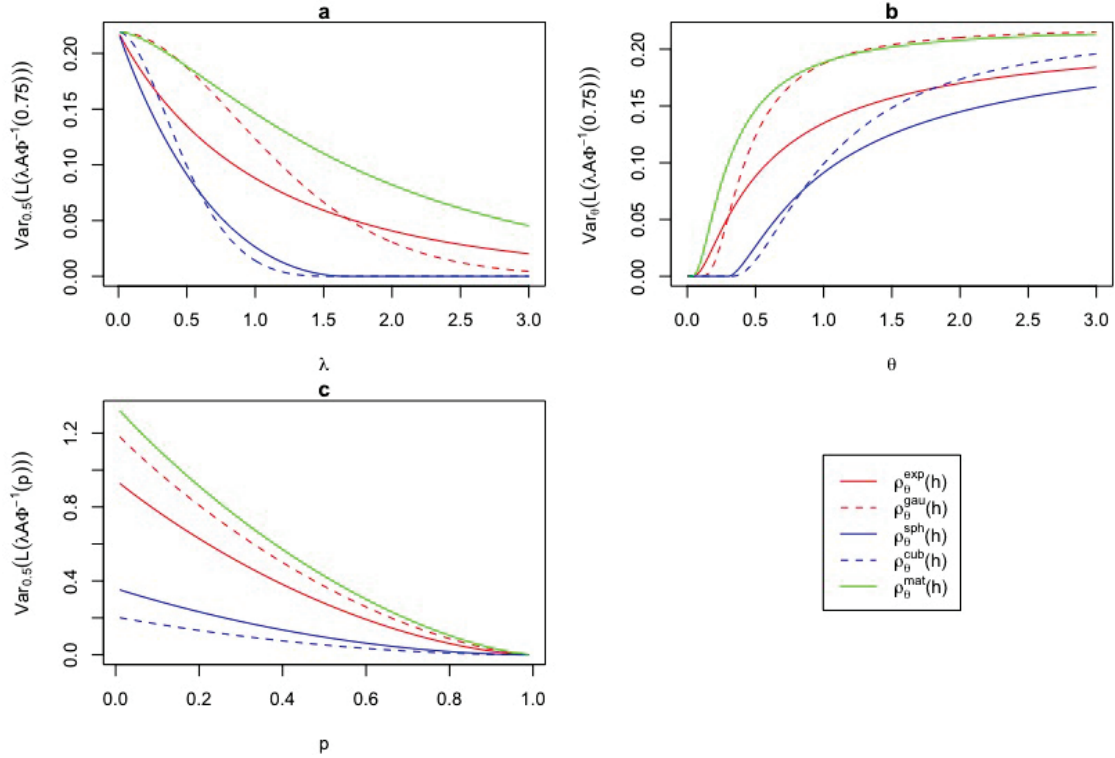


Figure 4.2: The behavior of $\mathcal{R}_1(\lambda \mathcal{A}, \mathcal{D}_{X,u}^+)$ for $\mathcal{A} = [0, 1]^2$ -exponential, Gaussian, spherical, cubic and Matérn with $\kappa = 1$ non-negative correlation functions. The graphs (a), (b) and (c) show the behavior of $\mathcal{R}_1(\lambda \mathcal{A}, \mathcal{D}_{X,u}^+)$ for a fixed $h = 0.30$ with respect to the following: (a) λ , when $u = \Phi^{-1}(0.75)$ and $\theta = 0.50$; (b) θ , when $u = \Phi^{-1}(0.75)$ and $\lambda = 1$; (c) $u = \Phi^{-1}(p)$, $p \in [0, 1]$, when $\lambda = 1$ and $\theta = 0.50$.

To tackle the behavior with respect to θ we choose $\lambda = 1$ and $u = \Phi^{-1}(0.75)$.

To study the behavior of the variance with respect to the threshold $u = \Phi^{-1}(p)$, $p \in [0, 1]$, we set $\lambda = 1$ and $\theta = 0.50$. The behavior of $\mathcal{R}_1(\mathcal{A}, \mathcal{D}_{X,u}^+)$ only depends on $\mathcal{G}_\theta(h, u)$

4.1.2 Numerical computation

We generated isotropic standard spatial Gaussian processes X on $\mathbb{S} = \mathbb{R}^2$ with different non-negative correlation functions (exponential, Gaussian, spherical, cubic and Matérn with $\kappa = 1$) for $\theta = 0.5$. The process X is simulated on a (15×15) grid with $n = 125$ locations, uniformly distributed in the square $\mathcal{A} = [0, 1]^2$. Most of the time, the threshold u is chosen by the practitioner and its value depends on the considered phenomena. For example, in daily rainfall simulation study, the threshold

was chosen equal to 0.5_{mm} [74], while [40] considered the value of the threshold as its median or quantile when evaluating the performance of the exceedance probability estimator. In this study, we set the threshold $u = \Phi^{-1}(p)$ for $p := \{0.75, 0.85, 0.95\}$.

This section is devoted to a numerical study of the computation of $\mathcal{R}_1(\mathcal{A}, \mathcal{D}_{X,u}^+)$, where $\mathcal{A} = [0, 1]^2$. We compare the computation of $\mathcal{R}_1(\mathcal{A}, \mathcal{D}_{X,u}^+)$ by the one-dimensional integration using (3.1.3) with the intuitive Monte-Carlo computation (M1). The (M1) computation is obtained by generating a $m = 1000$ sample of X on the grid; that is,

$$L_j(\mathcal{A}, \mathcal{D}_{X,u}^+) = \frac{1}{|\mathcal{A}|} \left[\frac{1}{n-1} \right]^{2n-1} \sum_{i=1}^{n-1} (X(s_{ij}) - u)^+ \quad j = 1, \dots, m. \quad (4.1.1)$$

$$\mathcal{R}_0^{M1}(\mathcal{A}, \mathcal{D}_{X,u}^+) = \frac{1}{m} \sum_{j=1}^m L_j(\mathcal{A}, \mathcal{D}_{X,u}^+) \quad (4.1.2)$$

and

$$\text{Var}^{M1}(L(\mathcal{A}, \mathcal{D}_{X,u}^+)) = \frac{1}{m-1} \sum_{j=1}^m (L_j(\mathcal{A}, \mathcal{D}_{X,u}^+) - \mathbb{E}^{M1}[L(\mathcal{A}, \mathcal{D}_{X,u}^+)])^2 \quad (4.1.3)$$

where \mathbb{E}^{M1} represents the expectation calculated using Monte-Carlo computation. Boxplots in Figure 4.3 represent the relative errors over 100 (M1) computations with respect to the one-dimensional integration. Because exponential, Gaussian and Matérn correlation models have relatively simple forms, the relative errors are expected to be smaller compared to the spherical and cubic ones. For cubic and spherical models, the discontinuity at $h = \theta$ induces more instability in the simulations.

4.1.3 Piemonte case study

We terminate this section with the computation of the risk measure $\mathcal{R}_1(\mathcal{A}, \mathcal{D}_{X,u}^+)$ on pollution in the Piemonte data. The air pollution is measured by the concentration in PM_{10} , the particulate matter with an aerodynamic diameter less than $10\mu m$. The observed values of PM_{10} are frequently larger than the legal level fixed by the European directive 2008/50/EC (see [19] for details).

The data has been fitted and analyzed in [11]. The data contains the daily concentration of PM_{10} during the winter season 2005 March 2006. The authors considered 24 monitoring stations for estimating the parameters of this model and 10 stations for validation.

The log of PM_{10} has been fitted on an isotropic Gaussian process with Matérn

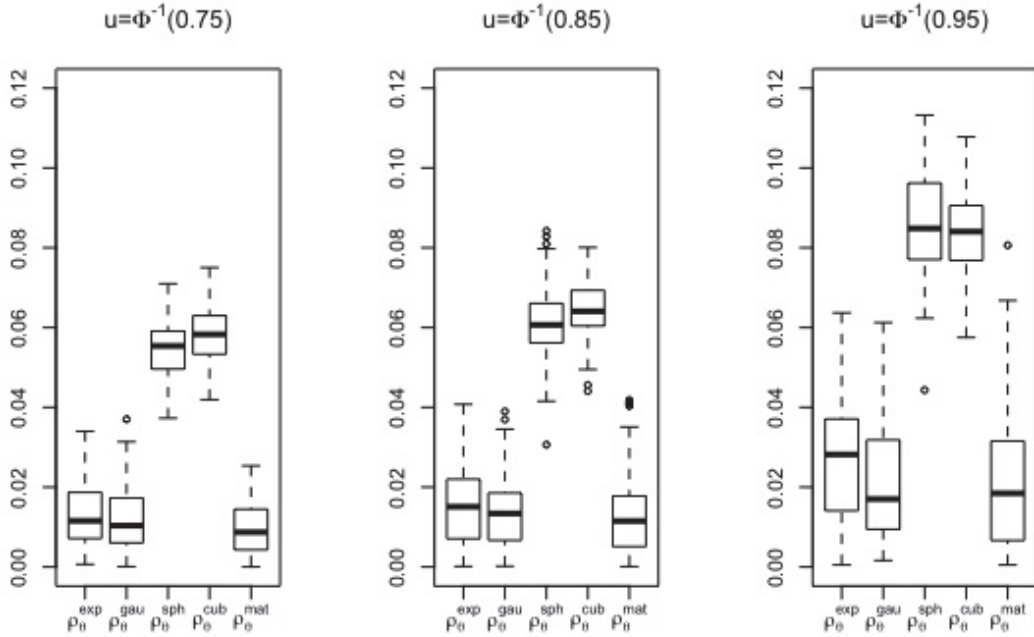


Figure 4.3: The boxplots represent the relative errors of $\mathcal{R}_1(\mathcal{A}, \mathcal{D}_{X,u}^+)$ between the one-dimensional integration computation and the M1 method for different thresholds $u = \Phi^{-1}(p)$, $p := \{0.75, 0.85, 0.95\}$ and five correlation functions (exponential, Gaussian, spherical, cubic and Matérn with $\kappa = 1$) for correlation length $\theta = 0.5$ over $\mathcal{A} = [0, 1]^2$.

auto-correlation function. In what follows, $Y = \log PM_{10}$. Following the parameter estimation (see [11]), we will use $\kappa = 1$ and $\theta = 100$. The estimation of the marginal parameters leads us to use $\mu = 3.69$ and $\sigma^2 = 1.2762$.

We use the above parameters to compute the risk measure

$$(\mathcal{R}_0(\lambda\mathcal{A}, \mathcal{D}_{Y, \log u}^+), \mathcal{R}_1(\lambda\mathcal{A}, \mathcal{D}_{Y, \log u}^+)),$$

with \mathcal{A} a square of side 10km and u the legal level, i.e. $u = 50$. We use Corollary 3.2; let $Y_0 = \frac{Y - \mu}{\sigma}$ and $u_0 = (\log(50) - 3.96) / \sqrt{1.2762} = 0.1965$, we have

$$\begin{aligned} \mathcal{R}_0(\lambda\mathcal{A}, \mathcal{D}_{Y, \log u}^+) &= \sqrt{1.2762}(\varphi(0.1965) - 0.1965\bar{\Phi}(0.1965)) \\ &= 0.3483621 \end{aligned}$$

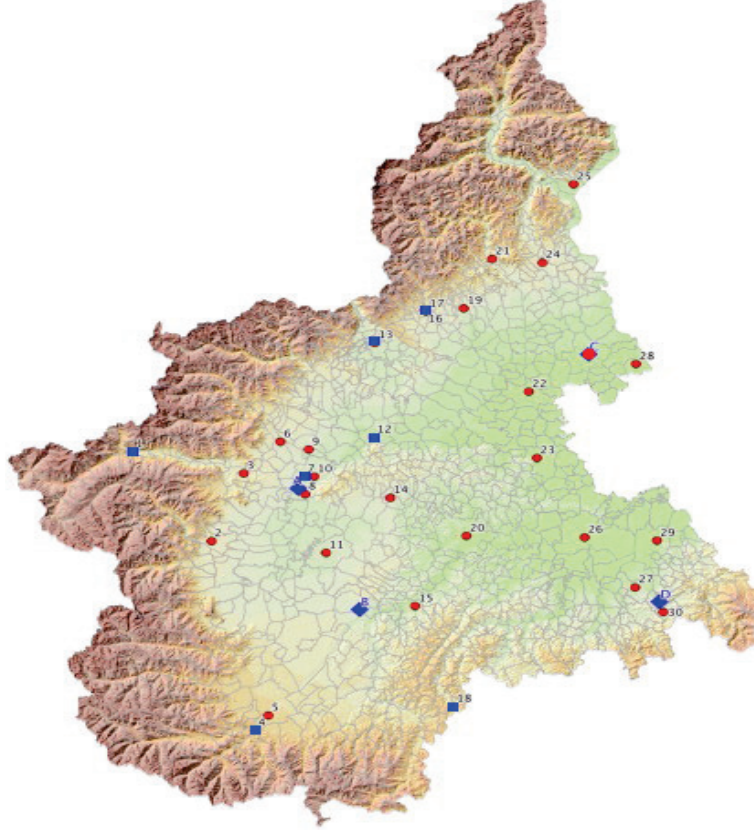


Figure 4.4: [11]. Locations of the 24 PM_{10} monitoring sites (red dots) and 10 validation stations (blue squares) in northern Italy between Alps and Appenises (Piemonte region).

and

$$\begin{aligned}\mathcal{R}_1(\lambda\mathcal{A}, \mathcal{D}_{Y, \log u}^+) &= 1.2762 \int_{h=0}^{14.15} f_s(h, 1) \mathcal{G}(h, 0.1956) dh. \\ &= 0.4119461.\end{aligned}$$

The random variable $L(\mathcal{A}, \mathcal{D}_{Y, \log u}^+)$ is the average over the square \mathcal{A} of the values of Y that exceed the legal threshold $\log u$. This is a quantity of interest for health public policies. Our study shows that the standard deviation of $L(\mathcal{A}, \mathcal{D}_{Y, \log u}^+)$ is large with respect to its expectations. This means that the dependence structure of the underlying process highly impacts the random variable $L(\mathcal{A}, \mathcal{D}_{Y, \log u}^+)$.

4.2 Computational aspects for extreme processes risk measure

In this section, we will study the behavior of the spatial covariance damage function and its spatial risk measure corresponding to a stationary and isotropic max-stable, inverse max-stable, and max-mixture processes. We shall use the correlation functions introduced in Section 2.2.1.

4.2.1 Analysis of the covariance damage function $\mathcal{Q}(h, \nu)$

As usual, we begin with covariance damage function in the study of the risk measure $\mathcal{R}_1(\mathcal{A}, \mathcal{D}_X^\nu)$.

Analysis of $\mathcal{Q}(h, \nu)$ of max-stable process

We study the behavior of $\mathcal{Q}(h, \nu)$ and $\mathcal{R}_1(\lambda\mathcal{A}, \mathcal{D}_X^\nu)$ for X , a TEG spatial max-stable process, with truncated parameter r , non-negative correlation function ρ and correlation length θ . We shall denote by $\mathcal{Q}_{\theta,r}(h, \nu)$ the covariance damage function. Five different models with different correlation functions (exponential, Gaussian, spherical, cubic and Matérn) are considered.

The behavior of $\mathcal{Q}_{\theta,r}(h, \nu)$ with respect to distance h is shown in Figure 4.5.(a). We set the power coefficient $\nu = 0.20$, $r = 0.25$ and $\theta = 0.20$. We have that, $\mathcal{Q}_{\theta,r}(h, \nu) = 0$ for any $h \geq 2r$; the decreasing speed changes according to the different dependence structures. It means the damage functions $\mathcal{D}_X^\nu(\cdot)$ and $\mathcal{D}_X^\nu(\cdot + h)$ belong to two domain (regions) dependence and two domain independence up to distance $h \geq 2r$. In other words, there is no compactness between $\mathcal{D}_X^\nu(\cdot)$ and $\mathcal{D}_X^\nu(\cdot + h)$ for all $h \geq 2r$.

The behavior of $\mathcal{Q}_{\theta,r}(h, \nu)$ with respect to θ is shown in Figure 4.5(b). Figure 4.5(c) shows the behavior of $\mathcal{Q}_{\theta,r}(h, \nu)$ with respect to the truncated parameter r . We set $\nu = 0.20$, $h = 0.25$ and $\theta = 0.20$.

Finally, we study the behavior of the spatial damage covariance function with respect to power coefficient ν . We set $h = 0.25$, $\theta = 0.20$ and $r = 0.25$. Figure 4.5.(d) shows that the covariance between the damage functions $\mathcal{D}_Y^\nu(\cdot)$ and $\mathcal{D}_Y^\nu(\cdot + h)$ increase with ν . This behavior seems natural in climatic phenomenon. For example, when the wind speed increases, the area impacted by the wind will increase.

Remark 4. *The global behavior of $\mathcal{Q}_{\theta,r}(h, \nu)$ for an inverse TEG is the same as for the TEG with the same parameters.*

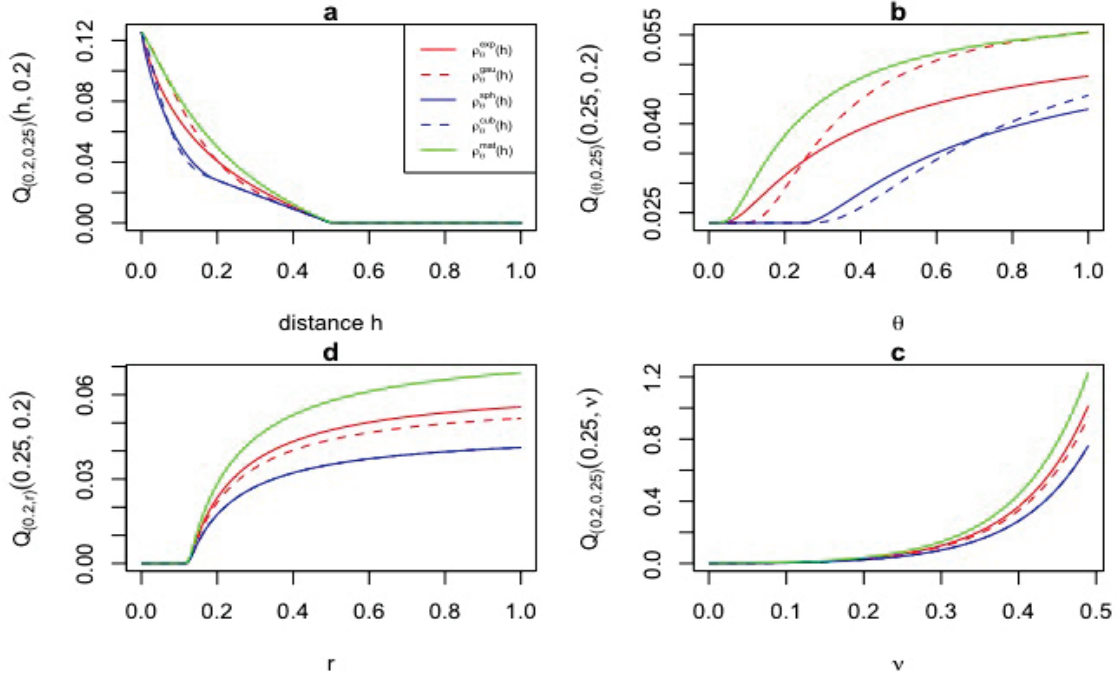


Figure 4.5: shows the behavior of $\mathcal{Q}_{\theta,r}(h, \nu)$ with respect to the power coefficient ν , the correlation length θ , the distance h and the truncated parameter r . Plain lines correspond to TEG and dashed lines correspond to inverse TEG. Five non-negative correlation functions (exponential, Gaussian, spherical, cubic and Matérn with $\kappa = 1$) have been examined. The graphs (a), (b), (c) and (d) show the behavior of $\mathcal{Q}_{\cdot}(\cdot, \cdot)$ with respect to the following: (a) the distance h , when $\nu = 0.2$, $\theta = 0.2$ and $r = 0.25$; (b) the correlation length θ , when $\nu = 0.2$, $r = 0.25$ and $h = 0.25$; (c) the truncated parameter r , when $\nu = 0.2$, $\theta = 0.20$ and $h = 0.25$; (d) the power coefficient ν , when $\theta = 0.20$, $r = 0.25$ and $h = 0.25$.

Analysis of $\mathcal{Q}(h, \nu)$ of max-mixture process

Max-mixture models with expression $Z := \max\{aX, (1-a)Y\}$ with TEG max-stable part denoted X and inverse TEG for the inverse max-stable part - denoted Y cover all possible dependence structures in one model (asymptotic dependence in a short distance, asymptotic independence in intermediate distances and independence in long distances). We have simulated five max-mixture models according to the correlation functions; X and Y have models with the same correlation functions but with different correlation lengths. r_X and r_Y denote the respective truncation parameter of X and Y ; ρ_X and ρ_Y denote the respective correlation functions of X and Y , and θ_X and θ_Y denote the respective correlation length. The mixing parameter is

denoted by a .

We set mixing parameter $a = 0.5$, $r_X = 0.15$, $\theta_X = 0.10$, $r_Y = 0.35$, $\theta_Y = 0.3$ and finally $\nu = 0.2$. In this model, the damage functions $\mathcal{D}_Z^\nu(\cdot)$ and $\mathcal{D}_Z^\nu(\cdot + h)$ are asymptotically dependent up to distance $h < 2r_X$, asymptotically independent when $2r_Y > h \geq 2r_X$ and independent for all $h \geq 2r_Y$. The decreasing speed depends on the correlation function, as shown in Figure 4.6.

Figure 4.7 shows the behavior of $\mathcal{Q}(h, \nu)$ with respect to each parameter. When

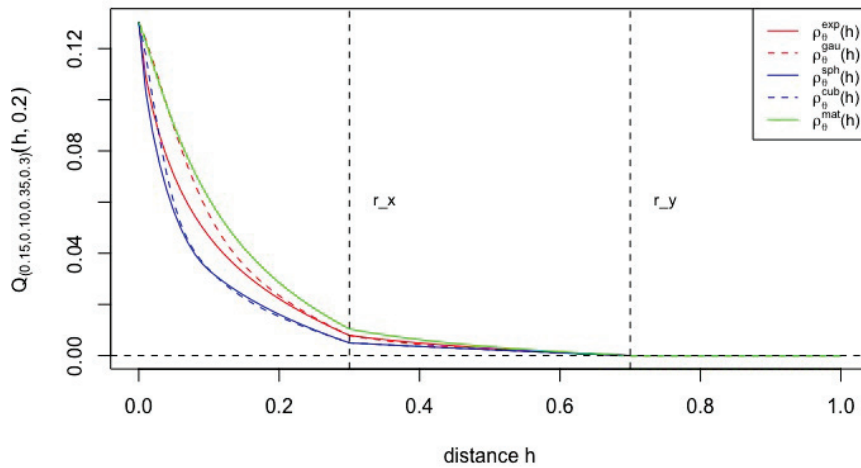


Figure 4.6: shows the behavior of $\mathcal{Q}(h, \nu)$ with respect to distance h . Five non-negative correlation functions (exponential, Gaussian, spherical, cubic and Matérn with $\kappa = 1$) have been examined when $a = 0.5$, $\nu = 0.2$ and X is TEG max-stable with $\theta_X = 0.15$ and $r_X = 0.10$; Y is an invariant TEG max-stable with $\theta_Y = 0.35$ and $r_Y = 0.30$.

it does not vary, each parameter is fixed to $a = 0.5$, $h = 0.25$, $\nu = 0.2$, $\theta_X = 0.1$, $\theta_Y = 0.3$, $r_X = 0.15$ and $r_Y = 0.35$. Graph (a) shows the behavior of \mathcal{Q} with respect to the mixing parameter a . The graphs from (b) to (f) shows the behavior of \mathcal{Q} with respect to the other parameters. The behavior is the same for max-stable processes.

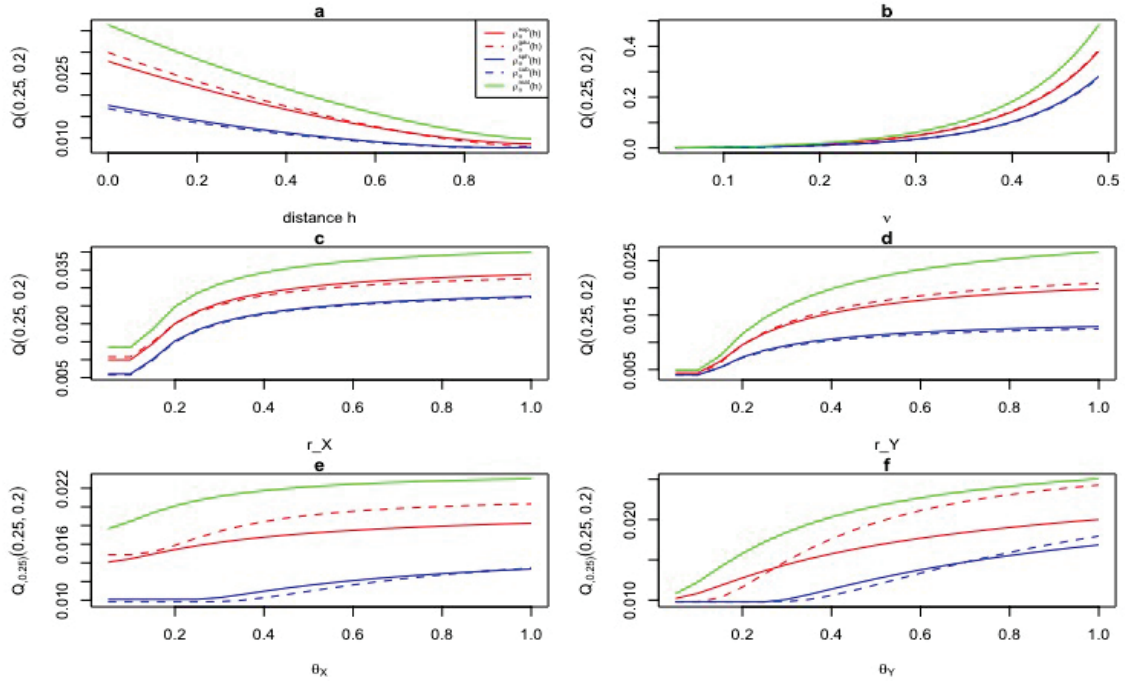


Figure 4.7: (a) shows the behavior of $\mathcal{Q}(h, \nu)$ with respect to mixing parameter a , the power coefficient ν , the correlation lengths θ_X, θ_Y , and truncated parameters r_X, r_Y . Five non-negative correlation functions (exponential, Gaussian, spherical, cubic and Matérn with $\kappa = 1$) have been examined. For $a = 0.5, h = 0.25, \nu = 0.2, \theta_X = 0.1, \theta_Y = 0.3, r_X = 0.15$ and $r_Y = 0.35$, the graphs (a),(b),(c),(d),(e) and (f) show the behavior of $\mathcal{Q}(\cdot, \cdot)$ with respect to the following: (a) the mixing parameter a ; (b) the power coefficient ν ; (c) the truncated parameter r_X ; (d) the truncated parameter r_Y ; (e) the correlation length θ_X ; (f) the correlation length θ_Y .

4.2.2 Numerical computation of $\mathcal{R}_1(\mathcal{A}, \mathcal{D}^\nu)$

In this study, we have computed $\mathcal{R}_1(\mathcal{A}, \mathcal{D}^\nu)$ for different max-stable processes X , inverse max-stable processes Y and max-mixture processes Z . We considered X a TEG with parameters r_X and θ_X , Y a Smith process with σ_Y^2 . The process Z is max-mixture between X and Y . Max-stable and inverse max-stable models are achieved for $a = 1$ and $a = 0$, respectively. We compute $\mathcal{R}_1(\mathcal{A}, \mathcal{D}^\nu)$ using (3.2.3) and (3.2.5), i.e. a three-dimensional integration. For these models, the reduction to a one-dimensional integration does not seem possible. We shall compare this computed value with the Monte Carlo estimation obtained by simulating the process Z . In this simulation study, the TEG has the following parameters: $r_X = 0.25$, non-negative exponential correlation function with $\theta_X = 0.20$. The inverse max-

stable Y is given by a Smith max-stable process Y' with $\sigma_{Y'}^2 = 1$. The process Z is simulated with $n = 50$ locations, uniformly distributed in the square $\mathcal{A} = [0, 1]^2$. We set the power coefficient $\nu := \{0.05, 0.15, 0.25, 0.35, 0.40\}$ and mixing parameter $a := \{0, 0.25, 0.5, 0.75, 1\}$.

The intuitive Monte-Carlo computation (M1) is obtained by the same manner in risk measure for the Gaussian. Boxplots in Figure 4.8. represent the relative errors over 100 (M1) simulations with respect to the three-dimensional integration. It shows that risk measure is hardly estimated by Monte Carlo for ν greater than 0.30. Recall that in the three-dimensional integration, we used (3.2.5). Using (3.2.4) creates numerical issues when ν approaches 0.4.

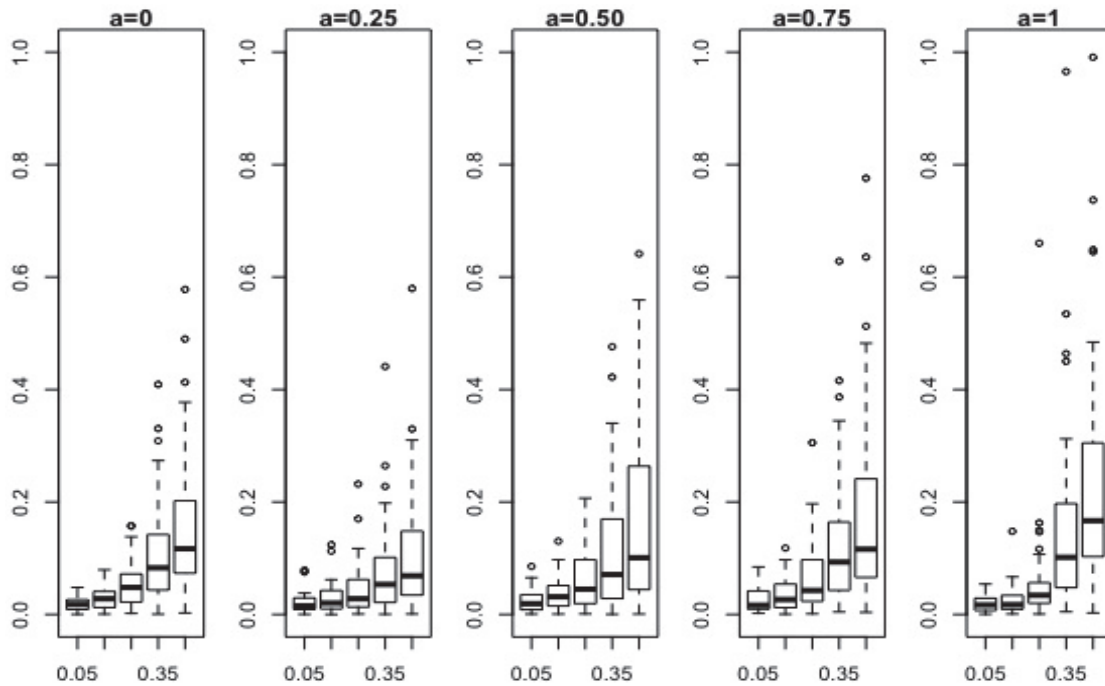


Figure 4.8: The boxplots represent the relative errors of the Monte Carlo estimation of $\text{Var}(L(\mathcal{A}, \mathcal{D}_Z^\nu))$ with respect to the three-dimensional integration for a different power coefficient $\nu := \{0.05, 0.15, 0.25, 0.35, 0.40\}$ and a mixing parameter $a := \{0, 0.25, 0.5, 0.75, 1\}$ with parameters $r_X = 0.25$ and $\theta_X = 0.20$ corresponding to max-stable X and with $\sigma^2 = 1$ corresponding to Y over a square $\mathcal{A} = [0, 1]^2$.

4.2.3 Behavior of $\mathcal{R}_1(\lambda\mathcal{A}, \mathcal{D}^\nu)$

We are going to study the behavior of $\mathcal{R}_1(\lambda\mathcal{A}, \mathcal{D}^\nu)$ with respect to λ for $\mathcal{A} = [0, 1]^2$, a square and several extreme models with fixed $h = 0.3$ and $\nu = 0.20$. Concerning the max-stable X , we considered two models: the first one is TEG with $r = 0.25$ and non-negative exponential correlation function with correlation length $\theta = 0.20$. The second one is Smith with $\sigma^2 = 0.6$. The same models with the same parameters are studied for inverse max-stable processes. Figure 4.9 shows that $\mathcal{R}_1(\lambda\mathcal{A}, \mathcal{D}_W^\nu)$, for

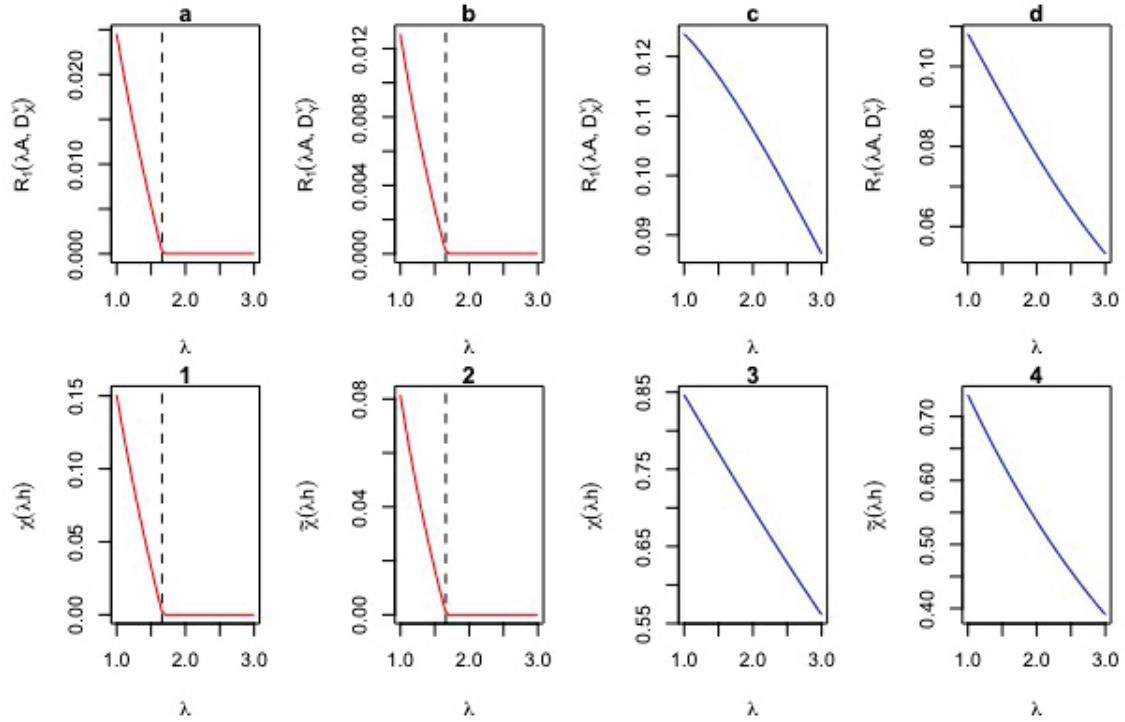


Figure 4.9: The graphs represent the behavior of $\mathcal{R}_1(\lambda\mathcal{A}, \mathcal{D}_X^\nu)$ with respect to λ for $\nu = 0.20$, a square $\mathcal{A} = [0, 1]^2$ and the corresponding relation to tail and lower tail dependence coefficients. Four models are considered: (a) TEG model with truncated parameter $r_X = 0.25$ and exponential correlation function with correlation length $\theta_X = 0.20$; (b) inverse TEG max-stable with the same parameters as in (a); (c) Smith max-stable process with $\sigma^2 = 0.6$; (d) inverse Smith max-stable process with the same parameters as in (c). Finally, the graphs (1), (2), (3) and (4) represent the tail and lower tail dependence coefficients corresponding to each model receptively; $h = 0.3$.

each same max-stable models X and inverse max-stable Y the behaviors are very similar; the difference resides in the fact that X is riskier than Y . Their behavior also

mimics the one of $\chi(h)$ in the max-stable case, or $\bar{\chi}(h)$ in the inverse max-stable case.

For max-mixture models, we evaluated $\mathcal{R}_1(\lambda\mathcal{A}, \mathcal{D}_Z^\nu)$ with respect to λ and mixing parameter a . We considered two models:

- MM1: X is TEG with the same setting in TEG max-stable above and Y is inverse Smith with $\sigma_Y^2 = 0.8$.
- MM2: X is TEG max-stable with the same in MM1 and Y is inverse TEG with $r_Y = 0.45$ and non-negative exponential correlation function with correlation length $\theta = 0.40$.

Figure 4.10.(a) shows the behavior of $\mathcal{R}_1(\lambda\mathcal{A}, \mathcal{D}_Z^\nu)$ for the max-mixture model MM1. It shows the relative height value for $\mathcal{R}_1(\lambda\mathcal{A}, \mathcal{D}_Z^\nu)$ up to $0.3\lambda < 2r_X$ and the amount of the risk converge to zero for all $0.3\lambda \geq 2r_X$ with speed decreasing dependence on the parameter of Smith model σ_Y^2 with dependence structure and asymptotic dependence when $0.3\lambda < 2r_X$ and asymptotic independence for all $0.3\lambda \geq 2r_X$. Figure 4.10.(b) shows the behavior of $\mathcal{R}_1(\lambda\mathcal{A}, \mathcal{D}_Z^\nu)$ with respect to the max-mixture model MM2. We can see the same behavior of asymptotic dependence part in MM1 when $0.3\lambda < 2r_X$, asymptotic independence when $2r_X \leq 0.3\lambda < 2r_Y$ and independence for all $0.3\lambda \geq 2r_Y$.

The fact that the rupture at $2r_Y$ is low implies that this parameter would certainly be difficult to estimate on data. Combining the graphs (1) and (2) with (I) and (II) respectively results in the same behavior of the risk measure in graphs (a) and (b). This is why we propose dependence measures in the next chapter, they combine these dependence structures. Figures 4.11.(a) and (b) shows the behavior of $\mathcal{R}_1(\lambda\mathcal{A}, \mathcal{D}_Z^\nu)$ with respect to a .

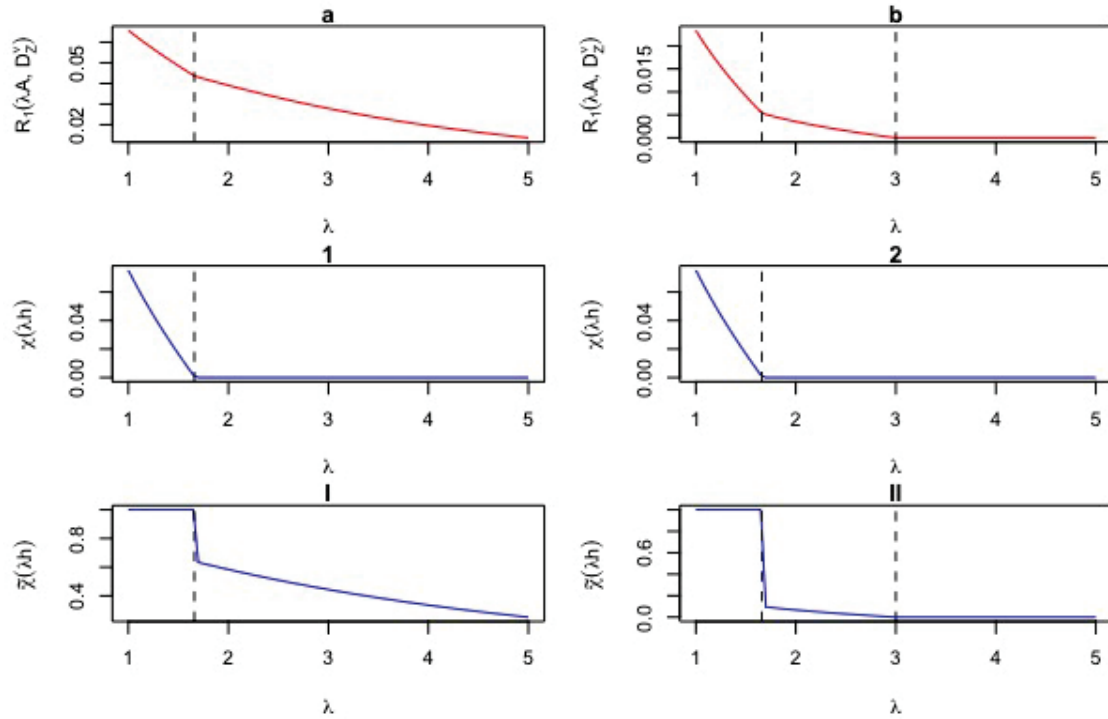


Figure 4.10: shows the behavior of $\mathcal{R}_1(\lambda\mathcal{A}, D_Z^V)$, $\chi(h)$ and $\bar{\chi}(h)$ for two max-mixture models.

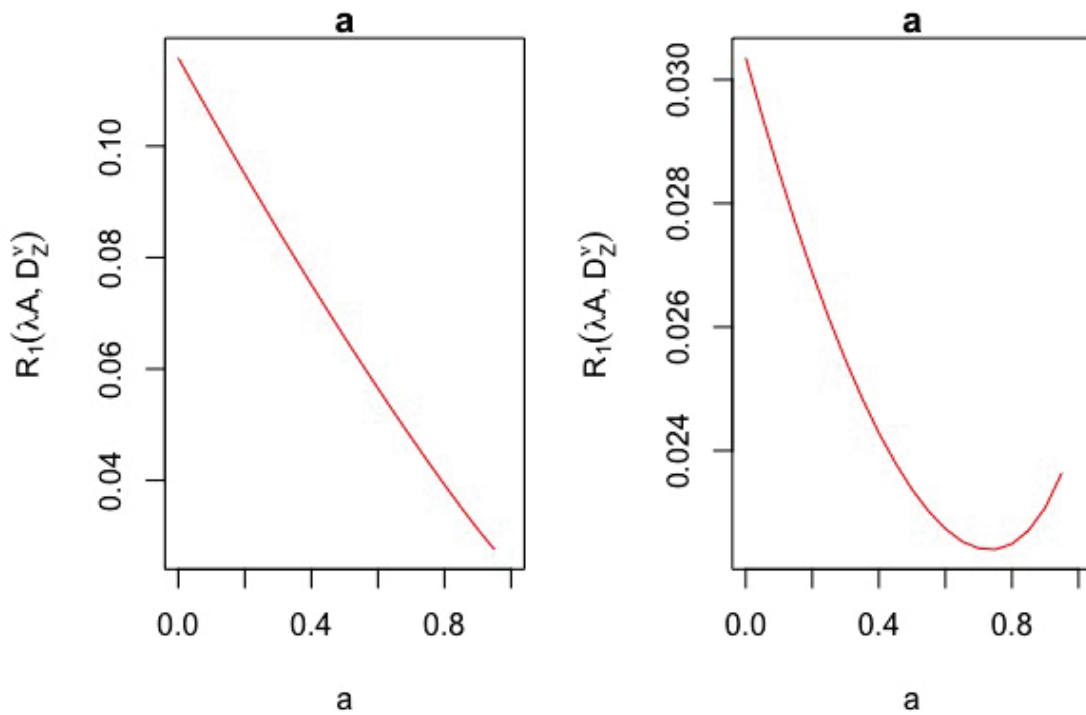


Figure 4.11: shows the behavior of $\mathcal{R}_1(\lambda\mathcal{A}, D_Z^V)$ with respect to mixing parameter a for two max-mixture models : (a) MM1 model; (b) MM2 model.

Chapter 5

Estimation parameters of spatial max-mixture model

In this chapter, we propose to estimate the parameters of max-mixture processes by minimization of the least squares F -madogram error (LS-madogram). We begin by recalling the definition of the F -madogram and calculate it for max-mixture spatial processes. Then, we prove that LS-madogram leads to consistent estimation of the parameters, provided that they are identified by the F -madogram. A simulation study is conducted in order to study the estimation performance and to compare LS-madogram estimation with the maximization of the composite likelihood. This is an alternative approach based on least squares for $\chi(h, u)$ and $\bar{\chi}(h, u)$; the results were convincing (see the Appendix B).

5.1 F -madogram for max-mixture spatial process

In extreme value theory and therefore for spatial extremes, one of the main concerns is to find a dependence measure that can quantify the dependences between locations. Many authors have proposed several such measures, especially for max-stable processes (recall Section 2.3 where we discussed deeply on these tools).

The χ and $\bar{\chi}$ dependence measures are designed to quantify asymptotic dependence and asymptotic independence respectively. Max-mixture processes have been introduced in order to provide both behaviors. We are then faced with the question of finding an adapted tool which would give information on more than one dependence structure. Recall ([9] and Proposition 2.3) that we have for a max-mixture process:

$$\chi(h) = a(2 - \Theta(h))$$

and

$$\bar{\chi}(h) = \mathbb{1}_{[h^* < h]}(h) + (2\eta(h) - 1)\mathbb{1}_{[h^* \geq h]},$$

where $h^* = \inf\{h, \Theta(h) \neq 0\}$, Θ is the extremal coefficient of the max-stable part and η is the tail dependence coefficient of the asymptotic independence part.

In [24], the F -madogram has been introduced for max-stable processes. There exists several definitions of madograms. For example, in [53], the λ -madogram is considered in order to take into account the dependence information from the exponent measure $V_h(u, v)$ when $u \neq v$. This λ -madogram has been extended in [33] to evaluate the dependence between two observations located in two disjoint regions in \mathbb{R}^2 . [36] adopted an F -madogram suitable for asymptotic independence instead of asymptotic dependence only. Finally, [7] used F -madogram as a test statistic for asymptotic independence bivariate maxima.

The F -madogram is defined in Definition 2.14. Below, we calculate $\nu^F(h)$ for a max-mixture process. It appears that contrary to χ and $\bar{\chi}$, it combines the parameters coming from the AD and the AI parts.

Recall that for a stationary process Z with distribution function F , the F -madogram is defined as

$$\nu^F(h) = \frac{1}{2} \mathbb{E}|F(Z(s)) - F(Z(s+h))|.$$

We have $\nu^F(h) \in [0, \frac{1}{6}]$ and $\nu^F(h) = 0$ if $Z(s)$ and $Z(s+h)$ are co-monotonic. $\nu^F(h) = \frac{1}{6}$ if $Z(s)$ and $Z(s+h)$ are independent (this result may be found in [24] and we give the proof below - Lemma 5.2 - for completeness).

Proposition 5.1. *Let Z be a max-mixture process, with mixing coefficient $a \in [0, 1]$. Let X be its max-stable part with extremal coefficient $\Theta(h)$. Let Y be its inverse max-stable part with tail dependence coefficient $\eta(h)$. Then, the F -madogram of Z is*

$$\begin{aligned} \nu^F(h) = & \\ & \frac{a(\Theta(h) - 1)}{a(\Theta(h) - 1) + 2} - \frac{a\Theta(h) - 1}{2a\Theta(h) + 2} - \frac{1/\eta(h)}{a\Theta(h) + (1-a)/\eta(h) + 1} \beta\left(\frac{a\Theta(h) + 1}{(1-a)}, 1/\eta(h)\right), \end{aligned} \quad (5.1.1)$$

where β is beta function.

Proof. We have

$$\nu^F(h) = \frac{1}{2} \mathbb{E}|F(Z(s)) - F(Z(s+h))|. \quad (5.1.2)$$

The equality $|a - b|/2 = \max(a, b) - (a + b)/2$ leads to

$$\nu^F(h) = \mathbb{E}[\max(F(Z(s)), F(Z(s+h)))] - \mathbb{E}[F(Z(s))]. \quad (5.1.3)$$

Let $M(h) = \max(F(Z(s)), F(Z(s+h)))$, we have:

$$\begin{aligned}\mathbb{P}(M(h) \leq u) &= \mathbb{P}(\max(F(Z(s)), F(Z(s+h))) \leq u) \\ &= \mathbb{P}(F(Z(s)) \leq u, F(Z(s+h)) \leq u) \\ &= \mathbb{P}(Z(s) \leq F^{-1}(u), Z(s+h) \leq F^{-1}(u)).\end{aligned}\tag{5.1.4}$$

The probability distribution function of the max-mixture spatial process Z is given in Equation (2.3.37) and leads to

$$\begin{aligned}\mathbb{P}(M(h) \leq u) &= e^{-\frac{a\Theta(h)}{F^{-1}(u)}} \left[2e^{-\frac{(1-a)}{F^{-1}(u)}} - 1 + e^{-\frac{1}{\eta(h)g(F^{-1}(h),a)}} \right] \\ &= u^{a\Theta(h)} [2u^{(1-a)} - 1 + (1 - u^{(1-a)})^{1/\eta(h)}], \quad u \in [0, 1].\end{aligned}$$

We deduce that the density of $M(h)$ satisfies the following:

$$\begin{aligned}f_{M(h)}(u) &= (2a(\Theta(h)-1)+2)u^{a(\Theta(h)-1)} - a\Theta(h)u^{a\Theta(h)-1} + a\Theta(h)u^{a\Theta(h)-1}(1-u^{(1-a)})^{1/\eta(h)} \\ &\quad - \frac{(1-a)}{\eta(h)}u^{a(\Theta(h)-1)}(1-u^{(1-a)})^{\frac{1}{\eta(h)}-1}.\end{aligned}\tag{5.1.5}$$

Therefore,

$$\mathbb{E}[M(h)] = \int_0^1 u f_{M(h)}(u) du = \frac{2a(\Theta(h)-1)+2}{a(\Theta(h)-1)+2} - \frac{a\Theta(h)}{a\Theta(h)+1} + A_1 - A_2$$

where,

$$A_1 := a\Theta(h) \int_0^1 u^{a\Theta(h)} (1 - u^{(1-a)})^{1/\eta(h)} du$$

and

$$\begin{aligned}A_2 &:= \frac{1}{\eta(h)} \beta\left(\frac{a\Theta(h)+1}{(1-a)} + 1, 1/\eta(h)\right) \\ &= \frac{\gamma\Gamma(\alpha+1)\Gamma(\gamma)}{\Gamma(\alpha+\gamma+1)}.\end{aligned}$$

Let $t = u^{(1-a)}$, this leads to

$$A_1 := \frac{a\Theta(h)}{(1-a)} \int_0^1 t^{a(\Theta(h)+1)/(1-a)} (1-t)^{1/\eta(h)} dt.$$

Using the beta function $\beta(x, y) = \int_0^1 t^{x-1} (1-t)^{y-1} dt$, we get

$$A_1 := \frac{a\Theta(h)}{(1-a)} \beta\left(\frac{a\Theta(h)+1}{(1-a)}, \frac{1}{\eta(h)} + 1\right).$$

It is well-known that $\beta(x, y) = \frac{\Gamma(x)\Gamma(y)}{\Gamma(x+y)}$ and $\Gamma(x+1) = x\Gamma(x)$. Let us denote $\alpha = \frac{a\Theta(h)+1}{(1-a)}$ and $\gamma = \frac{1}{\eta(h)}$, we have

$$\begin{aligned} A_1 &= \left[\alpha - \frac{1}{(1-a)} \right] \frac{\Gamma(\alpha)\Gamma(\gamma+1)}{\Gamma(\alpha+\gamma+1)} \\ &= \frac{\gamma\Gamma(\alpha+1)\Gamma(\gamma)}{\Gamma(\alpha+\gamma+1)} - \frac{\gamma}{(1-a)(\alpha+\gamma)} \frac{\Gamma(\alpha)\Gamma(\gamma)}{\Gamma(\alpha+\gamma)} \\ &= \frac{\gamma\Gamma(\alpha+1)\Gamma(\gamma)}{\Gamma(\alpha+\gamma+1)} - \frac{\gamma}{(1-a)(\alpha+\gamma)} \beta(\alpha, \gamma) \end{aligned}$$

In the same way, we can get A_2 :

$$\begin{aligned} A_2 &= \frac{1}{\eta(h)} \beta\left(\frac{a\Theta(h)+1}{(1-a)} + 1, 1/\eta(h)\right) \\ &= \frac{\gamma\Gamma(\alpha+1)\Gamma(\gamma)}{\Gamma(\alpha+\gamma+1)} \\ &= \frac{\alpha\gamma}{\alpha+\gamma} \beta(\alpha, \gamma). \end{aligned}$$

Finally, we get:

$$\mathbb{E}[M(h)] = \frac{2a(\Theta(h)-1)+2}{a(\Theta(h)-1)+2} - \frac{a\Theta(h)}{a\Theta(h)+1} - \frac{\beta\left(\frac{a\Theta(h)+1}{(1-a)}, 1/\eta(h)\right)}{\eta(h)(1-a)\left[\frac{a\Theta(h)+1}{(1-a)} + (1/\eta(h))\right]}.$$

Recall that $\mathbb{E}(F(Z(s))) = \frac{1}{2}$ because $F(Z(s)) \sim \mathcal{U}([0, 1])$ and return to equation (5.1.3) to get equation (5.1.1). \square

Lemma 5.2. *Let Z be a stationary PQD (positive quadrant dependence) process. If $Z(s)$ and $Z(s+h)$ are perfectly dependent (or co-monotonic), then $\nu^F(h) = 0$. If $Z(s)$ and $Z(s+h)$ are independent, then $\nu^F(h) = \frac{1}{6}$.*

Proof. We have for any PQD random variables X and Y with respective margins F and G and joint distribution function H the following inequality.

$$F(x)G(y) \leq H(x, y) \leq \min\{F(x), G(y)\} \quad (5.1.6)$$

where the lower and upper bounds are reached respectively for complete independence and complete dependence (see [59]).

For any non-negative random variable X , we have $\mathbb{E}[X] = \int_{\mathbb{R}^+} [1 - F(x)]dx$. Then, in the independence case:

$$\begin{aligned} \mathbb{P}(M(h) \leq u) &= \mathbb{P}(X(s) \leq F^{-1}(u), X(s+h) \leq F^{-1}(u)) \\ &= \mathbb{P}(X(s) \leq F^{-1}(u))\mathbb{P}(X(s+h) \leq F^{-1}(u)) \\ &= u^2. \end{aligned} \quad (5.1.7)$$

Therefore,

$$\begin{aligned} \nu_U^F(h) &= \mathbb{E}[M(h)] - \mathbb{E}[F(X(s))] \\ &= \int_0^1 [1 - u^2]du - \frac{1}{2} = 1/6 \end{aligned} \quad (5.1.8)$$

In the complete dependence case, we have

$$\begin{aligned} \mathbb{P}(M(h) \leq u) &= \mathbb{P}(X(s) \leq F^{-1}(u), X(s+h) \leq F^{-1}(u)) \\ &= \min [\mathbb{P}(X(s) \leq F^{-1}(u)), \mathbb{P}(X(s+h) \leq F^{-1}(u))] \\ &= \mathbb{P}(X(s) \leq F^{-1}(u)) = u. \end{aligned} \quad (5.1.9)$$

Therefore,

$$\begin{aligned} \nu^F(h) &= \mathbb{E}[M(h)] - \mathbb{E}[F(X(s))] \\ &= \int_0^1 [1 - u]du - \frac{1}{2} = 0. \end{aligned} \quad (5.1.10)$$

The bounds of $\nu^F(h)$ follow:

$$0 \leq \nu^F(h) \leq 1/6 \quad (5.1.11)$$

with bounds reached for complete dependence and independence, respectively. \square

In the particular cases where $a = 1$ or $a = 0$, Proposition 5.1 reduces to known results for max-stable processes (see [24]) and inverse max-stable processes (see [36]).

Corollary 5.3. *The F -madogram for a max-stable spatial process is given by*

$$2\nu^F(h) = \frac{\Theta(h) - 1}{\Theta(h) + 1}. \quad (5.1.12)$$

The F -madogram of an asymptotically independent spatial process is given by

$$2\nu^F(h) = \frac{1 - \eta(h)}{1 + \eta(h)} \quad (5.1.13)$$

Proof. The F -madogram $\nu^F(h)$ for a max-stable process is easily obtained by letting a go to 1 in Equation (5.1.1):

$$\nu^F(h) = \frac{\Theta(h) - 1}{2(\Theta(h) + 1)} - \frac{1/\eta(h)}{\Theta(h) + 1} \lim_{a \rightarrow 1} \beta \left(\frac{a\Theta(h) + 1}{(1-a)}, 1/\eta(h) \right).$$

We have, as x goes to infinity and for fixed y , $\beta(x, y) \sim \Gamma(y)x^{-y}$. Therefore, we obtain equation (5.1.12).

The F -madogram for asymptotically independent processes is obtained by letting a go to 0 in equation (5.1.1):

$$\begin{aligned} \nu^F(h) &= \frac{1}{2} - \frac{1}{\eta(h) + 1} \beta \left(1, 1/\eta(h) \right) \\ &= \frac{1}{2} - \frac{1}{(\eta(h) + 1) \Gamma(\frac{1}{\eta(h)} + 1)} \Gamma(1/\eta(h)) \\ &= \frac{1}{2} - \frac{\eta(h)}{\eta(h) + 1}. \end{aligned} \tag{5.1.14}$$

Hence, the result. □

5.2 Model inference

This section is devoted to the parametric inference for max-mixture processes. We begin with the presentation of the maximum composite likelihood estimation, then we present the least squares madogram. Finally, we shall compare these two methods.

5.2.1 Parametric Estimation using Composite Likelihood

Consider $(Z^k(s_1), \dots, Z^k(s_D))$, $k = 1, \dots, N$, be N independent copies of a spatial process $(Z(s))_{s \in \mathbb{S}}$, observed at D locations s_1, \dots, s_D . A standard way to perform parameter estimation is by maximization of the likelihood. This method requires the computation of the likelihood of $(Z(s_1), \dots, Z(s_D))$. Even if it is theoretically available, it is not computationally tractable for D greater than 2 or 3 (see [27, 67]). Indeed, the distribution function is given by (2.3.4) and the density function would be obtained by the chain rule derivation which leads to a huge amount of terms.

Therefore, the composite likelihood inference will be a more appropriate approach for the estimation [49, 70]. Asymptotic properties of this estimator has been proved in [25]. This approach has been applied successfully to spatial max-stable processes by [26] and [55] and is also used to identify the parameters of data exceedances over

a large threshold, for example, [8] and [67].

Our interest in this study lies in max-mixture models; two studies [9] and [73] highlight on these models; therefore, we will take the composite likelihood proposed by [9] as the control for evaluating the performance of the proposed non-linear least square estimator, which will be introduced in the next section.

If the pairwise density of Z can be computed and its parameter ψ is identifiable, then it is possible to estimate ψ by maximizing the pairwise weighted log likelihood. For simplicity, we denote Z_i^k for $Z^k(s_i)$. Let

$$\hat{\psi}_L = \max_{\psi} \mathcal{P}(\psi),$$

where

$$\mathcal{P}(\psi) = \sum_{k=1}^N \sum_{i=1}^{D-1} \sum_{j>i}^D w_{ij} \log \mathcal{L}(Z_i^k, Z_j^k; \psi) =: \sum_{k=1}^N \mathcal{P}_k(\psi). \quad (5.2.1)$$

where \mathcal{L} is the likelihood of the pair (Z_i^k, Z_j^k) and $w_{i,j} \geq 0$ is the weight that specifies the contribution for each pair. In [8], it is suggested to take $w_{i,j} = 0$ for any pair separated by distance over a specific value δ and $w_{i,j} = 1$ otherwise.

In [21], it is suggested to consider a censor approach of the likelihood, taking into account a threshold. Let $G(\cdot, \cdot)$ be a pairwise distribution function and consider the thresholds u_1 and u_2 ; the likelihood contribution is

$$\mathcal{L}(z_1, z_2; \psi) = \begin{cases} \partial_{12}^2 G(z_1, z_2; \psi) & \text{if } z_1 > u_1, z_2 > u_2, \\ \partial_1 G(z_1, z_2; \psi) & \text{if } z_1 > u_1, z_2 \leq u_2, \\ \partial_2 G(z_1, z_2; \psi) & \text{if } z_1 \leq u_1, z_2 > u_2, \\ G(z_1, z_2; \psi) & \text{if } z_1 \leq u_1, z_2 \leq u_2, \end{cases}$$

where ∂_i is the differentiation with respect to the variable z_i . In [73], the censored likelihood is used in order to improve the estimation of the parameters related to asymptotic independence. This censored approach was also applied by [9] for the estimation of parameters of max-mixture processes. In this paper, the replications Z^1, \dots, Z^N of Z are assumed to be α -mixing rather than independent. We denote generically by ψ the parameters of the model. In [9], it is proved, under some smoothness assumptions on the composite likelihood, that the composite maximum likelihood estimator $\hat{\psi}_L$ for max-mixture processes is asymptotically normal as N goes to infinity with asymptotic variance

$$\mathcal{G}(\psi) = \mathcal{J}(\psi)[\mathcal{K}(\psi)]^{-1}\mathcal{J}(\psi),$$

where $\mathcal{J}(\psi) = \mathbb{E}[-\nabla^2 \mathcal{P}(\psi)]$, $\mathcal{K}(\psi) = \text{var}(\nabla \mathcal{P}(\psi))$. The matrix $\mathcal{G}(\psi)$ is called the Godambe information matrix (see [9] and theorem 3.4.7 in [37]).

An estimator $\hat{\mathcal{J}}$ of $\mathcal{J}(\psi)$ is obtained from the Hessian matrix computed in the optimization algorithm. The variability matrix $\mathcal{K}(\psi)$ has to be estimated too. In our context, we have independent replications of Z and N is large compared with respect to the dimension of ψ . Then, we can use the outer product of the estimation of $\hat{\psi}$. Let

$$\hat{\mathcal{K}}(\psi) = N^{-1} \sum_{k=1}^N \nabla \mathcal{P}_k(\hat{\psi}) \nabla \mathcal{P}_k(\hat{\psi})'$$

or by Monte Carlo simulation with explicit formula of $\mathcal{P}_k(\psi)$ (see section 5. in [70]). In the case of samples of Z satisfying the α -mixing property, the estimation of $\mathcal{K}(\psi)$ can be done using a subsampling technique introduced by [32]; this was used in [9].

Finally, model selection can be done by using the composite likelihood information criterion [71]:

$$\text{CLIC} = -2 \left[\mathcal{P}(\hat{\psi}) - \text{tr}(\hat{\mathcal{J}}^{-1} \hat{\mathcal{K}}) \right].$$

Considering several max-stable models, the one that has the smallest CLIC will be chosen. In [67], the criterion $\text{CLIC}^* = (D - 1)^{-1} \text{CLIC}$ is proposed. It is close to Akaike information criterion (AIC).

5.2.2 Semi-parametric estimation using NLS of F-madogram

In this section, we shall define the non-linear least square estimation procedure of the parameters set ψ corresponding to the max-mixture model Z using the F -madogram. This procedure can be considered as an alternative method to the composite likelihood method.

Consider Z^t , $t = 1, \dots, T$ as copies of an isotropic max-mixture process Z with unit Fréchet marginal laws (F denotes the distribution function of a unit Fréchet law). It may be independent copies for example, if the data is recorded yearly (see [53]) or we shall consider that $(Z^t)_{t=1, \dots, T}$ satisfies an α -mixing property ([9]). Let \mathcal{H} be a finite subset of \mathbb{S} , $J(x, y) = \frac{1}{2}|x - y|$ and $Y_{h,t} = J(F(Z^t(s)), F(Z^t(s+h)))$, $t = 1, \dots, T$ and $h \in \mathcal{H}$. Therefore, for $t = 1, \dots, T$, the vectors $(Y_{h,t})_{h \in \mathcal{H}}$ have the same law and are considered either independent or α -mixing (in t). The main motivation for using the F -madogram in estimation is that it contains the dependence structure information for a fixed h of $Y_{h,t}$ (see section 3.2 in [7]).

In what follows, we make the assumption that the vectors $(Y_{h,t})_{h \in \mathcal{H}}$ are i.i.d. Note

that from the definition of the F -madogram, we have $\mathbb{E}[Y_{t,h}] = \nu^F(h, \psi)$ where $\nu^F(h, \psi)$ is the F -madogram of Z with parameters ψ defined in (2.14). If Z has an unknown true parameter ψ_0 on a compact set $\Psi \subset \mathbb{R}^d$, we rewrite

$$Y_{h,t} = \nu^F(h, \psi_0) + \varepsilon_{h,t}. \quad (5.2.2)$$

The vectors $(\varepsilon_{h,t})_{h \in \mathcal{H}}$ are i.i.d errors with $\mathbb{E}[\varepsilon_{h,t}] = 0$ and $\text{Var}(\varepsilon_{h,t}) = \sigma_h^2 > 0$ is finite and unknown.

Let

$$\mathcal{L}(\psi) = \sum_{h \in \mathcal{H}} \frac{1}{T} \sum_{t=1, \dots, T} (Y_{t,h} - \nu^F(h, \psi))^2 \quad (5.2.3)$$

Any vector $\hat{\psi}_T$ in Ψ which minimizes $\mathcal{L}(\psi)$ will be called a least square estimate of ψ_0 .

$$\hat{\psi}_T \in \underset{\psi \in \Psi}{\text{argmin}} \mathcal{L}(\psi). \quad (5.2.4)$$

Theorem 5.4. *Assume that $\Psi \subset \mathbb{R}^d$ is compact and that $\psi \mapsto \nu^F(h, \psi)$ is continuous for all $h \in \mathcal{H}$. We assume that the vectors $(Y_{h,t})_{h \in \mathcal{H}}$ are i.i.d. Let $(\hat{\psi}_T)_{T \in \mathbb{N}}$ be least square estimators of ψ_0 ; then, any limit point (as T goes to infinity) ψ of $(\hat{\psi}_T)_{T \in \mathbb{N}}$ satisfies $\nu(h, \psi) = \nu(h, \psi_0)$ for all $h \in \mathcal{H}$.*

Remark 5. *Of course, if $\psi \rightsquigarrow (\nu(h, \psi))_{h \in \mathcal{H}}$ is injective, then theorem 5.4 implies that the least square estimation is consistent, i.e. $\psi_T \rightarrow \psi_0$ a.s. as T goes to infinity. In the examples considered below, it seems that the injectivity is satisfied provided $|\mathcal{H}| \geq d$, but we were unable to prove it.*

Proof. We follow the proof of Theorem II.5.1 in [5]. From (5.2.2), we have, for all $\psi \in \Psi$

$$\begin{aligned} \mathcal{L}(\psi) &= \sum_{h \in \mathcal{H}} \frac{1}{T} \sum_{t=1, \dots, T} (\nu^F(h, \psi_0) + \varepsilon_{h,t} - \nu^F(h, \psi))^2 \\ &= \sum_{h \in \mathcal{H}} (\nu^F(h, \psi_0) - \nu^F(h, \psi))^2 \\ &\quad + \frac{2}{T} \sum_{h \in \mathcal{H}} (\nu^F(h, \psi_0) - \nu^F(h, \psi)) \left(\sum_{t=1, \dots, T} \varepsilon_{h,t} \right) + \sum_{h \in \mathcal{H}} \frac{1}{T} \sum_{t=1, \dots, T} \varepsilon_{h,t}^2. \end{aligned}$$

From the law of large numbers, we have

$$\frac{1}{T} \sum_{h \in \mathcal{H}} \sum_{t=1, \dots, T} \varepsilon_{h,t}^2 \rightarrow \sum_{h \in \mathcal{H}} \sigma_h^2 \quad \text{a.s. as } T \rightarrow \infty$$

and for any $h \in \mathcal{H}$,

$$\frac{1}{T} \sum_{t=1, \dots, T} \varepsilon_{h,t} \rightarrow 0 \text{ a.s.}$$

Therefore,

$$\mathcal{L}(\psi) \rightarrow \sum_{h \in \mathcal{H}} \sigma_h^2 + \sum_{h \in \mathcal{H}} (\nu^F(h, \psi_0) - \nu^F(h, \psi))^2 \text{ a.s. as } T \rightarrow \infty.$$

Take a sequence $(\hat{\psi}_T)_{T \in \mathbb{N}}$ of least square estimators, taking if necessary a subsequence, we may assume that it converges to some $\psi^* \in \Psi$. Using the continuity of $\psi \rightsquigarrow \nu^F(h, \psi)$, we have

$$\mathcal{L}(\hat{\psi}_T) \rightarrow \sum_{h \in \mathcal{H}} \sigma_h^2 + \sum_{h \in \mathcal{H}} (\nu^F(h, \psi_0) - \nu^F(h, \psi^*))^2 \text{ a.s. as } T \rightarrow \infty.$$

Since $\hat{\psi}_T$ is a least square estimator, $\mathcal{L}(\hat{\psi}_T) \leq \mathcal{L}(\psi_0) \rightarrow \sum_{h \in \mathcal{H}} \sigma_h^2$. It follows that

$$\sum_{h \in \mathcal{H}} (\nu^F(h, \psi_0) - \nu^F(h, \psi^*))^2 = 0$$

and thus $\nu(h, \psi^*) = \nu(h, \psi_0)$ for all $h \in \mathcal{H}$. \square

The asymptotic normality of the least square estimators should also be obtained by following, e.g., [16] and using the asymptotic normality of the F -madogram obtained in [24]. Nevertheless, the calculation of the asymptotic variance will require to calculate the covariances between $\nu^F(h_1, \psi)$ and $\nu^F(h_2, \psi)$, which is not straightforward.

5.3 Simulation study

This section is devoted to some simulations in order to evaluate the performance of the least square estimator and to compare it with the maximum composite likelihood estimator.

5.3.1 Analysis the behavior of $\nu^F(h)$

In order to have a comprehensive view of the behavior of $\nu^F(h)$, we have plotted in Figure 5.1. below $h \rightsquigarrow \nu^F(h)$. We have considered two max-mixture models MM1 and MM2 described below.

MM1 is a max-mixture between a TEG max-stable process X with exponential correlation function $\rho(h)$, correlation lengths θ_X and \mathcal{B} is chosen as a disk with fixed radius r_X ; and an inverse Smith max-stable process Y with covariance matrix $\Sigma = \sigma_Y \mathbf{I}_d$. The model parameters are given by the parameter vector $\psi = (a, r_X, \theta_X, \sigma_Y)^T \in [0, 1] \times [0, \infty) \times [0, \infty) \times [0, \infty)$. In this model, the pairwise max-mixture processes $(Z(s), Z(s+h))$ are asymptotically dependent at distance h up to $2r_X$ and asymptotically independent for all $h \geq 2r_X$;

MM2 is a max-mixture between a TEG max-stable process X and an inverse TEG max-stable process Y . Each of these two processes has exponential correlation function with different correlation lengths θ_X and θ_Y and different fixed radius r_X and r_Y , respectively. The parameter vector is $\psi = (a, r_X, \theta_X, r_Y, \theta_Y)^T \in [0, 1] \times [0, \infty) \times [0, \infty) \times [0, \infty) \times [0, \infty)$. In this model, the pairwise max-mixture processes $(Z(s), Z(s+h))$ are asymptotically dependent at distance h up to $2r_X$, asymptotically independent for $2r_X \geq h < 2r_Y$ and independent for all $h \geq 2r_Y$.

Figure 5.1. shows the behavior of the F -madogram for the models MM1 and MM2. For MM1, we have chosen $a = 0.5$, $r_X = 0.25$, $\theta_X = 0.2$ and $\sigma_Y = 0.6$. For MM2, we have chosen the same parameters as in MM1 for a and X and we have set $r_Y = 1.35$ and $\theta_Y = 0.8$. In this Figure, $\nu^F(h)$ has two sill one corresponding to X and the second corresponding to Y . This is completely in accordance with the nested variogram concept as presented in [72]. In data analysis, these two levels of the sill gives the researcher a hint about whether there is more than one spatial dependence structure in the data. Therefore, before the estimation procedure, it is appropriate to investigate if there are more than one dependence structures.

Figure 5.1. also shows that the behavior of $\nu^F(h)$ is the same as the risk measure $\mathcal{R}_1(\mathcal{A}, \mathcal{D}_Z^\nu)$ in Figure(4.2.3)(a) and (b) corresponding to MM2 and MM1, respectively. Therefore, it is the same behavior for the covariance function $Q(h, \nu)$ corresponding to the same models.

Finally, we shall see that the fact that the F -madogram expresses with all the model parameters is useful for the parameter estimation. On the contrary, when one considers the tail dependence function $\chi(h)$, it only involves the parameters from the max-stable part. The lower tail dependence function $\bar{\chi}(h)$ only involves the parameters from the inverse max-stable part.

5.3.2 Comparison of the estimation performance of $\hat{\psi}_T$ and $\hat{\psi}_L$

Recall that $\hat{\psi}_T$ denotes the least square estimator of the parameter vector ψ and $\hat{\psi}_L$ denotes the composite likelihood estimator.

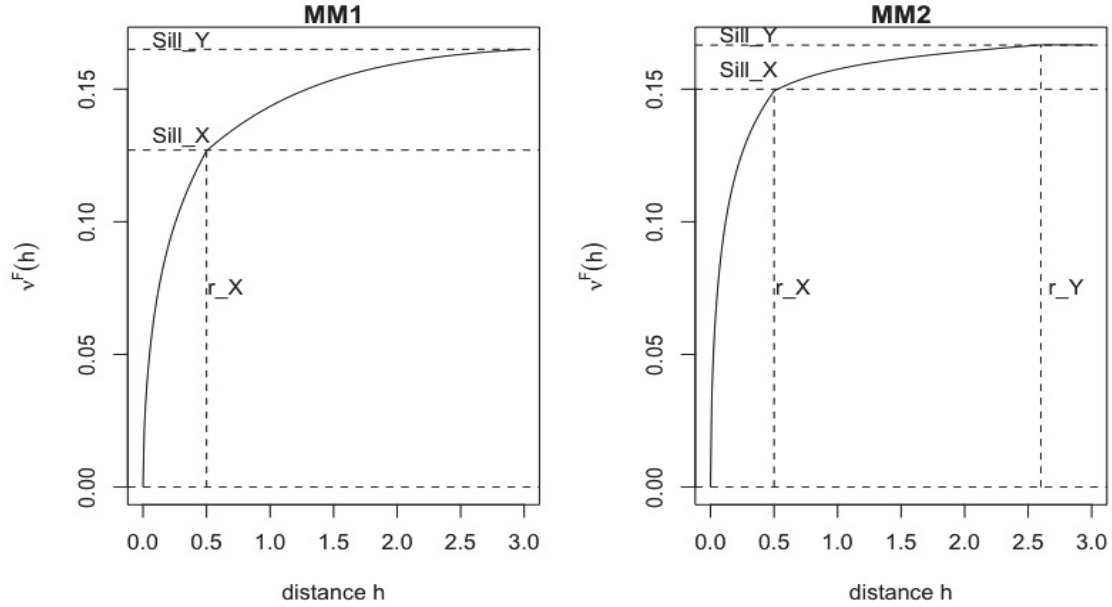


Figure 5.1: $h \rightsquigarrow \nu^F(h)$ for the max-mixture processes models MM1 and MM2. The model MM1 has correlation function $\rho(h) = \exp(-h/\theta_X)$, $r_X = 0.25$, $\theta_X = 0.2$ and $\sigma_Y = 0.6$. The model MM2 has correlation function $\rho_X(h) = \exp(-h/\theta_X)$ for X and $\rho_Y(h) = \exp(-h/\theta_Y)$ for Y with different correlation lengths θ_X and θ_Y . The fixed radiuses r_X and r_Y are plotted in the figure. For the two models, we set $a = 0.5$.

Outline the estimation experiment

In order to evaluate the performance of the non-linear least square estimator $\hat{\psi}_T$ as defined in (5.1.1), we have generated data from the two models, MM1 and MM2 above. The estimator $\hat{\psi}_T$ has been compared with true one ψ_0 and also with parameters estimated by composite likelihood estimator $\hat{\psi}_L$ proposed in [9] for the same data. For MM1, we considered 50 sites randomly and uniformly distributed in the square $\mathcal{A} = [0, 1]^2$. Since the dependence structure of MM2 is more complex, we have considered 150 sites randomly and uniformly distributed in the square $\mathcal{A} = [0, 3]^2$. For both models, the TEG X has parameters $r_X = 0.25$, $\theta_X = 0.20$. For inverse TEG Y , we set $r_Y = 1.3$, $\theta_Y = 0.9$.

For the two models MM1 and MM2, we have generated $T = 1000$ i.i.d observations for each site. These experiments replicated $J = 100$ time. We have considered several mixing parameters: $a := \{0, 0.25, 0.5, 0.75, 1\}$. For the composite likelihood estimator $\hat{\psi}_L$, we used the censored procedure with the threshold $u = 0.9$ of empirical quantile of data. The fitting of $\hat{\psi}_L$ was done using the code which was used in [9] with some modifications, since the MM2 model was not implemented.

Results on the parameters estimate

The following boxplots represent the error of estimated parameters, that is $(\hat{\psi}_T - \psi_0)$ and $(\hat{\psi}_L - \psi_0)$. Figures 5.2 and 5.3. display the performance of estimators for models MM1 and MM2, respectively. Generally, the estimators above worked well, although the variability in some estimates were relatively large, especially for the asymptotic independence parameters. It also shows some bias in the estimation of asymptotic independence model parameters.

It is well known that asymptotic independence is difficult to estimate, because the dependence between the process locations may decay very slowly when the distance increases (see [27]). Therefore, the estimation accuracy of the parameters is very sensitive, especially when dealing with more than one dependence structures. On one other hand, the fitting of $\alpha(h)$ which appears in TEG models in (2.3.25), is delicate and might quite get different estimates efficiency results with different data [26]. Furthermore, the dependence measures does not have all dependence information [24].

To compare the estimation efficiency between the estimators $\hat{\psi}_T$ and $\hat{\psi}_L$, the root mean square error (RMSE) was calculated for each estimated parameter based on the $J = 100$ experiments [75, 76]: $\hat{\psi}_j$ denotes the estimation (either least square or composite likelihood estimation) on the j th experiment.

$$\text{RMSE} = \left[J^{-1} \sum_{j=1}^J (\hat{\psi}_j - \psi)^2 \right]^{1/2}, \quad (5.3.1)$$

The barplots in Figures 5.4 and 5.5 display the RMSE for each parameter of MM1 and MM2 models. We see on these barplots that when a is close to 0 ($a = 0; 0.25$), the estimator $\hat{\psi}_T$ over-performs the estimator $\hat{\psi}_L$ and vice versa when $a \in \{0.75, 1\}$. For $a = 0.5$ the performance of the two estimators seems relatively equivalent.

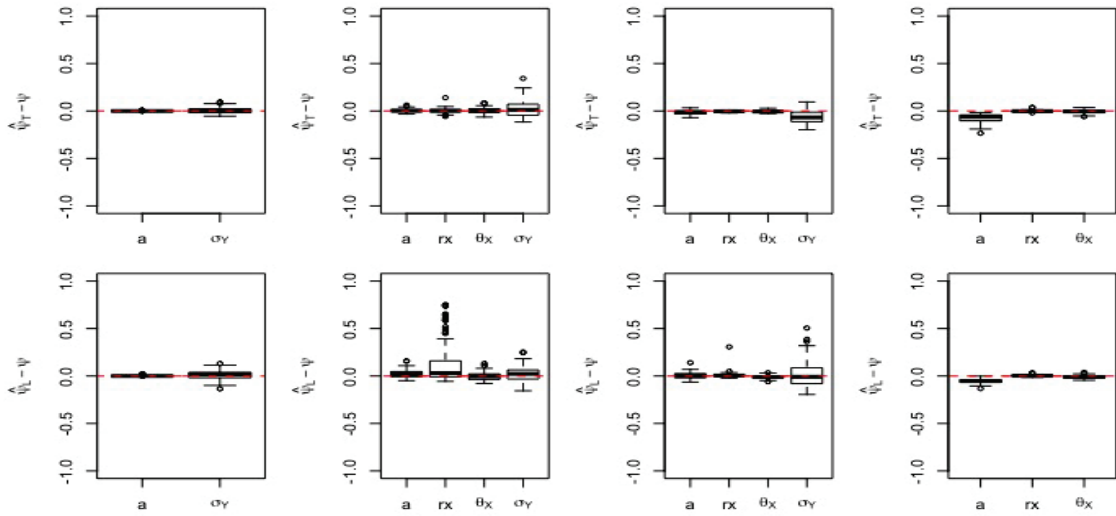


Figure 5.2: Boxplots display $(\hat{\psi} - \psi)$ of estimated parameters vector $\hat{\psi} = (\hat{a}, \hat{r}_X, \hat{\theta}_X, \hat{\sigma}_Y)^T$ for the MM1 model by the two estimators $\hat{\psi}_T$ and $\hat{\psi}_L$. The figures in the first row and from left to right concern the estimator $\hat{\psi}_T$ for $a \in \{0, 0.2, 0.75, 1\}$, the second row concerns $\hat{\psi}_L$. We have set, $r_X = 0.25$, $\theta_X = 0.20$ and $\sigma_Y = 0.6$ over a square $\mathcal{A} = [0, 1]^2$.

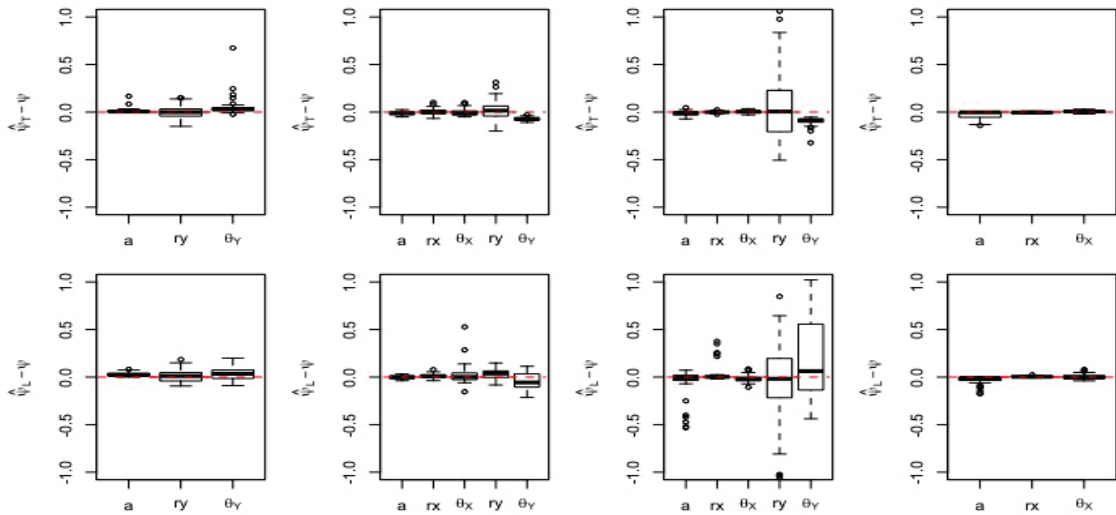


Figure 5.3: Boxplots display $(\hat{\psi} - \psi)$ of estimated parameters vector $\hat{\psi} = (\hat{a}, \hat{r}_X, \hat{\theta}_X, \hat{r}_Y, \hat{\theta}_Y)^T$ for MM2 model by the two estimators $\hat{\psi}_T$ and $\hat{\psi}_L$. The figures in the first row and from left to right concern the estimator $\hat{\psi}_T$ for $a \in \{0, 0.2, 0.75, 1\}$, the second row concerns $\hat{\psi}_L$. We have set, $r_X = 0.25$, $\theta_X = 0.20$, $r_Y = 1.3$ and $\theta_Y = 0.9$ over a square $\mathcal{A} = [0, 3]^2$.

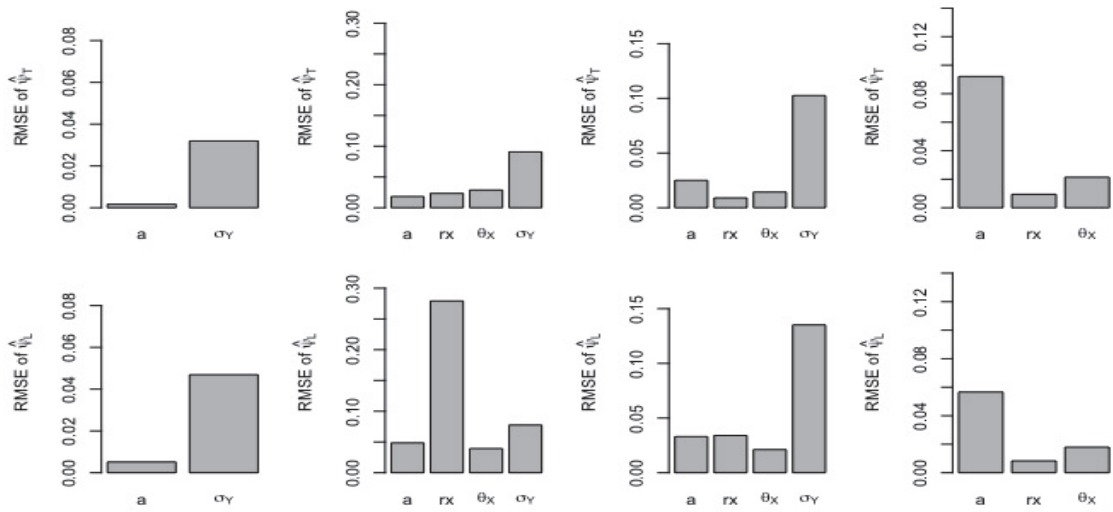


Figure 5.4: Barplots display the RMSE of $\hat{\psi}$ for each estimated parameters $\hat{\psi} = (\hat{a}, \hat{r}_X, \hat{\theta}_X, \hat{\sigma}_Y)^T$ for MM1 and the corresponding two estimators $\hat{\psi}_T$ and $\hat{\psi}_L$. The bars in the first row and from left to right represent the RMSE of the estimator $\hat{\psi}_T$ when $a := \{0, 0.2, 0.75, 1\}$, respectively and the same for the second row for $\hat{\psi}_L$. We set $r_X = 0.25$, $\theta_X = 0.20$ and $\sigma_Y = 0.6$ over a square $\mathcal{A} = [0, 1]^2$.

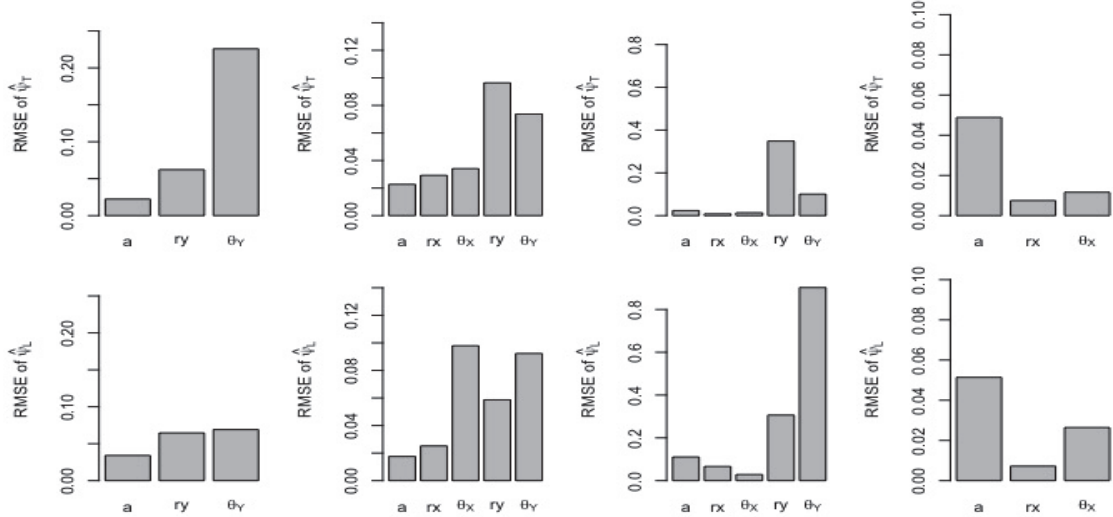


Figure 5.5: Barplots display the RMSE of $\hat{\psi}$ for each estimated parameters $\hat{\psi} = (\hat{a}, \hat{r}_X, \hat{\theta}_X, \hat{r}_Y, \hat{\theta}_Y)^T$ for MM2 and the corresponding two estimators $\hat{\psi}_T$ and $\hat{\psi}_L$. The bars in the first row and from left to right represent the RMSE of the estimator $\hat{\psi}_T$ when $a := \{0, 0.2, 0.75, 1\}$, respectively and the same for the second row for $\hat{\psi}_L$. We set $r_X = 0.25$, $\theta_X = 0.20$, $r_Y = 1.3$ and $\theta_Y = 0.9$ over a square $\mathcal{A} = [0, 3]^2$.

Chapter 6

Conclusions

6.1 Conclusion Remarks

We have proposed a spatial risk measure $\mathcal{R}(\mathcal{A}, \mathcal{D}_{X,u}^+)$ for Gaussian spatial process and developed the study of the risk measure $\mathcal{R}(\mathcal{A}, \mathcal{D}_X^\nu)$ for extreme spatial processes allowing asymptotic dependence and asymptotic independence. In addition, explicit formula of $\mathcal{R}(\mathcal{A}, \mathcal{D}_X^\nu)$ for TEG max-stable process has been provided. All these risk measures are sensitive with spatial dependence structure over a region. Such risk measures could calculate any bounded region but we took the benefit from the isotropic property of the processes to reduce the dimensional integration for some specific bounded region shapes, such as disk and square.

For asymptotic/ complete independence spatial processes, we showed by Corollaries 3.6 and 3.12 that we have only the loss magnitude $\mathcal{R}_0(\mathcal{A}, \mathcal{D}_X)$ to assess the risks, when the regions under study is big enough to make $\mathcal{R}_1(\mathcal{A}, \mathcal{D}_X)$ tends or equal to 0. In such a case, we can conclude that the corresponding damage functions $(\mathcal{D}_X(\cdot), \mathcal{D}(\cdot + h))$ belong to a not compact region with spatial independence.

We showed that some axioms are valid for any stationary processes. Properties such as anti-monotonicity is verified for isotropic Gaussian processes and isotropic stationary max-mixture processes (the same result holds for some max-stable processes, see [44]).

We emphasized the behavior of these risk measures with respect to the various parameters by a simulation study. It shows that the risk measures $\mathcal{R}(\mathcal{A}, \mathcal{D}_{X,u}^+)$ and $\mathcal{R}(\mathcal{A}, \mathcal{D}_X^\nu)$ are usually good tools in order to assess the risks, comparing to the intuitive Monte-Carlo computation.

With respect to the covariance damage function $\mathcal{G}(h, u)$ for Gaussian process, there are some difficulties in approximating the covariance of damage functions $(\mathcal{D}_{X,u}^+(\cdot), \mathcal{D}_{X,u}^+(\cdot + h))$, when the corresponding threshold u is high, even when a strong depen-

dence exists. The justification of this difficulty is that there is not enough data over u in order to approximate \mathcal{G} . We implemented $\mathcal{R}(\mathcal{A}, \mathcal{D}_{Y, \log u}^+)$ on the air pollution case study, and this example showed the interest of using the variance of $L(\mathcal{A}, \mathcal{D}_{Y, \log u}^+)$ as a spatial risk measure in concrete cases. With respect to $\mathcal{R}_1(\lambda \mathcal{A}, \mathcal{D}_X^\nu)$ for max-stable or inverse max-stable processes, we showed that their behavior also mimics the one of $\chi(h)$ in the max-stable case, or $\bar{\chi}(h)$ in the inverse max-stable case. For max-mixture, the behavior of $\mathcal{R}_1(\lambda \mathcal{A}, \mathcal{D}_X^\nu)$ mimics the proposed F-madogram $\nu^F(h)$.

We have also provided F-madogram $\nu^F(h)$ for the max-mixture process that can detect more than one dependence structure in a model (i.e. asymptotic dependence and asymptotic independence). The F-madogram presents the advantage of having both extremal coefficient $\Theta(h)$ of the max-stable process and $\eta(h)$ of the inverse max-stable in its expression. When $a = 1$, $\nu^F(h)$ is the F-madogram corresponding to a max-stable process introduced by [24] and so switches to $\Theta(h)$; when $a = 0$, $\nu^F(h)$ represents the F-madogram of an inverse max-stable and switches to $\eta(h)$. We defined a semi-parametric estimation procedure using F-madogram $\nu^F(h)$ as an alternative to composite likelihood. The simulation study showed that the estimation procedure based on $\nu^F(h)$ performs better than the composite likelihood procedure when the model is near to asymptotic independence.

6.2 Future work

Anisotropy is often observed in environmental phenomenon, especially when the regions are very large; but while isotropic models have been widely studied, only few studies have been treated as anisotropic case. For example, anisotropic variogram has been proposed. This variogram is based on coordinate transformation according to the type of anisotropy (geometric or zonal) (see [50] and [31]). In a case study in Middle European westerly winds data, the semivariogram was defined as a dependence structure of max-stable process in order to summarize the dependence parameters ([17]). While [13] inserted the geometric or zonal anisotropy into a spatial isotropic models, this procedure was adopted by [17] to propose an anisotropic Brown-Resnick max-stable model. Based on [50], our suggestion is to include the concept of anisotropy, such as the coordinate transformation of the risk measures and also in F-madogram so to be suitable for semi-parametric estimation procedure for anisotropic spatial processes. Finally, we could develop the risk measures in order to take into account the time dependence (spatio-temporal risk measures) and also to adapt the F-madogram in a spatio-temporal case and then develop the semi-parametric estimation procedure.

Appendix A

A.1 Moments of truncated bivariate Gaussian distribution

We shall present the results giving the moments of a truncated standard bivariate Gaussian random variable proved by [60]. Let $\ell(u, v, w)$ be total probability of the truncated bivariate standard Gaussian distribution with correlation function w , such that

$$\ell(u, v, w) = \frac{1}{2\pi(1-w^2)^{1/2}} \int_u^\infty \int_v^\infty e^{\left\{\frac{-1}{2(1-w^2)}[x^2-2wxy+y^2]\right\}} dx dy, \quad (\text{A.1.1})$$

where u and v are the truncated points corresponding to x and y respectively. Let $u = v$, then the first moment m_{10} and the product moment m_{11} respectively are

$$m_{10} = \frac{(1+\rho)\varphi(u)}{\ell(u, u, \rho)} \bar{\Phi}\left(\frac{u(1-\rho)}{(1-\rho^2)^{1/2}}\right) \quad (\text{A.1.2})$$

and

$$m_{11} = \rho + \frac{2\rho u\varphi(u)}{\ell(u, u, \rho)} \bar{\Phi}\left(\frac{u(1-\rho)}{(1-\rho^2)^{1/2}}\right) + \frac{(1-\rho^2)^{1/2}}{\sqrt{2\pi}\ell(u, u, \rho)} \varphi\left(\frac{(2u^2(1-\rho))^{1/2}}{(1-\rho^2)^{1/2}}\right). \quad (\text{A.1.3})$$

Proof. For sake of simplicity, we will only consider the case $u = v$. Recalling that

$$m_{10} = \frac{1}{2\pi(1-\rho^2)^{1/2}\ell(u, u, w)} \int_u^\infty e^{\frac{-1}{2(1-\rho^2)}y^2} \int_u^\infty x e^{\frac{-1}{2(1-\rho^2)}(x^2-2\rho xy)} dx dy.$$

By adding and subtracting $\rho^2 y^2$ in the expression $(x^2 - 2\rho xy)$, we get

$$= \frac{1}{2\pi(1-\rho^2)^{1/2}\ell(u, u, w)} \int_u^\infty e^{\frac{-1}{2}y^2} \int_u^\infty x e^{\frac{-1}{2(1-\rho^2)}(x-\rho y)^2} dx dy.$$

Let, $z_1 = x - \rho y / (1 - \rho^2)^{1/2}$. We set $x = z_1(1 - \rho^2)^{1/2} + \rho y$ and $v_1 = u - \rho y / (1 - \rho^2)^{1/2}$, such that:

$$\begin{aligned} \ell(u, u, w)m_{10} &= \frac{1}{2\pi(1 - \rho^2)^{1/2}} \int_u^\infty e^{\frac{-1}{2}y^2} \int_{v_1}^\infty (z_1(1 - \rho^2)^{1/2} + \rho y) e^{\frac{-1}{2}z_1^2} (1 - \rho^2)^{1/2} dz_1 dy \\ &= \frac{1}{2\pi} \int_u^\infty e^{\frac{-1}{2}y^2} \left[(1 - \rho^2)^{1/2} \int_{v_1}^\infty z_1 e^{\frac{-1}{2}z_1^2} dz_1 + \rho y \int_{v_1}^\infty e^{\frac{-1}{2}z_1^2} dz_1 \right] dy \\ &= \frac{(1 - \rho^2)^{1/2}}{2\pi} \int_u^\infty e^{\frac{-1}{2}(y^2 + v_1^2)} dy + \frac{\rho}{2\pi} \int_u^\infty y e^{\frac{-1}{2}y^2} Q(v_1) dy := A_1 + A_2, \end{aligned} \quad (\text{A.1.4})$$

where $Q(t) = \int_t^\infty e^{-\frac{1}{2}x^2} dx$.

For the first term A_1 in the equation (A.1.4) and by adding and subtracting $\rho^2 u^2$ in the the quantity $(y^2 + v_1^2)$, we get

$$A_1 = \frac{(1 - \rho^2)}{2\pi} e^{\frac{-1}{2}u^2} Q\left(\frac{u(1 - \rho)}{(1 - \rho^2)^{1/2}}\right) = (1 - \rho^2) \varphi(u) \bar{\Phi}\left(\frac{u(1 - \rho)}{(1 - \rho^2)^{1/2}}\right). \quad (\text{A.1.5})$$

By integrating by parts the second term A_2 , we get

$$A_2 = \rho(1 + \rho) \varphi(u) \bar{\Phi}\left(\frac{u(1 - \rho)}{(1 - \rho^2)^{1/2}}\right). \quad (\text{A.1.6})$$

Substituting the equations (A.1.5) and (A.1.6) in (A.1.4) we obtain:

$$\begin{aligned} \ell(u, u, w)m_{10} &= (1 - \rho^2) \varphi(u) \bar{\Phi}\left(\frac{u(1 - \rho)}{(1 - \rho^2)^{1/2}}\right) + \rho(1 + \rho) \varphi(u) \bar{\Phi}\left(\frac{u(1 - \rho)}{(1 - \rho^2)^{1/2}}\right) \\ &= (1 + \rho) \varphi(u) \bar{\Phi}\left(\frac{u(1 - \rho)}{(1 - \rho^2)^{1/2}}\right) \end{aligned}$$

and therefore the equation (A.1.2) satisfied.

Concerning the product moment m_{11} , recall that

$$m_{11} = \frac{1}{2\pi(1 - \rho^2)^{1/2} \ell(u, u, w)} \int_u^\infty y e^{\frac{-1}{2(1 - \rho^2)}y^2} \int_u^\infty x e^{\frac{-1}{2(1 - \rho^2)}(x^2 - 2\rho xy)} dx dy.$$

In the same way as for m_{10} , we get

$$\ell(u, u, w)m_{11} = \frac{(1 - \rho^2)^{1/2}}{2\pi} \int_u^\infty y e^{\frac{-1}{2}(y^2 + v_1^2)} dy + \frac{\rho}{2\pi} \int_u^\infty y^2 e^{\frac{-1}{2}y^2} Q(v_1) dy := A_3 + A_4. \quad (\text{A.1.7})$$

By adding and subtracting $\pm\rho^2u^2$ in the quantity $(y^2 + v_1^2)$ in the first term A_3 and letting $z_2 = (y - \rho u)/(1 - \rho^2)^{1/2}$ then by variable change, we get for $v_2 = (u(1 - \rho))/(1 - \rho^2)^{1/2}$

$$\begin{aligned}
A_3 &= \frac{(1 - \rho^2)^{1/2}}{2\pi} e^{\frac{-1}{2}u^2} \int_{v_2}^{\infty} (z_2(1 - \rho^2)^{1/2} + \rho u) e^{\frac{-1}{2}z_2^2} (1 - \rho^2)^{1/2} dz_2 \\
&= \frac{(1 - \rho^2)}{2\pi} e^{\frac{-1}{2}u^2} \left[(1 - \rho^2)^{1/2} e^{\frac{-1}{2}v_2^2} + \rho u Q(v_2) \right] \\
&= \frac{(1 - \rho^2)}{2\pi} \left[(1 - \rho^2)^{1/2} e^{\frac{-1}{2(1-\rho^2)}2u^2(1-\rho)} + \rho u e^{\frac{-1}{2}u^2} Q(v_2) \right]. \\
&= (1 - \rho^2) \left[\frac{(1 - \rho^2)^{1/2}}{\sqrt{2\pi}} \varphi\left(\frac{(2u^2(1 - \rho))^{1/2}}{(1 - \rho^2)^{1/2}}\right) + \rho u \varphi(u) \bar{\Phi}\left(\frac{u(1 - \rho)}{(1 - \rho^2)^{1/2}}\right) \right]
\end{aligned} \tag{A.1.8}$$

By integration by parts the second term A_4 we get

$$\begin{aligned}
A_4 &= \rho u \varphi(u) \bar{\Phi}\left(\frac{u(1 - \rho)}{(1 - \rho^2)^{1/2}}\right) + \rho^2 \left[\frac{(1 - \rho^2)^{1/2}}{\sqrt{2\pi}} \varphi\left(\frac{(2u^2(1 - \rho))^{1/2}}{\sqrt{1 - \rho^2}}\right) \right. \\
&\quad \left. + \rho u \varphi(u) \bar{\Phi}\left(\frac{u(1 - \rho)}{(1 - \rho^2)^{1/2}}\right) \right] + \rho \ell(u, v, \rho).
\end{aligned} \tag{A.1.9}$$

Substituting equations (A.1.8) and (A.1.9) in (A.1.7), we obtain

$$\begin{aligned}
\ell(u, u, w) m_{11} &= (1 - \rho^2) \left[\frac{(1 - \rho^2)^{1/2}}{\sqrt{2\pi}} \varphi\left(\frac{(2u^2(1 - \rho))^{1/2}}{(1 - \rho^2)^{1/2}}\right) \right] + \rho u \varphi(u) \bar{\Phi}\left(\frac{u(1 - \rho)}{(1 - \rho^2)^{1/2}}\right) \\
&\quad + \rho^2 \left[\frac{(1 - \rho^2)^{1/2}}{\sqrt{2\pi}} \varphi\left(\frac{(2u^2(1 - \rho))^{1/2}}{(1 - \rho^2)^{1/2}}\right) + \rho u \varphi(u) \bar{\Phi}\left(\frac{u(1 - \rho)}{(1 - \rho^2)^{1/2}}\right) \right] \\
&\quad + \rho \ell(u, u, \rho)
\end{aligned}$$

and therefore the equation (A.1.3) satisfied. \square

A.2 Proof Corollary 3.5

Let X be an isotropic standard Gaussian process on $\mathbb{S} \subset \mathbb{R}^2$ with auto-correlation function ρ . Let $\mathcal{A} \subset \mathbb{S}$ be either a disk or a square. The mapping $\lambda \mapsto \mathcal{R}_1(\lambda \mathcal{A}, \mathcal{D}_{X,u}^+)$ is non-increasing if and only if $h \mapsto \rho(h)$, $h > 0$ is non-increasing and non-negative. Case where \mathcal{A} is a square.

Proof. Recalling that

$$\mathcal{R}_1(\lambda\mathcal{A}, \mathcal{D}_{X,u}^+) = \int_{h=0}^{\sqrt{2}R} f_{disk}(h, R) \mathcal{G}(\lambda h, u) dh, \quad (\text{A.2.1})$$

if the partial derivative $\frac{\partial}{\partial \lambda} \mathcal{G}(\lambda h, u)$ exists and is continuous then

$$\frac{\partial}{\partial \lambda} \mathcal{R}_1(\lambda\mathcal{A}, \mathcal{D}_{X,u}^+) = \int_{h=0}^{\sqrt{2}R} f_{disk}(h, R) \frac{\partial}{\partial \lambda} \mathcal{G}(\lambda h, u) dh. \quad (\text{A.2.2})$$

As f_{square} is a positive function of the variables of $\mathcal{R}_1(\lambda\mathcal{A}, \mathcal{D}_{X,u}^+)$ and also of the variables of $\mathcal{G}(\lambda h, u)$. Let then study the partial derivative of \mathcal{G} with respect to λ .

$$\begin{aligned} \frac{\partial}{\partial \lambda} \mathcal{G}(\lambda h, u) &= \frac{\partial}{\partial \lambda} \left[\ell(u, u, \rho(\lambda h)) (\rho(\lambda h) + u^2) \right] - \frac{\partial}{\partial \lambda} \left[2u\varphi(u) \bar{\Phi} \left(\frac{u(1 - \rho(\lambda h))}{(1 - \rho^2(\lambda h))^{1/2}} \right) \right] \\ &+ \frac{\partial}{\partial \lambda} \left[(1 - \rho^2(\lambda h))^{1/2} \varphi^2 \left(\frac{u}{(1 + \rho(\lambda h))^{1/2}} \right) \right] := \text{A31} + \text{A32} + \text{A33} \end{aligned} \quad (\text{A.2.3})$$

The first term in Equation (A.2.3)

In the article [34], the authors proved that the derivative of $\ell(u, u, w)$ with respect to w is $\varphi(u, u, w)$ and then we have

$$\begin{aligned} \text{A31} &= \frac{\partial}{\partial \lambda} \left[\ell(u, u, \rho(\lambda h)) (\rho(\lambda h) + u^2) \right] \\ &= h\rho'(\lambda h) \varphi(u, u, \rho(\lambda h)) (u^2 + h\rho(\lambda h)) + \rho'(\lambda h) \ell(u, u, \rho(\lambda h)) \\ &= h\rho'(\lambda h) [\varphi(u, u, \rho(\lambda h)) (u^2 + \rho(\lambda h)) + \ell(u, u, \rho(\lambda h))]. \end{aligned} \quad (\text{A.2.4})$$

Note that

$$\begin{aligned} \phi(u, u, w) &= \frac{1}{2\pi\sqrt{1-w^2}} \exp \left\{ \frac{-1}{2(1-w^2)} (u^2 + u^2 - 2u^2w) \right\} \\ &= \frac{1}{2\pi\sqrt{1-w^2}} \exp \left\{ \frac{-2u^2(1-w)}{2(1-w^2)} \right\} \\ &= \frac{1}{2\pi\sqrt{1-w^2}} \exp \left\{ \frac{-u^2}{(1+w)} \right\} \\ &= \frac{1}{(1-w^2)^{1/2}} \phi^2 \left(\frac{u}{(1+w)^{1/2}} \right). \end{aligned}$$

Therefore

$$A31 = h\rho'(\lambda h) \left[\frac{(u^2 + \rho(\lambda h))}{(1 - \rho^2(\lambda h))^{1/2}} \varphi^2 \left(\frac{u}{(1 + \rho^2(\lambda h))^{1/2}} \right) + \ell(u, u, \rho(\lambda h)) \right]. \quad (\text{A.2.5})$$

The second term in Equation (A.2.3)

$$\begin{aligned} A32 &= 2u\varphi(u)\varphi \left(\frac{u(1 - \rho(\lambda h))}{(1 - \rho^2(\lambda h))^{1/2}} \right) \frac{\partial}{\partial \lambda h} \left(\frac{u(1 - \rho(\lambda h))}{(1 - \rho^2(\lambda h))^{1/2}} \right) \\ &= h\rho'(\lambda h)\varphi(u)\varphi \left(\frac{u(1 - \rho(\lambda h))}{(1 - \rho^2(\lambda h))^{1/2}} \right) \left(\frac{-2u^2\rho(\lambda h)}{(1 + \rho(\lambda h))(1 - \rho^2(\lambda h))^{1/2}} \right). \end{aligned} \quad (\text{A.2.6})$$

Note that

$$\begin{aligned} \phi(u)\phi \left(\frac{u(1 - w)}{(1 - w^2)^{1/2}} \right) &= \frac{1}{\sqrt{2\pi}} \exp \left\{ \frac{-u^2}{2} \right\} \frac{1}{\sqrt{2\pi}} \exp \left\{ \frac{-u^2(1 - w)^2}{(1 - w^2)} \right\} \\ &= \frac{1}{2\pi} \exp \left\{ \frac{-u^2}{2} \left[1 + \frac{(1 - w)}{(1 + w)} \right] \right\} \\ &= \frac{1}{2\pi} \exp \left\{ \frac{-u^2}{(1 + w)} \right\} \\ &= \phi^2 \left(\frac{u}{(1 + w)^{1/2}} \right). \end{aligned} \quad (\text{A.2.7})$$

Therefore

$$A32 = h\rho'(\lambda h)\varphi^2 \left(\frac{u}{(1 + \rho(\lambda h))^{1/2}} \right) \left(\frac{-2u^2\rho(\lambda h)}{(1 + \rho(\lambda h))(1 - \rho^2(\lambda h))^{1/2}} \right). \quad (\text{A.2.8})$$

The third term in Equation (A.2.3)

$$A33 = h\rho'(\lambda h)\varphi^2 \left(\frac{u}{(1 + \rho(\lambda h))^{1/2}} \right) \left[\frac{u(1 - \rho^2(\lambda h))^{1/2}}{(1 + \rho(\lambda h))^{3/2}} - \frac{\rho(\lambda h)}{(1 - \rho^2(\lambda h))^{1/2}} \right]. \quad (\text{A.2.9})$$

Substituting equations (A.2.5), (A.2.8) and (A.2.9) in (A.2.3) gives

$$\begin{aligned} \frac{\partial}{\partial \lambda} \mathcal{G}(\lambda h, u) &= h\rho'(\lambda h)\varphi^2 \left(\frac{u}{(1 + \rho(\lambda h))^{1/2}} \right) \left[\frac{(u^2 + \rho(\lambda h))}{(1 - \rho^2(\lambda h))^{1/2}} + \frac{-2u^2\rho(\lambda h)}{(1 + \rho(\lambda h))(1 - \rho^2(\lambda h))^{1/2}} \right. \\ &\quad \left. + \frac{u(1 - \rho^2(\lambda h))^{1/2}}{(1 + \rho(\lambda h))^{3/2}} + \frac{-\rho(\lambda h)}{(1 - \rho^2(\lambda h))^{1/2}} \right] + h\rho'(\lambda h)\ell(u, u, \rho(\lambda h)) \end{aligned} \quad (\text{A.2.10})$$

$$\begin{aligned}
&= h\rho'(\lambda h)\varphi^2\left(\frac{u}{(1+\rho(\lambda))^{1/2}}\right)\left[\frac{u^2(1+\rho(\lambda h)-2\rho(\lambda h))+u(1-\rho(\lambda h))^{1/2}(1-\rho^2(\lambda h))^{1/2}}{(1+\rho(\lambda h))(1-\rho^2(\lambda h))^{1/2}}\right] \\
&\quad +h\rho'(\lambda h)\ell(u,u,\rho(\lambda h)) \\
&= h\rho'(\lambda h)\varphi^2\left(\frac{u}{(1+\rho(\lambda))^{1/2}}\right)\left[\frac{u^2(1-\rho(\lambda h))+u(1-\rho(\lambda h))(1+\rho(\lambda h))^{1/2}}{(1+\rho(\lambda h))(1-\rho^2(\lambda h))^{1/2}}\right] \\
&\quad +h\rho'(\lambda h)\ell(u,u,\rho(\lambda h)) \\
&= \rho'(\lambda h)\left\{h\varphi^2\left(\frac{u}{(1+\rho(\lambda))^{1/2}}\right)\left[\frac{u^2(1-\rho(\lambda h))+u(1-\rho(\lambda h))(1+\rho(\lambda h))^{1/2}}{(1+\rho(\lambda h))(1-\rho^2(\lambda h))^{1/2}}\right]\right. \\
&\quad \left.+h\ell(u,u,\rho(\lambda h))\right\}.
\end{aligned} \tag{A.2.11}$$

The positive term in the big arcs in Equation (A.2.11) gives that the spatial covariance function $\mathcal{G}(\lambda h, u)$ is non-increasing if and only if $\rho(\lambda h)$ is non-increasing as λ . Then,

$$\mathcal{R}_1(\lambda\mathcal{A}, \mathcal{D}_{X,u}^+) \searrow \quad \text{iff} \quad \frac{\partial}{\partial\lambda}\rho(\lambda h) \leq 0$$

□

Appendix B

Semi-Parametric estimation using dependence measures

B.1 Estimation procedure

The semi-parametric estimation procedure introduced in this section is based on the minimization of the square difference between the empirical dependence measure and the theoretical one. The dependence measures we adopted in this procedure are upper/ lower tail dependence measures $\chi(h, u)$ and $\bar{\chi}(h, u)$ respectively, in addition to the F-madogram $\nu^F(h)$. We shall evaluate the performance of this procedure according to max-mixture model Z defined in 2.16.

Consider $Z^t, t = 1, \dots, T$, T copies of an isotropic max-mixture process Z with unit Frechet margin F . Then $(Z^t)_{t=1, \dots, T}$ are i.i.d observations and satisfy α -mixing property. Let \mathcal{H} be a finite subset of \mathbb{S} and $\psi \in \Psi$, $\Psi \subset \mathbb{R}^d$ is compact and $\psi \mapsto \nu^F(h, \psi)$ is continuous for all $h \in \mathcal{H}$. The estimation procedure is obtained as following:

First step, we need to calculate the empirical $\hat{\chi}(h, u)$ and $\hat{\bar{\chi}}(h, u)$. It is easy to write the empirical versions from the empirical distributions. We get,

$$\hat{\chi}(h, u) = 2 - \frac{\log \left(T^{-1} \sum_{t=1}^T \mathbb{1}_{\{U_t(s) < u, U_t(s+h) < u\}} \right)}{\log \left(T^{-1} \sum_{t=1}^T \mathbb{1}_{U_t(s) < u} \right)}$$

and

$$\hat{\bar{\chi}}(h, u) = \frac{2 \log \left(T^{-1} \sum_{t=1}^T \mathbb{1}_{\{U_t(s) > u\}} \right)}{\log \left(T^{-1} \sum_{t=1}^T \mathbb{1}_{\{U_t(s) > u, U_t(s+h) > u\}} \right)} - 1.$$

From the empirical F-madogram introduced in [24], we have

$$\hat{\nu}^F(h) = T^{-1} \sum_{t=1}^T 0.5 |U_t(s) - U_t(s+h)|,$$

where $U_t = F(Z^t)$ and F has Frechet margin.

Second step: we solve one of the following optimization problems

$$\hat{\psi}_\chi = \operatorname{argmin}_\psi \sum_{h \in \mathcal{H}} (\hat{\chi}(h, u) - \chi_\psi(h, u))^2$$

or

$$\hat{\psi}_{\bar{\chi}} = \operatorname{argmin}_\psi \sum_{h \in \mathcal{H}} (\hat{\chi}(h, u) - \bar{\chi}_\psi(h, u))^2$$

or

$$\hat{\psi}_\nu = \operatorname{argmin}_\psi \sum_{h \in \mathcal{H}} (\hat{\nu}^F(h) - \nu^F(h, \psi))^2.$$

From the definition of max-mixture model, it easy to deduce the corresponding upper /lower tail dependence measures

$$\begin{aligned} \chi_\psi(h, u) &= 2 - \frac{\log \mathbb{P}(F(Z(s)) < u, F(Z(s+h)) < u)}{\log \mathbb{P}(F(Z(s)) < u)} \\ &= 2 - \frac{\log \mathbb{P}(Z(s) < F^{-1}(u), Z(s+h) < F^{-1}(u))}{\log \mathbb{P}(Z(s) < F^{-1}(u))} \end{aligned}$$

From the definition of max-mixture, we have

$$\begin{aligned} &= 2 - \frac{\log (u^{a\Theta_X(h; \psi_X)} [2u^{(1-a)} - 1 + (1 - u^{(1-a)})^{\Theta_Y(h; \psi_Y)}])}{\log(u)} \\ &= 2 - a\Theta_X(h; \psi_X) - \frac{\log (2u^{(1-a)} - 1 + (1 - u^{(1-a)})^{\Theta_Y(h; \psi_Y)})}{\log(u)}. \end{aligned} \tag{B.1.1}$$

In the same way, we have also

$$\bar{\chi}_\psi(h, u) = \frac{2 \log(1 - u)}{\log \left(1 - 2u + u^{a\Theta_X(h; \psi_X)} [2u^{(1-a)} - 1 + (1 - u^{(1-a)})^{\Theta_Y(h; \psi_Y)}] \right)} - 1. \tag{B.1.2}$$

When $\psi := \{a, \psi_X, \psi_Y\}$.

B.2 Evaluating the performance of the estimators

In order to evaluate the performance of the estimators $\hat{\psi}$ corresponding to the different dependence measures $\chi(h, u)$, $\bar{\chi}(h, u)$ and $\nu^F(h)$, we adopted the model MM1 in section 5.3.1 with the same setting used in evaluation. We change the number of sites N to 50 (instead of 100 in section 5.3.1 and the threshold is fixed to $u = 0.9$). The following boxplots and barplots represent the performance of the proposed estimators for the three dependence measures mentioned previously or $a := \{0, 0.25, 0.75, 1\}$. For $a = 0.5$, we have approximately the same result as in the case $a = 0.25$.

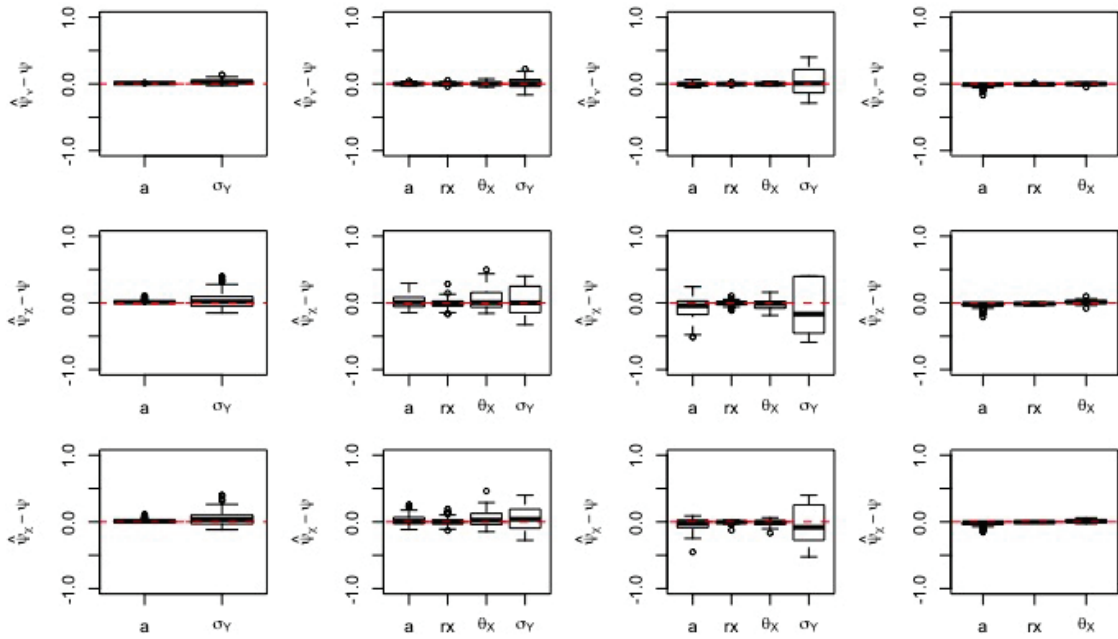


Figure B.1: Boxplots display $(\hat{\psi} - \psi)$ of estimated parameters vector $\hat{\psi} = (\hat{a}, \hat{r}_X, \hat{\theta}_X, \hat{\sigma}_Y)^T$ for MM1 model using the three different estimators $\hat{\psi}_\chi$, $\hat{\psi}_{\bar{\chi}}$ and $\hat{\psi}_\nu$. The first row corresponds to the estimator $\hat{\psi}_\chi$, the second row concerns $\hat{\psi}_{\bar{\chi}}$ and the third $\hat{\psi}_\nu$. From left to right, we fixed $a := \{0, 0.2, 0.75, 1\}$. We have set $r_X = 0.25$, $\theta_X = 0.20$ and $\sigma_Y = 0.6$ over a square $\mathcal{A} = [0, 1]^2$.

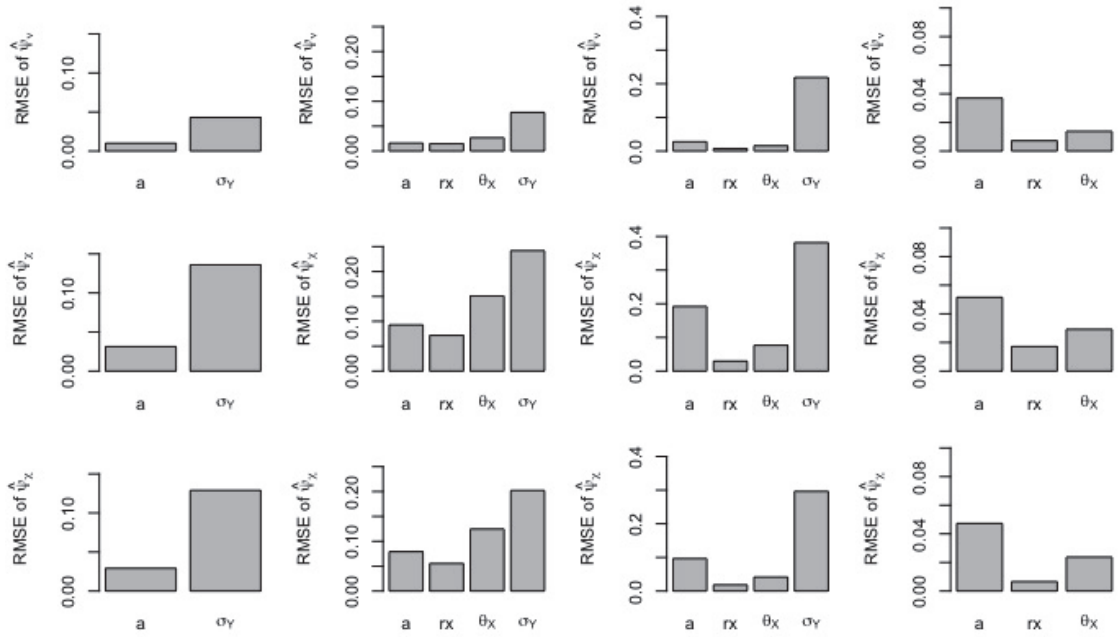


Figure B.2: Barplots represent the root mean square error RMSE of estimated parameters vector $\hat{\psi} = (\hat{a}, \hat{r}_X, \hat{\theta}_X, \hat{\sigma}_Y)^T$ for MM1 model corresponding to the three estimators $\hat{\psi}_\chi$, $\hat{\psi}_{\bar{X}}$ and ψ_ν . The first line corresponds to the results obtained for $\hat{\psi}_\chi$, second to the results for $\hat{\psi}_{\bar{X}}$ and third to ψ_ν . From left to right, we represent the results for $a := \{0, 0.2, 0.75, 1\}$. We have set $r_X = 0.25$, $\theta_X = 0.20$ and $\sigma_Y = 0.6$ over a square $\mathcal{A} = [0, 1]^2$.

Bibliography

- [1] P. Abrahamsen. *A review of Gaussian random fields and correlation functions*. Norsk Regnesentral/Norwegian Computing Center, 1997.
- [2] A. AghaKouchak and N. Nasrollahi. Semi-parametric and parametric inference of extreme value models for rainfall data. *Water resources management*, 24(6):1229–1249, 2010.
- [3] M. Ahmed, V. Maume-Deschamps, P. Ribereau, and C. Vial. Spatial risk measure for gaussian processes. *arXiv preprint arXiv:1612.08280*, 2016.
- [4] M. Ahmed, V. Maume-Deschamps, P. Ribereau, and C. Vial. Risk measures for max-stable and max-mixture spatial processes. Submitted, 2017.
- [5] A. Antoniadis, J. Berruyer, and C. René. *Régression non linéaire et applications*. Economica, 1992.
- [6] P. Artzner, F. Delbaen, J.-M. Eber, and D. Heath. Coherent measures of risk. *Mathematical finance*, 9(3):203–228, 1999.
- [7] J-N. Bacro, L. Bel, and C. Lantuéjoul. Testing the independence of maxima: from bivariate vectors to spatial extreme fields. *Extremes*, 13(2):155–175, 2010.
- [8] J-N. Bacro and C. Gaetan. Estimation of spatial max-stable models using threshold exceedances. *Statistics and Computing*, 24(4):651–662, 2014.
- [9] J-N. Bacro, C. Gaetan, and G. Toulemonde. A flexible dependence model for spatial extremes. *Journal of Statistical Planning and Inference*, 172:36–52, 2016.
- [10] J-N. Bacro and G. Toulemonde. Measuring and modelling multivariate and spatial dependence of extremes. *Journal de la Société Française de Statistique*, 154(2):139–155, 2013.
- [11] S. Bande, R.a Ignaccolo, and O. Nicolis. Spatio-temporal modelling for pm10 in piemonte. *Atti della XLIII Riunione Scientifica della SIS*, pages 87–90, 2006.

-
- [12] J. Beirlant, Y. Goegebeur, J. Segers, and J. Teugels. *Statistics of extremes: theory and applications*. John Wiley & Sons, 2006.
- [13] J. Blanchet and A.C. Davison. Spatial modeling of extreme snow depth. *The Annals of Applied Statistics*, pages 1699–1725, 2011.
- [14] F. Bosello and R. Roson. Estimating a climate change damage function through general equilibrium modeling. ISSN 1827-3580, 2007.
- [15] B. M. Brown and S. I. Resnick. Extreme values of independent stochastic processes. *Journal of Applied Probability*, pages 732–739, 1977.
- [16] S. Buhl, R. A. Davis, C. Klüppelberg, and C. Steinkohl. Semiparametric estimation for isotropic max-stable space-time processes. *submitted*, 2016.
- [17] S. Buhl and C. Klüppelberg. Anisotropic brown-resnick space-time processes: estimation and model assessment. *Extremes*, 19(4):627–660, 2016.
- [18] T.A. Buishand. Bivariate extreme-value data and the station-year method. *Journal of Hydrology*, 69(1):77–95, 1984.
- [19] M. Cameletti, F. Lindgren, D. Simpson, and H. Rue. Spatio-temporal modeling of particulate matter concentration through the spde approach. *AStA Advances in Statistical Analysis*, 97(2):109–131, 2013.
- [20] T. N. Chase, K. Wolter, R. A. Pielke Sr, and I. Rasool. Was the 2003 european summer heat wave unusual in a global context? *Geophysical Research Letters*, 33, 2006.
- [21] S. Coles, J. Bawa, L. Trenner, and P. Dorazio. *An introduction to statistical modeling of extreme values*, volume 208. Springer, 2001.
- [22] S. Coles, J. Heffernan, and J.A. Tawn. Dependence measures for extreme value analyses. *Extremes*, 2(4):339–365, 1999.
- [23] S. Coles and F. Pauli. Models and inference for uncertainty in extremal dependence. *Biometrika*, 89(1):183–196, 2002.
- [24] D. Cooley, P. Naveau, and P. Poncet. Variograms for spatial max-stable random fields. In *Dependence in probability and statistics*, pages 373–390. Springer, 2006.
- [25] R. A. Davis and C. Y. Yau. Comments on pairwise likelihood in time series models. *Statistica Sinica*, pages 255–277, 2011.

-
- [26] A. C. Davison and M. Gholamrezaee. Geostatistics of extremes. In *Proceedings of the Royal Society of London A: Mathematical, Physical and Engineering Sciences*, volume 468, pages 581–608. The Royal Society, 2012.
- [27] A.C. Davison, R. Huser, and E. Thibaud. Geostatistics of dependent and asymptotically independent extremes. *Mathematical Geosciences*, 45(5):511–529, 2013.
- [28] L. De Haan. A spectral representation for max-stable processes. *The annals of probability*, pages 1194–1204, 1984.
- [29] L. De Haan and T. T. Pereira. Spatial extremes: Models for the stationary case. *The annals of statistics*, pages 146–168, 2006.
- [30] M.G. Donat, T. Pardowitz, G.C. Leckebusch, U. Ulbrich, and O. Burghoff. High-resolution refinement of a storm loss model and estimation of return periods of loss-intensive storms over germany. *Natural Hazards and Earth System Sciences*, 11(10):2821–2833, 2011.
- [31] M.D. Ecker and A. E. Gelfand. Spatial modeling and prediction under stationary non-geometric range anisotropy. *Environmental and Ecological Statistics*, 10(2):165–178, 2003.
- [32] C. Edward. The use of subseries values for estimating the variance of a general statistic from a stationary sequence. *The Annals of Statistics*, pages 1171–1179, 1986.
- [33] C. Fonseca, L. Pereira, H. Ferreira, and A.P. Martins. Generalized madogram and pairwise dependence of maxima over two regions of a random field. *KY-BERNETIKE*, 51(2):193–211, 2015.
- [34] A. Genz. Numerical computation of rectangular bivariate and trivariate normal and t probabilities. *Statistics and Computing*, 14(3):251–260, 2004.
- [35] D. A. Griffith. Spatial autocorrelation. In *International Encyclopedia of Human Geography*, pages 308 – 316. Elsevier, Oxford, 2009.
- [36] A. Guillou, P. Naveau, and A. Schorgen. Madogram and asymptotic independence among maxima. *REVSTAT-Statistical Journal*, 12(2):119–134, 2014.
- [37] X. Guyon. *Random fields on a network: modeling, statistics, and applications*. Springer Science & Business Media, 1995.

- [38] J. Herrera, R. G. and Diaz, J. M. Trigo, J. Luterbacher, and E. M. Fisher. A review of the european summer heat wave of 2003. *Critical Reviews in Environmental Science and Technology*, 40:267–306, 2010.
- [39] P. Hougaard. *Analysis of multivariate survival data*. Springer Science & Business Media, 2012.
- [40] R. Ignaccolo, D. Sylvan, and M. Cameletti. Modeling pollutant threshold exceedance probabilities in the presence of exogenous variables. In *Spatial2 Conference: Spatial Data Methods for Environmental and Ecological Processes, Foggia (IT), 1-2 September 2011*. IT, 2011.
- [41] Z. Kabluchko, M. Schlather, and L. De Haan. Stationary max-stable fields associated to negative definite functions. *The Annals of Probability*, pages 2042–2065, 2009.
- [42] C. Keef, J.A. Tawn, and C. Svensson. Spatial risk assessment for extreme river flows. *Journal of the Royal Statistical Society: Series C (Applied Statistics)*, 58(5):601–618, 2009.
- [43] E. Koch. *Tools and models for the study of some spatial and network risks: Application to climate extremes and contagion in France*. PhD thesis, ISFA, university of Claude Bernard Lyon1, ISFA, University of Claude Bernard Lyon1, 7 2014.
- [44] E. Koch. Spatial risk measures and applications to max-stable processes. *To appear in Extremes*, 2015.
- [45] P. A. Krokmal. Higher moment coherent risk measures. *Quantitative Finance*, 7(4):373–387, 2007.
- [46] C.D. Lai and M. Xie. Concepts of stochastic dependence in reliability analysis. In *Handbook of Reliability Engineering*, pages 141–156. Springer, 2003.
- [47] A.W. Ledford and J.A. Tawn. Statistics for near independence in multivariate extreme values. *Biometrika*, 83(1):169–187, 1996.
- [48] E. L. Lehmann. Some concepts of dependence. *The Annals of Mathematical Statistics*, pages 1137–1153, 1966.
- [49] B.G. Lindsay. Composite likelihood methods. *Contemporary Math.*, pages 221–239, 1988.

-
- [50] H. Manto. Modelling of geometric anisotropic spatial variation. *Mathematical Modelling and Analysis*, pages 361–366, 2005.
- [51] C. Martin. Les inondations du 15 juin 2010 dans le centre var : réflexion sur un épisode exceptionnel. *Etudes de Géographie Physique*, XXXVII:41–76, 2010.
- [52] D. Moltchanov. Distance distributions in random networks. *Ad Hoc Networks*, 10(6):1146–1166, 2012.
- [53] P. Naveau, A. Guillou, D. Cooley, and J. Diebolt. Modelling pairwise dependence of maxima in space. *Biometrika*, 96(1):1–17, 2009.
- [54] P. J. Northrop. An efficient semiparametric maxima estimator of the extremal index. *Extremes*, 18(4):585–603, 2015.
- [55] S. A. Padoan, M. Ribatet, and S. A. Sisson. Likelihood-based inference for max-stable processes. *Journal of the American Statistical Association*, 105(489):263–277, 2010.
- [56] O. Payrastre, E. Gaume, P. Javelle, B. Janet, P. Fourmigué, P. Lefort, A. Martin, B. Boudevillain, P. Brunet, G. Delrieu, L. Marchi, Y. Aubert, E. Dautrey, L. Durand, Lang. J., L. Boissier, J. Douvinet, C. Martin, I. Ruin, and TTO2D Team of HYMEX. Analyse hydrologique de la catastrophe du 15 juin 2010 dans la région de draguignan (var, france). In *Congrès SHF : Evénements extrêmes fluviaux et maritimes, Paris*, 2012.
- [57] M. Re. Winterstorms in europe ii—analysis of 1999 losses and loss potentials. *Publication of Munich Re*, 2001.
- [58] M. Re. Natural catastrophes 2012 analyses, assessments, positions 2013 issue. *Topics Geo*, pages 1–66, 2013.
- [59] J. Reimann. Positively quadrant dependent bivariate distributions with given marginals. *Periodica Polytechnica Civil Engineering*, 32(1-2):3–21, 1988.
- [60] S. Rosenbaum. Moments of a truncated bivariate normal distribution. *Journal of the Royal Statistical Society. Series B (Methodological)*, pages 405–408, 1961.
- [61] M. Schlather. Models for stationary max-stable random fields. *Extremes*, 5(1):33–44, 2002.
- [62] M. Schlather and J.A. Tawn. Inequalities for the extremal coefficients of multivariate extreme value distributions. *Extremes*, 5(1):87–102, 2002.

-
- [63] M. Schlather and J.A. Tawn. A dependence measure for multivariate and spatial extreme values: Properties and inference. *Biometrika*, 90(1):139–156, 2003.
- [64] P. K. Sen. The impact of wassily hoeffding’s research on nonparametrics. In *The Collected Works of Wassily Hoeffding*, pages 29–55. Springer, 1994.
- [65] M. Sibuya. Bivariate extreme statistics, i. *Annals of the Institute of Statistical Mathematics*, 11(2):195–210, 1959.
- [66] R. L. Smith. Max-stable processes and spatial extremes. *Unpublished manuscript, Univer*, 1990.
- [67] E. Thibaud, R. Mutzner, and A.C. Davison. Threshold modeling of extreme spatial rainfall. *Water resources research*, 49(8):4633–4644, 2013.
- [68] A. Tsanakas and E. Desli. Risk measures and theories of choice. *British Actuarial Journal*, 9(04):959–991, 2003.
- [69] U. Ulbrich, A.H. Fink, M. Klawa, and J.G. Pinto. Three extreme storms over europe in december 1999. *Weather*, 56(3):70–80, 2001.
- [70] C. Varin, N. Reid, and D. Firth. An overview of composite likelihood methods. *Statistica Sinica*, pages 5–42, 2011.
- [71] C. Varin and P. Vidoni. A note on composite likelihood inference and model selection. *Biometrika*, pages 519–528, 2005.
- [72] H. Wackernagel. Multivariate nested variogram. In *Multivariate Geostatistics*, pages 172–180. Springer, 1998.
- [73] J.L. Wadsworth and J.A. Tawn. Dependence modelling for spatial extremes. *Biometrika*, 99(2):253–272, 2012.
- [74] C. Yang, R.E. Chandler, V.S. Isham, and H.S. Wheeler. Spatial-temporal rainfall simulation using generalized linear models. *Water Resources Research*, 41(11), 2005.
- [75] F. Zheng, E. Thibaud, M. Leonard, and S. Westra. Assessing the performance of the independence method in modeling spatial extreme rainfall. *Water Resources Research*, 51(9):7744–7758, 2015.
- [76] F. Zheng, S. Westra, M. Leonard, and S. A. Sisson. Modeling dependence between extreme rainfall and storm surge to estimate coastal flooding risk. *Water Resources Research*, 50(3):2050–2071, 2014.